THE ROLE OF AUTOPHAGY IN EARLY DEVELOPMENT AND TUMOR SUPPRESSION USING A ZEBRAFISH MODEL SYSTEM

APPROVED BY SUPERVISORY COMMITTEE

Beth Levine, M.D.

James F. Amatruda, M.D., Ph.D.

James Brugarolas, M.D., Ph.D.

John Abrams, Ph.D.

Ondine Cleaver, Ph.D.

DEDICATION

I would like to dedicate this dissertation to my family.

ACKNOWLEDGEMENT

To my mentors, Dr. Levine and Dr. Amatruda.

I would like to acknowledge my mentors, Dr. Levine and Dr. Amatruda. Under your support, I have gained the confidence to move onto the next step. I truly appreciate all of your patience, understanding, and guidance.

THE ROLE OF AUTOPHAGY IN EARLY DEVELOPMENT AND TUMOR SUPPRESSION USING A ZEBRAFISH MODEL SYSTEM

by

EUNMYONG LEE

DISSERTATION

Presented to the Faculty of the Graduate School of Biomedical Sciences

The University of Texas Southwestern Medical Center at Dallas

In Partial Fulfillment of the Requirements

For the Degree of

DOCTOR OF PHILOSOPHY

The University of Texas Southwestern Medical Center

Dallas, Texas

Aug, 2013

Copyright

by

EUNMYONG LEE, 2013

All Rights Reserved

THE ROLE OF AUTOPHAGY IN EARLY DEVELOPMENT AND TUMOR SUPPRESSION USING A ZEBRAFISH MODEL SYSTEM

EUNMYONG LEE, Ph.D.

The University of Texas Southwestern Medical Center at Dallas, 2013

BETH LEVINE, M.D., JAMES F.AMATRUDA, M.D., Ph.D.

Autophagy is an evolutionarily conserved lysosomal degradation pathway which involves the sequestration of cytoplasmic components into a double membraned structure called the autophagosome. By using genetically manipulated autophagy-deficient models, important roles for autophagy in development and tumorigenesis have been suggested.

Genetic analyses indicate that autophagy is essential for eukaryotic differentiation and development. However, little is known about whether autophagy contributes to morphogenesis during embryonic development. To address this question, the role of autophagy in early development was examined using zebrafish, a model system for studying vertebrate tissue and organ morphogenesis. Active autophagy was observed in multiple tissues during early embryonic development, as evidenced by the presence of autophagosomes in electron microscope images or

GFP-LC3 puncta in autophagy reporter fish line *Tg(cmv::GFP-LC3)*. Knockdown of autophagy genes by morpholinos caused defects in morphogenesis, increased numbers of dead cells, abnormal heart development, and reduced survival. Further analyses of cardiac development in autophagy-deficient zebrafish revealed defects in cardiac looping, abnormal chamber morphology, aberrant expression of cardiac valve markers and an abnormal cardiac gene expression program. Moreover, *atg5* deficient mice displayed cardiac defects including abnormal chamber septation. These results indicate that autophagy is necessary for normal cardiac morphogenic and gene expression programs during vertebrate development.

There is some controversy about whether autophagy promotes or inhibits tumorigenesis. The genetic relationship between autophagy deficiency and tumor susceptibility suggests the importance of autophagy in tumor suppression, but the molecular mechanisms are poorly understood. To study the role of autophagy in tumor suppression, transgenic fish that express dominant-negative autophagy proteins were generated. In a *p53*-mutant background, an impaired autophagy fish line *Tg(mitfa:dnatg5)* was prone to develop tumors, including malignant peripheral nerve sheath tumors (MPNSTs). The tumors in a heterozygous mutant *p53* background displayed loss of heterozygosity (LOH) for *p53*, and expression of dnAtg5 accelerated LOH of *p53*, suggesting a possible role for autophagy in the regulation of genomic stability during oncogenesis.

TABLE OF CONTENTS

LIST OF FIGURES

LIST OF TABLES

LIST OF ABBREVIATIONS

mTOR – Mammalian target of rapamycin

ULK1-Unc-51-like kinase 1

PI3K-Phosphatidylinositol-3-kinase

UVRAG-UV radiation resistance-associated gene

EM-Electron microscope

MO-Morpholino

ZFNs-Zinc finger nucleases

ENU-Ethylnitrosourea

hpf-hours post fertilization

MPNST-Malignant peripheral nerve sheath tumor

dpf-days post fertilization

PTU-Phenylthiourea

PFA-Paraformaldehyde

H&E-Hematoxylin and Eosin

AVC-Atrioventricular canal

AV-Atrioventricular

cmlc2-cardiac myosin light chain 2

MEF-Murine embryonic fibroblasts

VSD-Ventricular septal defect

mitfa-microphthalmia-associated transcription factor a

LOH-Loss-of-heterozygosity

CHAPTER ONE:

Introduction

1.1 Autophagy in development and disease

Autophagy, which means “self-eating”, is an intracellular degradation pathway which involves lysosomal degradation [1]. Unlike the proteasomal pathway, it degrades misfolded proteins, large protein aggregates and cellular organelles [2]. Autophagy involves the delivery of these cytoplasmic components into the lysosome for their degradation [3]. The importance of autophagy was recognized after discovery of several autophagy involved proteins in yeast [4].

Autophagy is a tightly regulated process that is activated by several stimuli, such as starvation or metabolic stresses. The main function of autophagy is to provide nutrients and ATP by degrading surplus proteins [3]. After the study of several genetically altered model organisms, other roles for autophagy have been revealed. Autophagy maintains cellular homeostasis by removing misfolded proteins and damaged organelles [2] . It has been shown to be important for life span extension, dead cell clearance, genomic stability, and to play a role in several types of diseases [2, 5-7].

Autophagy is a conserved pathway in eukaryotes, as indicated by the similarity of protein complex formations which are involved in the pathway [8]. Multiple model organisms have been used to study the physiological and pathological roles of autophagy. Here, I will review the roles of autophagy in development and tumor suppression that have emerged from studies in other model organisms and introduce zebrafish as a new model system for studying the role of autophagy in these processes.

1.2 Autophagy overview

Autophagy degrades cellular contents by sequestering them within a double membraned structure called the autophagosome. Several stimuli, such as nutrient starvation, protein aggregation, damaged organelles, DNA damage, hypoxia, redox stress and intracellular pathogens activate autophagy mostly through inhibition of mammalian target of rapamycin (mTOR) [9]. In normal conditions, mTOR complex1 interacts with the autophagy protein complex, which contains unc-51-like kinase 1 (ULK1), Atg13 and FIP200 [9]. In the process of autophagy-inducing stress, mTOR1 dissociates from this complex and activates ULK. Once activated, autophagy proceeds via four major steps- vesicle nucleation, vesicle elongation, autophagosome formation and fusion with lysosomes, and vesicle breakdown and degradation [2].

Vesicle nucleation Vesicle nucleation involves the initial formation of an isolation membrane that surrounds the targeted material for degradation. This step is mediated by a Class III phosphatidylinositol-3 kinase (PI3 kinase) complex that contains the autophagy protein Beclin 1 [2]. The activity of this complex is negatively regulated by Bcl-2 family proteins and positively regulated by Beclin 1 interacting proteins such as UV radiation resistance-associated gene (UVRAG), Bif1, and Ambra1 [9].

Vesicle elongation Vesicle elongation involves the expansion and completion of the autophagosomal membrane. There are two ubiquitin-like molecules essential for autophagosome formation, Atg12 and Atg8 (also known as LC3 in mammals). Atg5 is conjugated to Atg12, with the help of Atg7, an E1-like ligase, and forms a protein complex with Atg16 which is thought to be involved in membrane recruitment [9]. Pro-Atg8/LC3 is cleaved by Atg4 and conjugated to

phosphatidylethanolamine (PE) by Atg7, Atg10, and Atg3 [9]. Lipidated LC3 is the only autophagy protein that stably associates with the autophagosomal membrane [2]. In addition to its role in autophagosome membrane formation, LC3 can recruit several adaptor proteins to the autophagosome, including the ubiquitin-binding protein p62 [9].

Docking and fusion After autophagosomes are formed, they fuse with lysosomes and become autolysosomes. Inside autophagosomes, the sequestered contents are degraded.

Vesicle breakdown and degradation The sequestered materials are degraded by lysosomal hydrolases, and recycled for cellular processes used in cellular biosynthetic pathways.

Several techniques are available to monitor autophagy. First, autophagosomes are detectable by electron microscopy (EM) [10]. When there is activated autophagy, increased numbers of autophagosomes and autolysosomes are detected. Second, Atg8/LC3 can be used to mornitor autophagy [11]. Atg8/LC3 is the only protein that stably associates with the autophagosomal membrane [11]. Therefore, the detection of membrane-associated Atg8/LC3 is used to monitor autophagosome formation by immunoblot analysis to detect lipidated LC3 or by immunofluorescence analysis to detect redistribution of GFP-tagged LC3, from a diffuse cytoplasmic appearance to distinct intracellular puncta. Third, p62 degradation can be used to measure autophagic flux [12]. P62 is a substrate for LC3, and targeted to the autophagosome. When autophagy is activated, p62 is degraded rapidly.

1.3 Autophagy in development and differentiation

It has been known that autophagy is active during development [13]. During development or differentiation, cells undergo dramatic morphological changes. In theory, autophagy might be

involved in the phenotypic rapid change of cells or the remodeling of tissues by degrading and providing cellular building block materials in a response to environmental developmental signals. Indeed, genetically altered models have revealed a role for autophagy during development and differentiation.

Autophagy in early embryonic development

Fertilized mammalian eggs use maternally-derived RNAs and proteins at the earliest stages of development. At the 2- to 4-cell stages, the eggs start to degrade the maternal mRNA and proteins and synthesize their own zygotic proteins. The earliest onset of autophagy is in fertilized eggs in mammals, but the pathway becomes highly active within 4 hours after fertilization [14]. Knockout of maternal *Atg5* results in embryonic lethality at 4 the to 8 cell stages [15]. In the nematode *C. elegans*, it has been shown that autophagy genes play a role in embryonic apoptotic corpse clearance [16] and elimination of paternal mitochondria [17, 18]. Thus, it is clear that autophagy is involved in remodeling of cells during early embryonic development.

Autophagy in mouse embryonic development

Some autophagy gene knockouts result in embryonic lethality. For example, null mutations of *beclin 1*, *FIP200*, and *Ambra1*are embryonic lethal [13]. *Beclin 1*$^{-/-}$ mice show abnormally small size, with increased cell death [19]. Ambra1 is one of the proteins in the Beclin 1/class III PI3K complex. *Ambra1*$^{-/-}$ is embryonic lethal at E10-14 with neuronal tube closure defects, hyperproliferation, and increased cell death in neural tissues [20]. FIP200 is a ULK1-interacting protein, and *FIP200*$^{-/-}$ mice are lethal at day E13.5-16.5 with defective heart and liver development [21].

Mice with homozygous deletion of *Atg3, Atg5, Atg7, Atg9* and *Atg16L1* are born at normal Mendelian ratios but die within a day [22-26]. Atg3 acts as a specific E2-like enzyme for Atg8/LC3. Atg7 is an E1-like enzyme for Atg5 and Atg8 during autophagosomal membrane elongation [9]. Atg9 is the only transmembrane protein among the autophagy-related proteins and is proposed to be involved in membrane transport to the preautophagosome [9]. Atg16L1 forms a multimeric complex with the Atg5-Atg12 complex during autophagosomal membrane elongation [9]. *Atg3, Atg5, Atg7, Atg9,* and *Atg16L1* knockout mice are deficient in serum amino acids and are thought to die because of neonatal nutrient starvation [22-26]. The ability of some autophagy null mutants to be born at normal Mendelian ratios suggested that the role of autophagy might be dispensable for morphogenesis during embryonic development.

It is not clear why the knockout of different autophagy genes results in different phenotypes during development. There are several possibilities. First, each gene may have different functions in additional pathways besides autophagy. Second, the phenotypes could be related to the different steps in autophagy that different genes function in. Beclin 1, Ambra1, and FIP200, which result in embryonic lethality when knocked out, are involved in vesicle nucleation, the initiation step in autophagy, whereas *Atg3, Atg5, Atg7, Atg9*, and *Atg16L1* are involved later in autophagosome expansion and completion [13]. Third, it is possible that there are compensatory mechanisms for some of the genes.

Autophagy in differentiation

Under starvation or other stress conditions, lower organisms change their morphology as an adaptive response. Studies of genetically altered mutants revealed an essential role for autophagy

in starvation induced differentiation or development, including sporulation in yeast, fruiting body formation in *Dictyostelium discoideum*, and dauer formation in *C. elegans* [7, 27, 28].

In normal conditions, autophagy also plays a role in differentiation of multicellular organisms. Autophagy gene tissue-specific knockout mouse models showed roles for autophagy in erythrocyte differentiation, B-and T-cell lymphocyte differentiation, and adipocyte differentiation [13]. Erythroblasts contain nuclei and cellular materials that are eliminated during maturation of erythrocytes. *ULK1* knockout mice show impaired clearance of mitochondria and ribosomes in erythroid cells [29]. Hematopoietic cell-specific *Atg7* knockout mice accumulate damaged mitochondria in erythrocytes, display anemia and die at 8-12 weeks [30]. Also, hematopoietic cell-specific $Atg7^{-/-}$, B-cell specific $Atg5^{-/-}$, T-cell specific $Atg5^{-/-}$ and T-cell specific $Atg7^{-/-}$ have reduced numbers of B-cells and/or T-cells [30-33].

1.4 Autophagy in cancer

The role of autophagy in tumorigenesis is complex. On one hand, autophagy acts as a tumor suppressor; however, on the other hand, autophagy acts as pro-survival mechanism for tumor cells. Thus, the role of autophagy may be different in different stages of tumorigenesis. Although autophagy prevents tumor initiation, it is thought to act as pro-survival mechanism in established tumors by providing nutrients into tumor cells under metabolic stress [34].

Autophagy as a tumor suppressor

The role of autophagy in tumor suppression has been suggested by genetic studies. More than 40% of human breast, ovarian, and prostate tumors have monoallelic disruption of *BECN1* [35]. Monoallelic loss of *Becn1* in mice results in spontaneous malignancies including lung

adenocarcinoma, hepatocellular carcinoma, lymphoma, and mammary neoplastic lesions [19]. *Atg4C* deficiency increases chemically-induced fibrosarcomas [36] and *Atg5* or *Atg7* knockout mice develop benign liver tumors [37]. Deletion of *Bif-1* which interacts with Beclin 1 through UVRAG results in spontaneous tumors [38]. In addition, the relationship between autophagy and cancer-regulatory signaling pathways further suggested a role for autophagy in tumor suppression. Autophagy is activated by tumor suppressors, such as PTEN, TSC1 and TSC2, thorough mTOR inhibition/ULK1 activation [34]. Also, oncogenic pathways such as AKT inhibit autophagy by activation of mTOR and direct phosphorylation of Beclin 1 [34].

Taken together, these reports suggest the importance of autophagy in tumor suppression, but the molecular mechanisms are not well understood. One hypothesis is that autophagy prevents tumor initiation by reducing metabolic stress, such as damage to mitochondria, which can result in tumorigenic signals, including ROS and pro-inflammatory signals [34].

Autophagy as pro-survival mechanism for tumor cells

Autophagy also acts as pro-survival mechanism for tumor cells that are under metabolic stress, including hypoxia and insufficient vasculature, by providing nutrients and thereby potentially leading to chemoresistance [39]. In support of autophagy as a pro-oncogenic pathway, there are several lines of evidence. First, up-regulated autophagy has been found in several tumors [39]. However, this may also reflect its role as a tumor suppressor mechanism, since massive induction of autophagy may kill tumor cells through autophagic cell death. Second, autophagy inhibitors have been tested for their efficacy in cancer therapy with some promising results in pre-clinical models [34]. Third, genetic inhibition of *Atg5* impairs tumor growth of pancreatic cancer cells in a mouse xenograft model [40].

Autophagy in tumor prevention or cancer treatment

As discussed above, albeit controversial, increasing evidence suggests that autophagy plays a role in tumor regulation. Therefore, a better understanding of the mechanisms by which autophagy is involved in tumorigenesis would be beneficial in developing new strategies to target autophagy in tumor prevention or cancer treatment. The zebrafish model system offers a unique opportunity to gain such an understanding and to elucidate the specific contexts in which it has pro- or anti-tumor function.

1.5 Zebrafish as a model system

Zebrafish as a model for embryonic development

Danio rerio, known as zebrafish, is one of the widely used model systems for embryonic development. As a model system for embryonic development, it has several advantages. First, it shares similar mechanisms of embryonic development with mammals [41, 42]. Early development is fast, with most tissues were generated within a week. Techniques are available for their genetic manipulation; forward and reverse genetics are available. Efficient knockdown of genes can be achieved using morpholinos (MOs), anti-sense oligonucleotides. Transgenic fish are available by introducing new genes into germ cells using transposon systems, or by disrupting the gene using zinc finger nucleases (ZFNs), fused transcription activator-like effectors to a FokI cleavage domain (TALEN) as well as mutation by *N*-ethyl-*N*-nitrosourea (ENU) mutagenesis [43-46]. Lastly, it is cost-efficient model, which is easy to maintain and zebrafish have a large offspring size.

In the zebrafish, one of the most well-studied tissues is the cardiac system. The mechanism for cardiac development is evolutionary conserved [47]. Unlike other model systems, zebrafish can survive for several days without proper cardiac function by passive diffusion of oxygen from their skin to the tissues [41]. Given their transparency, easy genetic manipulation, and ability to survive with cardiac defects, zebrafish have provided important information for understanding higher eukaryotic cardiac development. Zebrafish have a two-chambered heart. The progenitor cells line up and migrate to form a cone-like shape that develops as a linearized cardiac tube. The heart starts to beat around 24 hours post fertilization (hpf). Around 36 hpf, the linearized cardiac tube is tilted to the left, which is referred to as jogging, and around 48 hpf, it undergoes looping. The atrioventricular cushion starts to develop and each chamber in the linearized cardiac tube becomes specified as either atrium or ventricle around 48 hpf [41, 48].

Zebrafish as a model for cancer

Zebrafish has been widely used as a developmental model. Recently, zebrafish has become a popular model system for studying human diseases including cancer. Zebrafish show high similarity with humans for gene function in organ development and physiology [46]. By using genetic manipulation, zebrafish develop many types of tumors which show similar histology with human tumors [49]. Live imaging is possible, which can be used to monitor the progression of tumors in zebrafish. For example, the leukemia and lymphomas induced by the expression of *Myc-GFP* under the control of the *rag2* promoter were visualized by GFP expression using fluorescence microscopy [50]. Furthermore, given its small size, zebrafish can be used as efficient *in vivo* model for therapeutic target screening [51].

As a non-mammalian animal, it has some disadvantages as a disease model system including for cancer. It does not have all of the same organs as mammals, such as lung and mammary gland [49]. As a cancer model, it has generally a lower tumor incidence than in mice, and it has a different spectra of tumors than in mammals [51]. p53 mutant fish show a lower tumor incidence (28%) than in mice (>70%) and the onset of tumor in also somewhat delayed [52, 53]. The tumor types caused by p53 mutation are Malignant Peripheral Nerve Sheath Tumors (MPNSTs), which are different than sarcomas in mouse models [52]. It also has duplicated genes which may affect the functions of oncogenes or tumor suppressors [51].

Despite these limitations, the advantages of zebrafish model system for the study of cancer such as its suitability for screening and imaging make it as a powerful diseases model system. Taken together, zebrafish as a disease model can prove very useful for understanding disease pathogenesis and as platform for the discovery of therapeutic agents.

CHAPTER TWO:

The role of autophagy in zebrafish development

2.1 Introduction

Autophagy is active during development and differentiation. During development, cells and organisms undergo massive morphological changes, necessitating the breakdown of established material and rebuilding of cellular structures [13]. Based on the known role of autophagy, as a cellular degradation pathway that provides nutrient and energy, it is not surprising to that autophagy is emerging as a crucial pathway in development and differentiation.

Since autophagy is an evolutionarily conserved pathway that uses similar proteins, several model organisms have been used to investigate the role of autophagy during development and differentiation. In lower organisms, autophagy acts as an adaptive response to environmental stimuli. When autophagy genes are deleted, yeast show defects in sporulation under starvation conditions [27]. In amoeba, autophagy deficiency results in abnormal fruiting body formation during starvation conditions [28]. In multicellular organisms, the role of autophagy extends to other cellular processes that need active recycling of cellular materials. For example, autophagy deficient worms display defects in apoptotic corpse clearance, and autophagy mutant flies show abnormalities in larval development, synapse formation and eye development [16, 54]. Several knockout mouse models were generated and analyzed to investigate systemic or tissue specific roles of autophagy during development and differentiation. As discussed above, some autophagy deficient mouse models are embryonic lethal, such as systemic knockout of *beclin 1, FIP200* or gene trap of *Ambra1* [19-21, 55]. Other knockout mouse models for key autophagy components, *Atg3, Atg5, Atg7, Atg9,* and *Atg16L1,* are viable during embryonic periods but die within 24

hours after birth [22-26]. Therefore, to better understand the role of autophagy in embryonic development, more studies are needed. Even though tissue-specific autophagy-deficient mouse models have been used to reveal role of autophagy during tissue morphogenesis, because of technical difficulties in studying the role of autophagy in morphogenesis, more tractable model systems are needed.

Zebrafish (*Danio rerio*) has been used as a model for development and diseases. It is comparable with mammals in many aspects, but more efficient as a model system because of its fast embryonic development, tractability due to its transparency, and manageability for genetic studies. Given these advantages, the morphogenesis and patterning of several tissues have been studied using zebrafish as a model system. The heart is one of the organs that have been well-studied. Unlike mammals, cardiac function in zebrafish embryos is dispensable for several days during early development [41]. Embryos can uptake oxygen directly from their skin, which enables the fish to survive for several days without proper cardiac function [41].

Given these benefits as a tractable model system for early embryonic development, I used zebrafish to study the role for autophagy in embryonic development. Here, I report that autophagy is essential for cardiac morphogenesis in zebrafish. First we tested whether zebrafish could be used as a model for autophagy. By imaging autophagosomes, we confirmed the occurrence of autophagy during embryonic development. Next, we investigated the role of autophagy during embryonic development. Knockdown of key autophagy components, *atg5, beclin 1* and *atg7*, using autophagy MOs resulted in systemic developmental defects including of the brain, body axis, and heart. Using the advantages of zebrafish as a model for cardiac development, we found that autophagy is essential for the regulation of cardiac patterning gene

expression. Further studies are needed to investigate the mechanistic regulation of cardiac morphogenesis by autophagy.

2.2 Methodology

Zebrafish strains and culture

Embryos from wild type AB strain were used for MO injection. Fish were raised and maintained under standard conditions [56]. Autophagy reporter fish *Tg(cmv:GFP-LC3)* (gift of Daniel Klionsky, University of Michigan) were previously described [57]. Cardiac reporter *Tg(cmlcs:GFP)* [58], and wnt reporter *Tg(tcfsiam:GFP)*fish [59] were previously described. *Tg(fli1:GFP)*fish were a gift of Dr. Nathan Lawson (University of Massachusetts) [60] and $tp53^{M214K}$ mutant zebrafish were a gift of Dr. A. Thomas, Look, Dana-Farber Cancer Institute [52]. All animal protocols were approved by the UT Southwestern Medical Center Institutional Animal Care and Use Committee.

Zebrafish embryonic cell culture

Approximately 50 autophagy MO- or control MO-injected embryos were used for primary cell culture. Injected embryos at the shield stage were sterilized with 70% ethanol, and dissociated in trypsin/EDTA solution. Primary cells were plated on a multi-chamber slide (Nunc) in LDF (Leibovitz 50%, DMEM 35%, F-12 15%) medium containing antibiotics and incubated at 25^{o}C [61].

Autophagy morpholinos

Translation-blocking MOs and splice-blocking MOs directed against *atg5, beclin 1* and *atg7* MOs were obtained from Gene-Tools (Philomath, OR). Control injections were done with standard control MO from Gene-Tools. The sequences of MOs targeted to inhibit translation are as follows:

Translation inhibiting morpholinos	
atg5 MO	5'-CACATCCTTGTCATCTGCCATTATC-3'
beclin 1 MO	5'-ACCTCAAAGTCTCCATGCTTCTTTC-3'
atg7 MO	5'-AGCTTCAGACTGGATTCCGCCATCG-3'

Splice blocking MOs were designed to inhibit splicing of the second exon and third intron in *atg5*, the first exon and first intron in *beclin 1*, and the first intron and second exon in *atg7*. The splice-MO sequences used are as follows:

Splice blocking morpholinos	
atg5 splice MO	5'-ATTCCTTTAACTTACATAGTAGGGT-3'
beclin 1 splice MO	5'-TGTTATTGTGTGTTACTGACTTGTA-3'
atg7 splice MO	5'-AGCTCGTTCTCCAAACTCACCGTTA-3'

Zebrafish RNA preparation and RT-PCR

RNA at 1 cell, sphere, germ ring, 5-somites, and 24 hpf stages of zebrafish embryos were purified by Trizol (Invitrogen) according to the manufacturer's instructions. After adding 0.5 ml of Trizol reagent, embryos were lysed with a blue pestle. cDNA was synthesized using 5 µg

purified RNA using a RT^2 HT first strand kit (Qiagen). To detect different autophagy transcripts, PCR reactions were performed using the follow primers:

Primers for RT-PCR	
atg5 377F	5'-GTCTTGCATTAGAGAGGcCG-3'
atg5 738R	5'-CTCTAGCAGGGGTTCAATGC-3'
atg5 exon2 F	5'-TGACAAGGATGTGCTTCGAG-3'
atg5 exon3 R	5'-ACCACATTTCCTCCACATCC-3'
atg5 intron2 R	5'-TTTAACAACCAAATGAACACTTATGTCTATTCAACTG -3'
beclin 1 F	5'-ACCCACTTTGTGAGGAGTGC-3'
beclin 1 R	5'-GTCCCTCATCCAGCTCTTTG-3'
atg7 F	5'-GATTCTGGCATCAGCTCACA-3'
atg7 exon2 R	5'-TTTGTCGGTGGATTTGAAGG-3'
atg7 intron1 R	5'- AAGCGGGTAAGGTTAATATTGCT -3'
ULK1b exon16 F	5'-GGCAACTATGGGCAGTCTGT-3'
ULK1b exon18 R	5'-ACCTGTGGAGAGAGCTGGAA-3'
GAPDH F	5'-TGGGTGTCAACCATGAGAAA-3'
GAPDH R	5'-TCAACGGTCTTCTGTGTTGC-3'
actin F	5'-GCTGTTTTCCCCTCCATTGTT-3'
actin R	5'-TCCCATGCCAACCATCACT-3'

Zebrafish cDNA cloning and mutagenesis

One-cell stages of wild type embryos were collected and lysed with 0.5 ml of Trizol (Invitrogen). cDNA was synthesized using 1μg purified RNA using a SuperScript First strand synthesis kit

(Invitrogen). To detect full length autophagy transcripts (*atg5* and *beclin 1*), PCR was performed using the follow primers:

Primers for RT-PCR	
atg5 BamH1 F	5'-CGGGATCCGCCATGGCAGATGAC-3'
atg5 Xba1 R	5'-GCTCTAGAGGCTTCAGTCACTCGGTGC-3'
beclin 1 BamH1 F	5'-CGGGATCCGCCATGGAGACTTTGA-3'
beclin 1 Xba1 R	5'-GCTCTAGAGCGGCGGCGCTATCGGTTGTAAAACTG-3'

PCR products were digested with BamH I and Xba I and cloned into pCS2 plus vector. Mutations were induced using a Quick change II XL site-directed mutagenesis kit (Stratagene) according to the manufacturer's protocol and verified by sequencing analysis. To induce mutations in *atg5* and *beclin 1* transcripts, PCR was performed using the follow primers:

Primers for mutation	
Mu atg5 F	5'-TCTTTTTGAAGGATCCGCCATGGCGGACGATAAAGACGTCCTTCGAGATGTTTGGTTTGGAAGG-3'
Mu atg5 R	5'-CCTTCCAAACCAAACATCTCGAAGGACGTCTTTATCGTCCGCCATGGCGGATCCTTCAAAAAGA-3'
Mu beclin 1 F	5'-CTTTTTGCAGGATCCGCCATGGAAACCTTAAGATTTTCTAGTAACACCATGCAGGT-3'
Mu beclin 1 R	5'-ACCTGCATGGTGTTACTAGAAAATCTTAAGGTTTCCATGGCGGATCCTGCAAAAAG-3'

mRNA in vitro transcription and purification

Mutated zebrafish *atg5* and *beclin 1* mRNAs were synthesized with mMessage mMachine SP6 kit (Ambion) using manufacturer's instruction.

Autophagy morpholinos and mRNA injections

2 nL of autophagy MOs and/or mRNAs were injected into the yolk at the 1 cell stage-embryos. For titration of translation-MOs, 0.1-0.5 mM of *atg5* MO, 0.2-1 mM of *beclin 1* MO, 0.5-2 mM of *atg7* MO were injected. Proper concentrations were selected as 0.3 mM of *atg5* MO, 1 mM of *beclin 1* MO and 1 mM of *atg7* MO, and used for further study. Standard control MO was injected at 1 mM. For rescue experiments, 10-20 pg of 5'-capped zebrafish mutant *atg5* mRNA or 2-30 pg of 5'-capped zebrafish mutant *beclin 1* mRNA were co-injected with *atg5* or *beclin 1* MO, respectively. Splice-MOs were injected with a concentration at 1-4 mM for *atg5* MO, and 0.5 mM-2 mM for *beclin 1* MO and *atg7* MO.

Western blotting

Two days post fertilization (dpf), embryos were anesthetized with Tricaine and incubated for 30 min on ice in lysis buffer containing 150 mM NaCl, 10 mM Tris pH7.4, 0.2% Triton X-100, 0.3% NP-40, 0.2 mM Na_3VO_4 and protease inhibitors (Roche). After centrifugation at 13,000 x *g*, supernatants were used for imunoblotting. Hearts were purified from 3 dpf larvae as described [62]. Atg5 antibody (Novus, NB110-53818), Beclin 1 antibody (Santa Cruz Biotechnology, sc-11427) and β-actin antibody (Millipore, MAB1501R) were used for western blotting.

Confocal microscope imaging of zebrafish primary cells and zebrafish embryos

Images of whole-mount zebrafish embryos were taken with a Nikon Coolpix 4500 camera mounted on a Leica MZ125 stereo dissecting microscope. Images of GFP-LC3 in primary cells

or zebrafish embryos were acquired using a Zeiss LSM 510 META confocal microscope. The embryos were treated with 0.003% 1-phenyl-2-thiourea (PTU) to reduce pigment at 24 hpf. For confocal imaging, embryos were maintained in 0.002% Tricaine and mounted in 3% low-melt agarose. Confocal z-stack images were used and analyzed by IMARIS.

Transmission electron microscope imaging

10 somite stage-embryos were fixed with 2.5% glutaraldehyde in 0.1 M cacodylate buffer pH 7.4 for 3 hours. Embryos were rinsed with 0.1 M cacodylate buffer pH 7.4 and postfixed with 2% osmium tetroxide containing 0.8% potassium ferricyanide in 0.1 M cacodylate for 1.5 hours, rinsed with water, then stained with 4% uranyl acetate in 50% ethanol for 1.5 hours, followed by dehydration with grade series of ethanol. After 100% ethanol, samples were treated with 100% propylene oxide and infiltrated with mixtures of propylene oxide and epon for 3 hours (2:1). Samples were placed in 100% resin 2 times, then into fresh resin and polymerized in an oven at 70˚C overnight. Thick sections were cut and stained with Toluidine blue in order to choose the correct orientation. Thin sections were post-stained with 2% aqueous uranyl acetate and lead citrate. Sections were imaged using a JEOL 1200 EX electron microscope at 120KV equipped with a Sis Morada 11 megapixel mount CCD camera.

Acridine orange staining

One dpf embryos were washed with PBS and incubated in PBS containing 2 μg/ml acridine orange for 30 min [63]. After staining, embryos were washed 5 times with E3 buffer. Mounted embryos in 3% methylcellulose were visualized using a Leica MZ16 FA fluorescent stereo dissecting microscope (Leica).

Survival assay

More than 100 embryos were injected with autophagy MO or control MO. The number of surviving injected embryos was counted daily for a month.

Histology

Injected zebrafish embryos were fixed at 3 dpf in 4% paraformaldehyde (PFA) for 48 hours and sagittal sections were stained with Hematoxylin and Eosin (H&E) for tissue morphology.

Immunohistochemistry

Injected zebrafish embryos were fixed at 3 dpf in 4% PFA for 48 hours and sagittal sections were prepared as paraffin embedded slides. For immunostaining, the slides were deparaffinized and baked for 15 min in Trilogy reagent (Cell Marque) in a pressure cooker for antigen retrieval. Endogenous peroxidase activity was quenched by 3% H_2O_2 in water for 30 min and nonspecific binding sites were blocked in 2.5% horse serum (Impress kit, Vector) for 30 min at room temperature. Slides were incubated overnight at 4˚C with β-catenin antibody (BD Transduction) at 1:250, washed with PBST 4 times and incubated with anti-mouse antibody conjugated with HRP (Impress kit, Vector) for 30 min in a wet chamber. After several washes with PBST, slides were developed with DAB solution, counterstained with hematoxylin (Invitrogen), dehydrated and mounted with Permount mounting media (Fisher).

In situ hybridization

Whole mount *in situ* hybridizations were performed using standard protocols with embryos at 2 dpf to detect *cmlc2, versican, bmp4, notch1b* and *nppa* and at 3 dpf to detect *foxn4* and *tbx5*. Riboprobes were synthesized using the following primers:

Primers for riboprobe synthesis	
cmlc2 F	5'-GTTGACCAGGCTTTTGCAGT-3'
cmlc2 R	5' TAATACGACTCACTATAGGGAGAATGATGCTCTACTCATAGTCAAG GAA-3'
bmp4 F	5'-CTGTCCACCAGAGACATCATGATTCC-3'
bmp4 R	5'- TAATACGACTCACTATAGGGAGACTTCATGATGGAATC-3'
notch1b F	5'-GGTTTTACGGGCTCGACCTG-3'
notch1b R	5'- TAATACGACTCACTATAGGGAGAATCACACTTCCCGTTATTAAAATA -3'
tbx2b F	5'-CTGATAGCGAGCACGAAATGGAC-3'
tbx2b R	5'- TAATACGACTCACTATAGGGAGAGGTTGTCCGGTGTTTAGTGGG-3'
foxn4 F	5'-CAGACAGAAGTCTGTTGACCCTG-3'
foxn4 R	5'- TAATACGACTCACTATAGGGAGAGCCAGGCAAAGTCCATTATACTG GG-3'
tbx5 F	5'-CTACCGGCCCCTAAGCTACT-3'
tbx5 R	5'- TAATACGACTCACTATAGGGAGAGCTGGCTTCATTCCAGTCAT-3'

T7 primer (TAATACGACTCACTATAGGGAGA) was added to reverse primers to facilitate antisense riboprobe synthesis. Riboprobe against *versican* was kindly provided by Dr. Didier Stainier (UCSF).

RNA preparation for microarray and real time PCR analyses

Zebrafish hearts were purified from control MO- or autophagy MO-injected embryos as described [62]. RNA from each group of injected embryos was purified at 3 dpf by Trizol (Invitrogen), digested with DNase and further purified using RNeasy columns (Qiagen). The purified RNAs were used for microarray.

Total RNA prepared from heart was used for quantitative RT-PCR. cDNA was synthesized using the RT^2 HT first strand kit (Qiagen). Quantitative PCR reaction for *foxn4* was performed with a QuantiFast SYBR Green PCR kit using an Applied Biosystems 7500 Real-time thermocycler. All signals were analyzed and normalized to β-actin mRNA. Primers for *foxn4* were obtained from Qiagen and primers for β-actin have been described previously [64].

2.3 Results

Autophagy is active in early embryonic development in zebrafish

To study the role of autophagy in early embryonic development in zebrafish, the temporal pattern of autophagy activation during zebrafish development was monitored. Unlike in mouse embryos, in which autophagy induction was observed at the 1-cell stage [14], it has been reported that autophagy is induced after 32 hpf in zebrafish because of delayed expression of proteins essential for autophagy [57]. To confirm the temporal expression pattern of autophagy transcripts, several autophagy key components, *atg5*, *beclin 1*, *atg7* and *ulk1b* were detected by a RT-PCR reaction (Figure 1.1A). All 4 transcripts were detected in 1-cell stage-embryos which implicated that they were maternally deposited. The inconsistency with a previous report [57] may be caused by different RT-PCR conditions. In the study by He *et al*.[57], the authors

amplified the full-length RNA for autophagy gene expression detection, but here, we performed the reactions for 2 exons of each transcript which are shorter than the full-length mRNA. It is possible that amplifying shorter segments of transcripts results in more sensitive amplification than amplification of the full-length transcripts.

To confirm the activation of autophagy in early embryonic development of zebrafish, 10 somite stage embryos were monitored for autophagosome structures by EM. We could detect early autophagosome and autolysosome structures (Figure 1.1B) which indicated the presence of autophagy at this stage.

To further confirm autophagy induction *in vivo*, we used the fluorescent autophagy reporter transgenic fish line *Tg(cmv:GFP-LC3)* [57]. During autophagy induction, LC3-I (which is diffusely distributed in the cytoplasm) becomes conjugated with phosphatidylethanolamine to form LC3-II, which stably associates with the autophagosomal membrane. GFP-tagged LC3-II accumulates in punctate structures (autophagosomes), thus serving as a useful *in vivo* marker of autophagy [11]. Using confocal microscopy, we detected the accumulation of GFP-LC3 puncta in zebrafish by the 15-somite stage indicating that similar to other organisms, autophagy is active during early development (Figure 1.1C).

Autophagy gene knockdown induces developmental defects

To investigate the role of autophagy in embryo morphogenesis, we used MOs to inhibit translation of zebrafish mRNAs encoding three key components of the autophagy machinery, *atg5, atg7, and beclin 1*. The knockdown of protein expressions by MO injection was performed with three different concentrations (Figure 1.2). At low concentrations of MO injections (0.1 mM for *atg5*, 0.2 mM for *beclin 1*, 0.5 mM for *atg7*), small numbers of morphants showed abnormal

developmental phenotypes such as twisted body shape at 2 dpf. The phenotypes were mild and did not affect their further development. At higher concentration of MO injections (0.5 mM for *atg5*, 2 mM for *atg7*), the majority of morphants exhibited severe developmental defects, having very small heads or in some cases no head at all and a very short twisted body at 2 dpf. These embryos failed to survive more than 3 days. These phenotypes were likely caused by nonspecific side effects of higher-than-desired MO concentrations. So, for further experiments, we decided to use concentrations of MOs that caused abnormal developmental phenotypes rather than classical off-target effect phenotypes.

First, we confirmed protein knockdowns by immune blot analysis of whole embryos at 48 hpf (Figure 1.3A). Atg5 is normally conjugated to Atg1*2* via a conjugation reaction that requires the action of the E1-like enzyme, Atg7 [9]. MO knockdown of Atg5 led to the expected loss of Atg5-Atg12 complex formation as well as free Atg5 (Figure 1.3A). Loss of the Atg5-Atg12 complex was similarly observed in *atg7* morphants. However, free Atg5 was increased in *atg7* morphants caused by the accumulation of protein which could not form the Atg5-Atg12 complex suggesting specific knockdown of Atg7 protein expression by *atg7* MOs injections. Embryos injected with *beclin 1* MOs did not show specific loss of Atg5-Atg12 complex, since Beclin 1 is not required for Atg5-Atg12 complex formation. Compared to control morphants, *beclin 1* morphants had decreased Beclin 1 protein expression (Figure 1.3A, bottom). Thus, *atg5*, *atg7*, and *beclin 1* MOs successfully inhibit protein expression of their target autophagy gene in zebrafish embryos.

Next, we evaluated whether autophagy MOs inhibit autophagy *in vivo*, using an autophagy reporter strain of fish, *Tg(cmv:GFP-LC3)* [57]. To efficiently quantify the effects of autophagy

MOs on zebrafish autophagy, we prepared primary cells from shield-stage *Tg(cmv:GFP-LC3)* embryos injected with control or autophagy MOs and counted the number of GFP-LC3 puncta per cell. Primary cells derived from shield-stage autophagy morphants displayed reduced numbers of GFP-LC3 puncta (Figure 1.3B, C), indicating that knockdown of *atg5, beclin 1* or *atg7* inhibits autophagosome accumulation *in vivo* (Figure 1.3B, C).

After demonstrating that the autophagy-specific MOs inhibit autophagy *in vivo*, we assessed the effects of autophagy inhibition on early zebrafish development. Autophagy morphants displayed reproducible abnormal developmental phenotypes including small heads (arrow) and eyes (asterisk), twisted body shapes, and pericardial edema (arrow head) at 2 dpf (Figure 1.4A, B). In general, the morphologic defects were similar when comparing *atg5, beclin 1* or *atg7* knockdown, although there were some differences in penetrance, with *beclin 1* morphants the most severely affected overall, and body morphology defects prominent in *atg7* (as well as *beclin 1*) morphants. Most strikingly, 62% of *atg5* morphants, 80% of *beclin 1* morphants, and 31% of *atg7* morphants exhibited cardiac defects such as pericardial edema, defective blood flow through the heart, defective heart looping, enlarged atria or linearized hearts (Figure 1.4A, B, Figure 1.5A). In comparison, more than 95% of fish were normal after control MO injection.

Autophagy gene knockdown results in increased numbers of dead cells

Autophagy genes are required for the clearance of dead cells during embryonic development in mice [5], chickens [65] and nematodes [16]. Mice with a null mutation in the autophagy gene, *AMBRA1,* have increased cell proliferation and cell death in the central nervous system [20] . To determine whether autophagy genes play a similar role in the regulation of cell death or dead cell clearance during zebrafish embryonic development, we stained embryos at 1

dpf with acridine orange (AO), and quantified the number of dead cells per unit area in a defined region of the embryo. Compared to control morphants, autophagy morphants showed a greater than 2-fold increase in numbers of dead cells (Figure 1.4C, D). These results indicate that autophagy may play an important role in either preventing cell death and/or the removal of dead cells during zebrafish development.

Autophagy gene knockdown affects long-term survival of zebrafish larvae

Certain autophagy genes are essential for embryonic survival of nematodes and mice [66, 67]. To evaluate whether autophagy inhibition during embryonic and early larval stages of development affects zebrafish viability, we followed more than 100 control or autophagy morphants for long-term survival. More than 60% of control morphants survived for more than 4 weeks. In contrast, survival was poor for autophagy morphants, with approximately 40% of *atg5* morphants and less than 10% of *beclin 1* or *atg7* morphants surviving more than 10 days (Figure 1.4E). As the translation-blocking effects of MOs generally wear off within 4-5 days after injection [68], these data suggest that autophagy during the first 4-5 days of development is essential for long-term fish viability.

Autophagy occurs during cardiac development

Autophagy morphants showed striking cardiac defects at 2 dpf (Figure 1.4A,B, Figure 1.5A). To further investigate the role of autophagy during cardiac morphogenesis, we first confirmed whether autophagy is active during cardiac development. Using an autophagy reporter fish strain *Tg(cmv:GFP-LC3)*, GFP-tagged LC3-II accumulation in the cardiac region was monitored by confocal microscopy at 2 dpf and 3 dpf. Autophagosomes were found in atrioventricular canal (AVC) and cardiomyocytes at 2 dpf (Figure 1.5B, left). At 3 dpf, increased

numbers of autophagosomes were detected in cardiomyocytes, endocardial cells and AVC indicating autophagy is occurring during cardiac development (Figure 1.5B, right).

Autophagy morphants showing cardiac defects or control morphants were monitored at 2 dpf to evaluate the levels of autophagy. Compared to control morphants, *atg5, beclin 1* and *atg7* morphants showed reduced numbers of autophagosomes in the heart at 2 dpf (Figure 1.6A) as visualized by z-stack images at high magnification (Figure 1.6A, lower). At 3 dpf, *atg5* and *atg7* morphants showed significantly reduced numbers of autophagosomes throughout the entire heart. *beclin 1* morphants also showed a trend toward reduced numbers of autophagosomes in the heart that did not reach statistical significance (Figure 1.6B, C).

Inhibition of autophagy induces cardiac defects

During zebrafish heart development, cardiac progenitor cells migrate from the lateral mesoderm and form a linear heart tube around 24 hpf. The heart tube subsequently tilts slightly to the left and undergoes looping around 2 dpf, representing a structural change from a linearized tube to a 3-dimensional chamber [41]. To better understand the cardiac defects in autophagy morphants, control and *atg5* MOs were injected into the transgenic strain *Tg(cmlc2:GFP)* which expresses GFP in cardiac myocytes, and the shape of heart was examined. At 2 dpf, control morphants had normal looping of their hearts. However, *atg5* morphants showed cardiac defects, such as enlarged atrium or linearized heart without looping (Figure 1.7A).

To further understand the cardiac defects in autophagy morphants, histological analyses were performed with control or autophagy MO-injected embryos at 3 dpf. Serial sections of hearts from autophagy morphants showed enlarged atria compared to those of control morphants, as well as incorrect looping at 3 dpf (Figure 1.7B). In control morphants, the atrium was properly

placed caudally and to the left of the ventricles. However, in autophagy morphants, the atrium was enlarged and cardiac looping was defective, resulting in the atrium and ventricle appearing in the same histologic plane. Additionally, all three autophagy morphants exhibited accumulation of blood cells in the atrium compared to the ventricle, suggesting that autophagy inhibition might cause defects in cardiac valve development and circulatory defects.

As autophagy morphants showed incorrect looping and potential cardiac valve defects by histological analysis (Figure 1.7B), we sought to further confirm these defects using *in situ* hybridization with cardiac-specific and atrioventricular (AV) valve-specific markers. To assess cardiac looping, we performed *in situ hybridization* to detect gene expression of the cardiac myosin light chain 2 (*cmlc2*) at 48 hpf. Control morphants displayed a normal looping pattern, resulting in the ventricle being placed slightly rostral and to the right of the atrium. In contrast, autophagy morphant hearts showed defects including failure to develop distinct heart tubes (data not shown) and failure of looping resulting in co-linear orientation of the two chambers (Figure 1.8A, C).

To further analyze cardiac valve development in autophagy morphants, we performed *in situ* hybridization to detect expression of three genes, *versican, bmp4,* and *notch1b,* which have been shown to be important in cardiac valve development [69] (Figure 1.8B, D). Atrioventricular canal development involves the regulation of multiple signaling networks in cardiomyocytes and endocardial cells [69-71]. In control MO-injected embryos, the expression of *versican, bmp4,* and *notch1b* is confined to the region of the AV valve. In contrast, these genes were misexpressed after knockdown of autophagy genes. v*ersican* was ectopically expressed throughout the ventricle in *atg5* and *atg7* morphants, and its expression was increased in the AV

valve and in parts of the atrium and ventricle in *beclin 1* morphants. The cardiomyocyte marker *bmp4* and the endocardial marker *notch1b* were ectopically expressed, most strikingly in the ventricle, in about 50% of autophagy morphants. In some autophagy morphants, the expression of *bmp4* and *notch1b* was markedly decreased or absent (Figure 1.8B, D). Thus, autophagy gene knockdown leads to defective cardiac looping, defective valve formation and ectopic expression of valve markers, suggesting that inhibition of autophagy disrupts gene regulatory networks critical for proper cardiac morphogenesis.

Autophagy gene knockdown alters the gene expression pattern of the developing heart

To further examine the effects of autophagy inhibition on cardiac gene expression, we purified RNA from the hearts of control and autophagy morphants at 3 dpf and profiled gene expression by microarray analyses. Altogether 109 genes were predictive of an altered autophagy state (Figure 1.9A). Transcripts that were differentially regulated in autophagy morphants included a large number of genes that are important for cardiac development and function, including *slc12a9, nup155, lrpprc, snrpbcrsp7/MED26* and *spred1*. The differentially expressed genes were enriched for fundamental biologic processes including cell cycle, hematopoiesis, tRNA metabolism and non-coding RNA metabolic processes. Most strikingly, morphants exhibited significant differential expression of transcription factors with roles in development, including *foxn4, dbx1b, eed, eng1a, hoxb2a, hoxc10a, hoxc1a, msxc, mynn, vox, ved* and *npas4* (Figure 1.9B). The magnitude of these effects was greatest for *atg7* morphants, but similar changes were also observed in *atg5* and *beclin 1* morphants. We confirmed the differential expression of *dbx1b, eed, hoxb2a, her15.1, mynn, msxc* and *znf2la* by quantitative RT-PCR of

RNA from purified hearts (Figure 1.10). These data demonstrate that developmental cardiac gene transcription programs are aberrant in autophagy morphant zebrafish.

We performed additional studies to validate the abnormal expression of *foxn4*, previously shown to be critical for proper AVC formation in zebrafish [72]. To validate the differential expression of *foxn4* in autophagy morphant fish, we performed quantitative RT-PCR on purified heart mRNA (Figure 1.9C). In agreement with the microarray results, *foxn4* expression was upregulated in all three autophagy morphants (Figure 1.9C). *tbx5* normally cooperates with *foxn4* to regulate expression of *tbx2b* during formation of the AVC. Misexpression of *tbx2b* causes defective AV canal development and impaired cardiac function [72]. *In situ* hybridization showed that autophagy knockdown caused increased expression and mislocalization of *tbx5* in the developing heart (Figure 1.9D, E). Consistent with this result, autophagy morphants exhibited expanded expression of *tbx2b* throughout the atrium and ventricle as well as in the AVC (Figure 1.9D, E). Taken together, these data indicate a critical role for autophagy in regulating cardiac development and proper patterning of the AV canal.

Autophagy gene knockdown may alter Wnt signal transduction pathway

The Wnt signaling pathway has been known to be involved in body axis formation and plays important roles in several tissues, such as brain, cardiac valve, and hematopoietic stem cells during embryonic development and in stem cell maintenance in adulthood [73]. Transgenic fish lines with constitutively active Wnt signaling show defects in cardiac development such as looping defects and excessive endocardiac cushion development [69]. Previous reports demonstrated that autophagy negatively regulates Wnt signaling by degradation of Dishevelled (Dvl) during metabolic stress, as evidenced by murine embryonic fibroblasts (MEF) from *Atg5*$^{-/-}$

and *Atg7*$^{-/-}$ mice showing extended Dvl2 half-life under starvation. [74]. These reports raised the hypothesis that modulated Wnt signaling in the AVC by impaired autophagy might be a possible mechanism of cardiac malformation. To investigate this hypothesis, autophagy morphants were examined for their Wnt signaling activity in the AVC. Immunostaining of cardiac tissue showed nuclear localization of β-catenin in endocardial cells indicating the activation of the Wnt signaling pathway in control and autophagy morphants at 3 dpf (Figure 1.11A). *beclin 1* and *atg7* morphants showed slightly increased levels of nuclear β-catenin in AVC but *atg5* morphants did not show significant differences from control morphants. These findings suggested that, while there might be crosstalk between autophagy and Wnt signaling, it was not consistent in the different autophagy morphants and therefore unlikely to provide an explanation for the observed cardiac defects in all three autophagy morphants. Unlike *apc* mutant fish in which Wnt signaling is constitutively active, autophagy and control morphants failed to display nuclear localized β-catenin in myocardial cells. To further assess the activation of Wnt signaling by impaired autophagy and support the hypothesis that autophagy attenuates Wnt signaling during cardiac morphogenesis, we monitored the wnt reporter strain *Tg(tcfsiam:GFP)* [59]. Control or *atg5* MO was injected into the offspring from the cross of a Wnt reporter female with a wild type male, and the embryo was monitored for GFP expression in AVC at 3 dpf. *Atg5* morphants showed 3 different GFP expression patterns:up regulation, no change, or down regulation compared to control morphants (Figure 1.11B). Further studies with larger numbers of embryos would be required to test whether autophagy affects Wnt signaling in zebrafish cardiac development.

Inhibition of autophagy does not affect vasculature

Cardiac morphogenesis can be influenced by several cardiac-extrinsic developmental factors such as blood circulation and vascular development [75-77]. Vascular defects can cause secondary cardiac defects by increasing cardiac afterload. To exclude vascular defects as a possible source of the cardiac phenotype of autophagy morphants, we monitored vascular development of morphants using the *Tg(fli1:EGFP)* line, which expresses GFP in endothelial cells, blood cells and endocardial cells [60]. Autophagy morphants did not show significant vasculature defects at 3 dpf (Figure 1.12), suggesting that the cardiac defects in autophagy morphants are not an indirect consequence of vascular abnormalities.

Cardiac defects was not fully rescued by mRNA injection

Next, we tested whether these knockdown phenotypes could be rescued by introducing mRNA. Autophagy MOs, including *atg5* or *beclin 1* MO were co-injected with *in vitro* transcribed full length mRNA containing 9-10 silent mutations in the region recognized by the MOs to inhibit their binding. The co-injected embryos still displayed abnormal phenotypes, but the severity of the phenotypes was improved compared to embryos injected with autophagy MOs alone. Co-injection of *atg5* MO with zebrafish mutant *atg5* mRNA showed a slight decrease in the percentage of cardiac defects (12%) and increase in the percentage of normal embryos (12%) but this did not reach statistical significance (Figure 1.13A). *Beclin 1* MO coinjected with zebrafish mutant *beclin 1* mRNA also resulted in an increased percentage of normal embryos (8%) and a decreased percentage of twisted body shape (15%) and cardiac defects (6%) (Figure 1.13B). To summarize, the embryos co-injected with autophagy gene mRNA with MO tended to have more mild abnormal phenotypes than autophagy MO alone injected embryos, but the abnormal phenotypes were not fully rescued by injection of synthetic mRNA. Immunoblots

suggested that the rescuing mRNA only produces protein for about the first 24 hpf: thus later phenotypes such as the cardiac developmental phenotypes would be unlikely to be fully rescued.

Inhibition of autophagy induces developmental defects in zebrafish with a p53 mutant background

MO injection can induce abnormal developmental phenotypes due to off-target effects that are attributed to p53-mediated cellular toxicity [78]. To exclude the possibility that the abnormal phenotypes of autophagy morphants were due to these off-target effects, we injected control and autophagy MOs into homozygous p53 mutant ($tp53^{M214K}$) fish [79] (Figure 1.14A, B). More than 80% of control morphants were normal at 2 dpf. Except for a slight decrease in the percentage of *atg7* knockdown embryos exhibiting small head size, autophagy morphants continued to exhibit developmental defects. One hundred percent of *atg5* morphants, more than 80% of *beclin 1* morphants and slightly more than 30% of *atg7* morphants showed cardiac defects. Overall, the cardiac defects due to autophagy MOs were not significantly affected by loss of p53 function, suggesting that the cardiac defects observed in a wild-type background of zebrafish were not caused by p53-dependent off-target effects.

Autophagy morphants showed increased numbers of dead cells at 1 dpf. A similar magnitude of increase in numbers of dead cells was also seen with injection of autophagy MOs into p53 mutant ($tp53^{M214K}$) embryos (Figure 1.14C, D). These results indicate that autophagy may play an important role in either preventing cell death and/or the removal of dead cells during zebrafish development.

Splice-morpholino injection also induces abnormal developmental phenotypes

Autophagy MO injections that inhibit the translation of *atg5*, *atg7* and *beclin 1* resulted in developmental phenotypes, including small heads, twisted body shape, and cardiac defects. To further confirm that these phenotypes were due to autophagy inhibition, we used another type of MO. Splice blocking-MOs were designed to inhibit the splicing of the exon 2-intron 2 junction in *atg5*, exon 1-intron 1 junction in *atg7*, and the exon 1-intron 1 junction in *beclin1* mRNA. Binding of the MOs to target gene inhibits splicing, alters the translation reading frame, and produces truncated RNAs with premature stop codons. Splicing inhibition by MO injection was confirmed by RT-PCR (Figure 1.15A). In control morphants, a spliced form of RNA was mainly detected at 2 dpf by RT-PCR. However, in autophagy morphants, non-spliced RNAs were more predominant than spliced form of RNAs. At a lower dose of MO injection, both forms of RNAs were detected but, at a higher dose of MOs injection, the spliced forms of RNA were hardly detected, indicating that splicing inhibition is splice MO-dose dependent. In order to optimize MO injections, several different concentrations were tested. Similar abnormal phenotypes to those found in translation-MO injected autophagy morphants were also observed in relationship to the injected MO concentration (Figure 1.15B, C). Different types of MOs induced similar abnormal phenotypes, both in wild type or p53-mutant backgrounds, suggesting these abnormal developmental phenotypes are truly caused by knockdown of autophagy genes.

2.4 Discussion

Here, I demonstrated that autophagy plays an essential role in normal morphogenesis in zebrafish cardiac development. Autophagy is active during the early period of embryogenesis stages in zebrafish as in other metazoans [14], and the knockdown of autophagy genes causes embryonic developmental defects. Furthermore, I demonstrated that autophagy is active during

cardiac development, and the knockdown of autophagy results in cardiac morphological and functional abnormalities, including mislooping of cardiac chambers, the formation of abnormal atrioventricular canals as well as increased embryonic lethality. These may be caused by the disruption of the cardiac gene expression program responsible for cardiac morphogenesis, leading to misregulation of cardiac specific transcription factors and ectopic expression of cardiac patterning genes.

In mouse embryos, autophagy is induced by fertilization and active during oocyte-to-embryo transition [14]. The viable phenotype of many mouse autophagy gene mutants has been attributed to maternally supplied autophagy factors [22-26]. Using the biochemical conversion of LC3-I to LC3-II as a marker of active autophagy, *He* and co-workers reported that autophagy was detectable in zebrafish embryos beginning at 32 hpf [57]. The authors explained the discrepancy of the delayed autophagy activation in zebrafish compared to other organisms by the function of yolk which serves as a source of nutrients during early development and the absence of autophagy transcripts, *atg9* and *ulk1* at 1 the cell stage. In this study, we detected autophagy in the somite stage (approximately 14-16 hpf) embryos, as evidenced by the presence of autophagic structures in EM analyses 10 somite stage-embryos and GFP-LC3 puncta, which mark autophagosomes in the cmv:GFP-LC3 transgenic reporter line at 15 somite stage-embryos. To further address the earlier appearance of autophagy in our experiments, the temporal expression pattern of autophagy transcripts was analyzed by RT-PCR. Unlike the previous report by He *et al*., *ulk1b, atg5, beclin 1 and atg7* transcripts were detected in 1 cell stage-embryos suggesting these transcripts were maternally supplied. The differences between our findings and those of the previous report may have to do with the increased sensitivity of confocal and electron microscopy methods to detect the occurrence of autophagy in individual cells as

compared to western blotting, as well as with our conditions for RT-PCR. To detect autophagy transcripts, we designed primers amplifying to two individual exons in each gene, not the full-length transcript. Also, even if there are no maternal autophagy transcripts in the 1 cell stage-embryo, the embryo starts to synthesize its own zygotic transcript and proteins as early as 4-6 hpf [14]. In our study, we detected increased levels of autophagy transcripts in sphere stage-embryos (4 hpf), indicating the beginning of zygotic gene transcription at this stage. In fact, we also detected autophagosome formation in primary cultures of cells prepared from shield-stage embryos (6 hpf). While it is possible that autophagy in this setting is a cellular response to *in vitro* culture and the absence of the yolk, our results indicate that embryonic cells are competent for autophagy from an early time in development. Taken together with our detection of robust autophagy occurring in intact, somite-stage embryos, as well as the presence of autophagy transcripts, these results indicate that autophagy is part of the early developmental program in zebrafish embryos during the period of active tissue morphogenesis and organogenesis.

It is perhaps somewhat surprising that extensive autophagy occurs during early fish development, since zebrafish embryos utilize yolk as their source of nutrient for several days until they can ingest and digest food. In this setting, autophagy may serve to support the high metabolic demands of tissues undergoing large-scale morphogenesis and cell movement, which could fulfill energetic needs beyond those supported by relatively slow diffusion of nutrients from the yolk. Alternatively, autophagy in developing zebrafish tissues may reflect an intrinsic role of the pathway in cellular differentiation, similar to what has been described in yeast sporulation, *Dictyostelium* fruiting body formation, and erythrocyte maturation [13].

Autophagy is essential for normal development in zebrafish as evidenced by abnormal phenotypes in the setting of autophagy gene knockdown. Knockdown of autophagy genes, *atg5, beclin 1* or *atg7* by either translation MOs or splicing MOs led to similar defects, including small heads, twisted body shape and cardiac defects. Previous studies in autophagy morphant fish have focused mostly on brain defects [80, 81]. Consistent with this, injection of autophagy MOs in p53 mutant transgenic fish line results in similar abnormal phenotypes, which rules out the possibility that the abnormal phenotypes were due to off-target effects of MOs [82]. When embryos were injected with MO and zebrafish full length mRNA that cannot be targeted by MOs, the abnormal phenotypes became less severe and the percentage of fish with abnormal phenotypes was partially decreased compared to MO injection alone. One possible explanation of this partial rescue is the challenge of temporal and spatial mRNA expression regulation. It is possible that the mRNA could not last long enough in the target tissue for full rescue of the abnormal phenotypes. Another possibility is the toxicity of mRNA injection. Hu *et al.* showed that overexpression of *atg5* mRNA itself can induce deformity and retardation, which makes it more challenging to distinguish the rescued MO-induced phenotype from mRNA overexpression-induced abnormalities [81].

Many autophagy genes are essential for functioning of the pathway. Like other organisms, such as yeast, nematodes and mice, knockdown of individual autophagy key components, such *atg5*, *beclin 1* or *atg7* alone was sufficient to inhibit autophagy and result in abnormal phenotypes. These phenotypes were dose-responsive in both translation-MOs and splicing-MOs. Even though the concentration was chosen based on the knockdown of protein expression, there were subtle differences in the phenotypes of each morphants - the most severe phenotypes were observed in *beclin 1* morphants, and the mildest phenotypes were observed in *atg7* morphants

when injected with translation MOs. One possible explanation is the different half-lives of maternally supplied proteins or different degrees of protein expression required in specific tissues. In splicing-MO-injected embryos, *atg5* morphants displayed more mild phenotypes than the other autophagy morphants. Though they showed impaired splicing, it is still possible that there was insufficient protein knockdown, which could be tested by additional western blot analysis. Interestingly, despite subtle differences among their phenotypes, all autophagy morphants showed impaired long-term survival, even beyond 5 days, after which time MOs do not effectively knockdown their target genes [83]. Even *atg7* morphants which have the mildest developmental phenotypes also showed poor long-term survival. Overall, these results indicated that autophagy plays a role in embryonic morphogenesis and long-term viability.

Autophagy is active during cardiac morphogenesis. One of the striking phenotypes observed in autophagy morphants is impaired cardiac development, including incorrect looping of the two chambers, mispatterning of AVC markers and altered expression of transcriptional factors. As MOs are reported to delay development, the ectopic expression of AVC markers in autophagy morphants could theoretically be explained as a result of developmental retardation. To rule out this possibility, autophagy morphants were synchronized by their morphological clock before analyzing their phenotypes. However, further experiments to monitor whether or not mispatterning of AVC marker expression persists are needed. To gain further insight into the connection between impaired autophagy and abnormal AVC development, microarray analyses were performed and showed altered expression of a large numbers of transcription factors. One of the transcription factors, *foxn4* was of particular interest since it has been reported to regulate AVC development, cooperating with *tbx5* to regulate expression of *tbx2b* [72]. This finding

suggests a model which autophagy is required for proper cardiac morphogenesis by regulating gene expression changes required for AVC formation.

Several signaling pathways have been implicated in proper formation of the AVC, including Notch, ErbB, TGF-β, and Wnt/β-catenin [69, 84, 85]. A recent report showed that autophagy can inhibit Wnt signaling by degrading Dishevelled [74]. Immunostaining for β-catenin in AVC of autophagy morphants did not showed a significant increase. However, the expression pattern of GFP was altered in Wnt reporter *Tg(tcfsiam:GFP)* which express GFP driven by Wnt target gene promoter after *atg5* MO injection. The GFP expression was altered in both directions, suggesting the possibility of altered Wnt signaling regulation by autophagy inhibition leading to abnormal AVC development. However, it is not still clear whether autophagy is negatively regulating Wnt signaling in the AVC during zebrafish development. It is also possible that inhibition of autophagy somehow impairs embryonic metabolism, which results in abnormal Wnt signaling. Further in-depth studies are needed to clarify the connection between Wnt signaling and autophagy in cardiac morphogenesis.

There are several implications of this work. First, autophagy is conserved in zebrafish as in the other eukaryotic organisms. Autophagy is active in early stages of embryonic development, especially in brain and heart, which need to undergo major morphological changes during development. Second, autophagy is essential for proper cardiac development, perhaps by regulating expression of transcription factors. These results suggest that autophagy genes should be examined as candidates for congenital heart disease. Furthermore, autophagy has been known to play a role in cardiac stress conditions [86]. It would be interesting to see whether regulation of gene expression by autophagy would play a role in cardiac stress and injury. Autophagy may

alter signaling pathways involved in AVC development. Additional roles for autophagy in modulating other pathways need to be addressed.

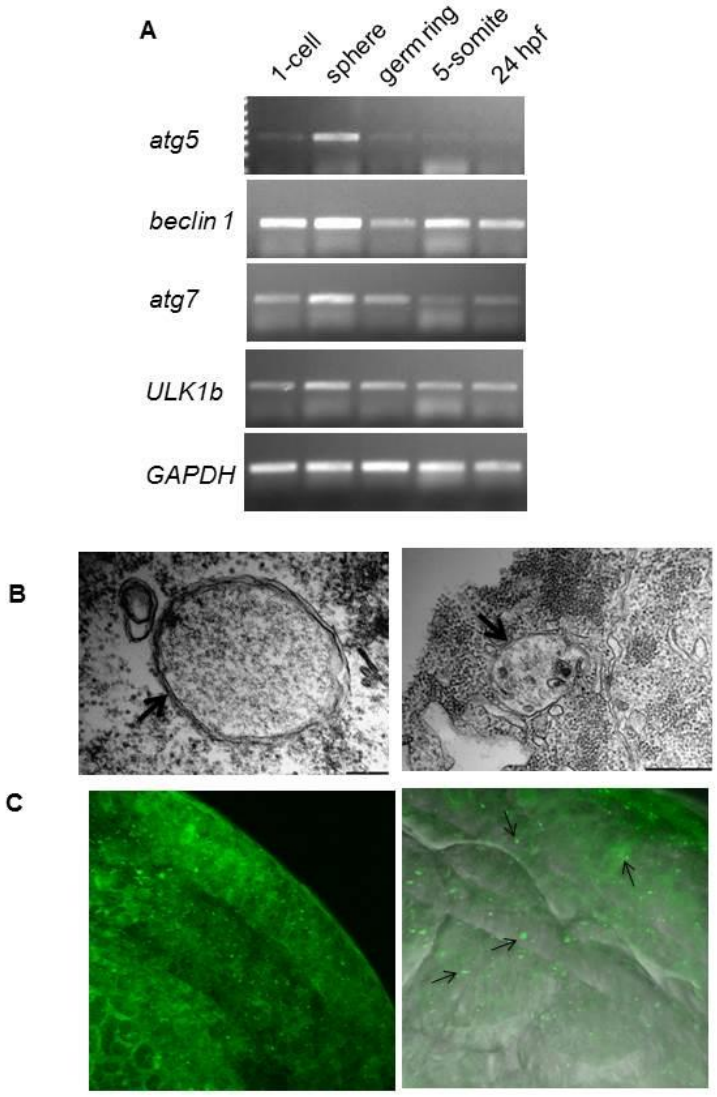

Figure 1.1. Autophagy is present during early zebrafish development.

(A) Autophagy transcripts are maternally deposited in zebrafish embryos. RT-PCR was performed with RNA isolated from 1-cell, sphere, germ ring, 5-somite and 24 hpf stage of wild-type embryos using gene-specific primers. **(B)** Early autophagosome (left) and autolysosomes (right) were detected from 10-somite stage embryos with electron microscopy. Scale bars, left=200 nm, right=500 nm. **(C)** GFP-LC3 puncta were visualized with confocal microscopy at 15-somite stage embryos from *Tg(cmv::GFP-LC3).* Left, z-stack images of somites. Right, GFP-LC3 puncta in somites merged with bright-field image.

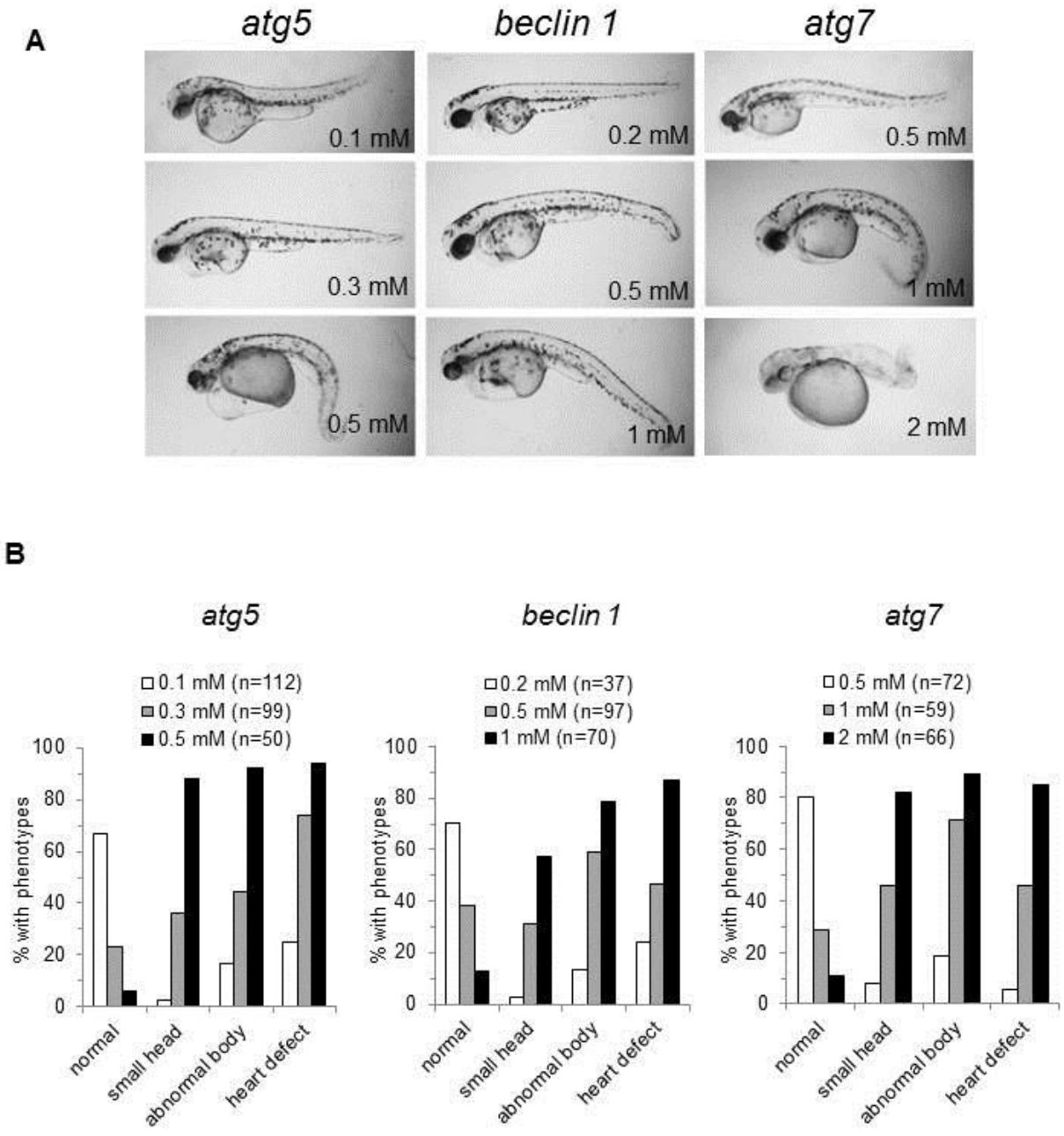

Figure 1.2. Autophagy morphants show a dose-dependent response.

(A) Representative images of autophagy morphants. Embryos were injected at the one-cell stage with three different concentrations of autophagy-specific morpholinos (MOs) and phenotypes were analyzed at 2 dpf. **(B)** Quantification of phenotypes depicted in **(A)**.

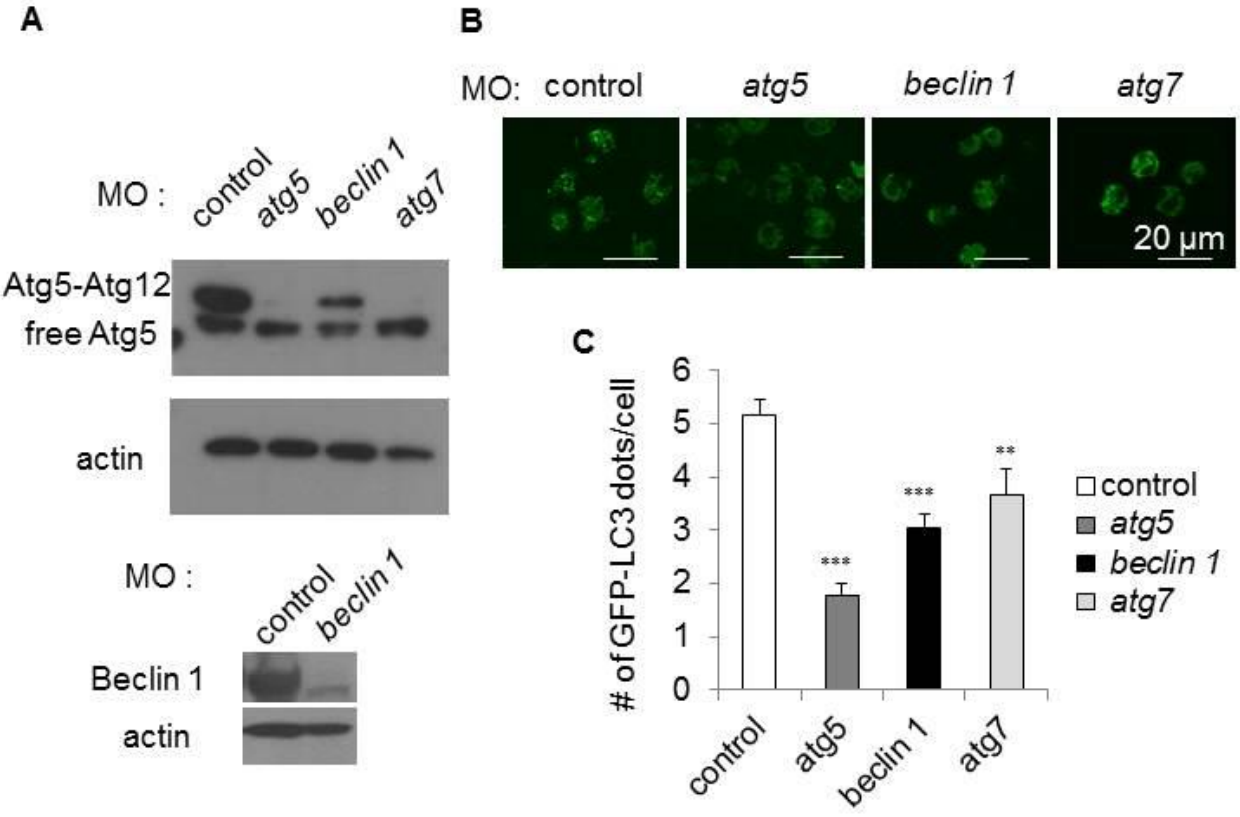

Figure 1.3. Autophagy is efficiently inhibited by autophagy gene knockdown.

(A) Expression of autophagy proteins after autophagy MO injection. Embryos were injected at the one-cell stage with control or autophagy-specific MOs, and lysates were prepared for immunoblot at 48 hpf. Top panel, immunoblot with anti-Atg5 antibody. Bottom panel, immunoblot with anti-Beclin 1 antibody. Actin is shown as a loading control. **(B** and **C)** Autophagy gene knockdown impairs autophagy in zebrafish. Primary cells were prepared from *Tg(cmv:GFP-LC3)* after MO injection and GFP-LC3 puncta were visualized with confocal microscopy. **(B)** Representative images of GFP-LC3 puncta in embryos injected with autophagy gene-specific and control MOs. **(C)** Quantification of data shown in **(B)**. Results represent the mean ± SEM from 50 to 100 cells in each group. ***P<0.001, **P<0.01, *P<0.05 for autophagy morphants versus control morphants; one-tailed t-test.

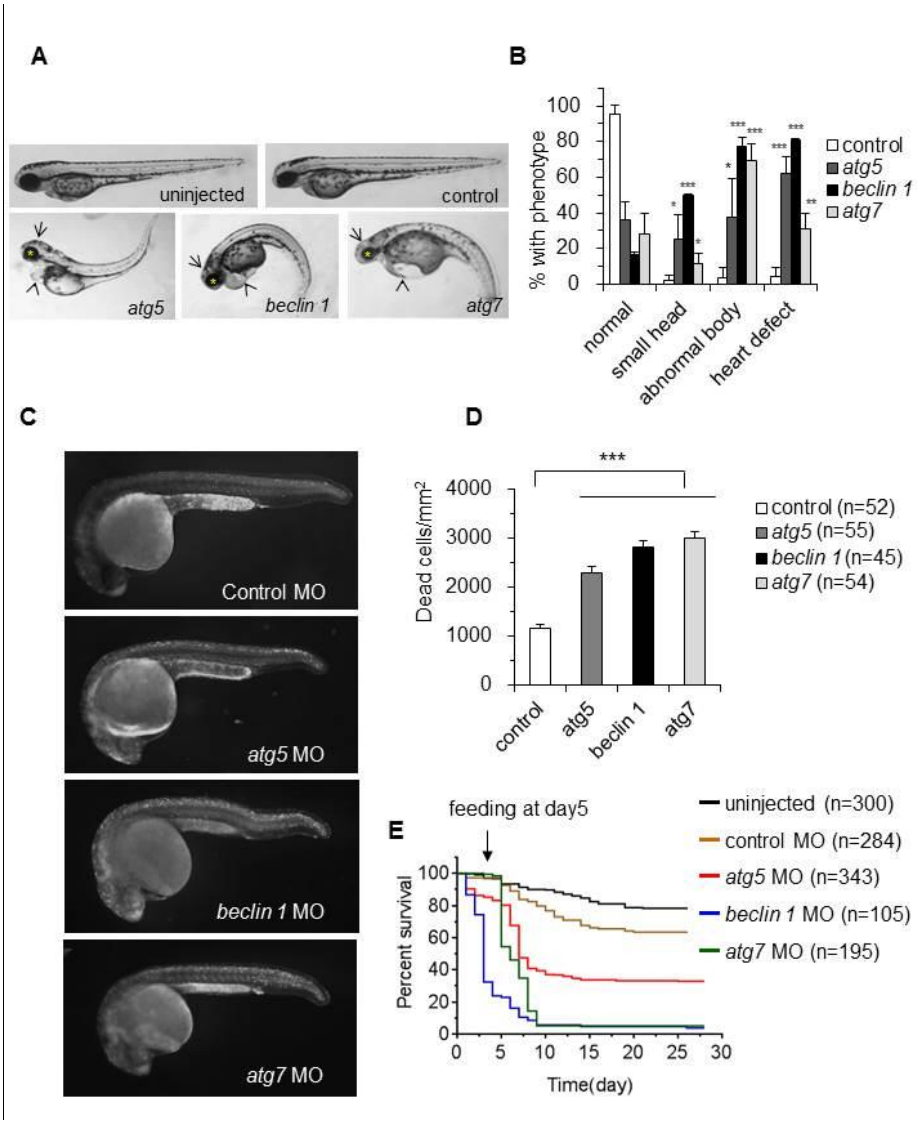

Figure 1.4. Autophagy gene knockdown in zebrafish results in developmental defects, increased numbers of dead cells and decreased survival.

(A and **B)** Morphology of autophagy morphants at 2 dpf. **(A)** Representative images of autophagy morphants which displayed small heads (arrows), abnormal eyes (asterisks), twisted body shapes and cardiac defects (arrowheads). **(B)** Quantification of phenotypes depicted in **(A)**. Results represent the mean ± SEM from 3 independent experiments. ***P<0.001, **P<0.01, *P<0.05 for autophagy morphants vs. control morphants; one-tailed *t*-test. **(C** and **D)** Acridine orange (AO) staining of control and autophagy morphants at 1dpf. AO-positive cells were counted in an area spanning from the end of the yolk extension to the end of tail. **(D)** Quantification of data shown in **(C)**. Results represent the mean ± SEM from more than 40 embryos in each group. ***P<0.001 for autophagy morphants vs. control morphants; one-tailed *t*-test. **(E)** Survival of control and autophagy gene morphants. ***P<0.001 for autophagy morphants vs. control morphants; Log-rank test.

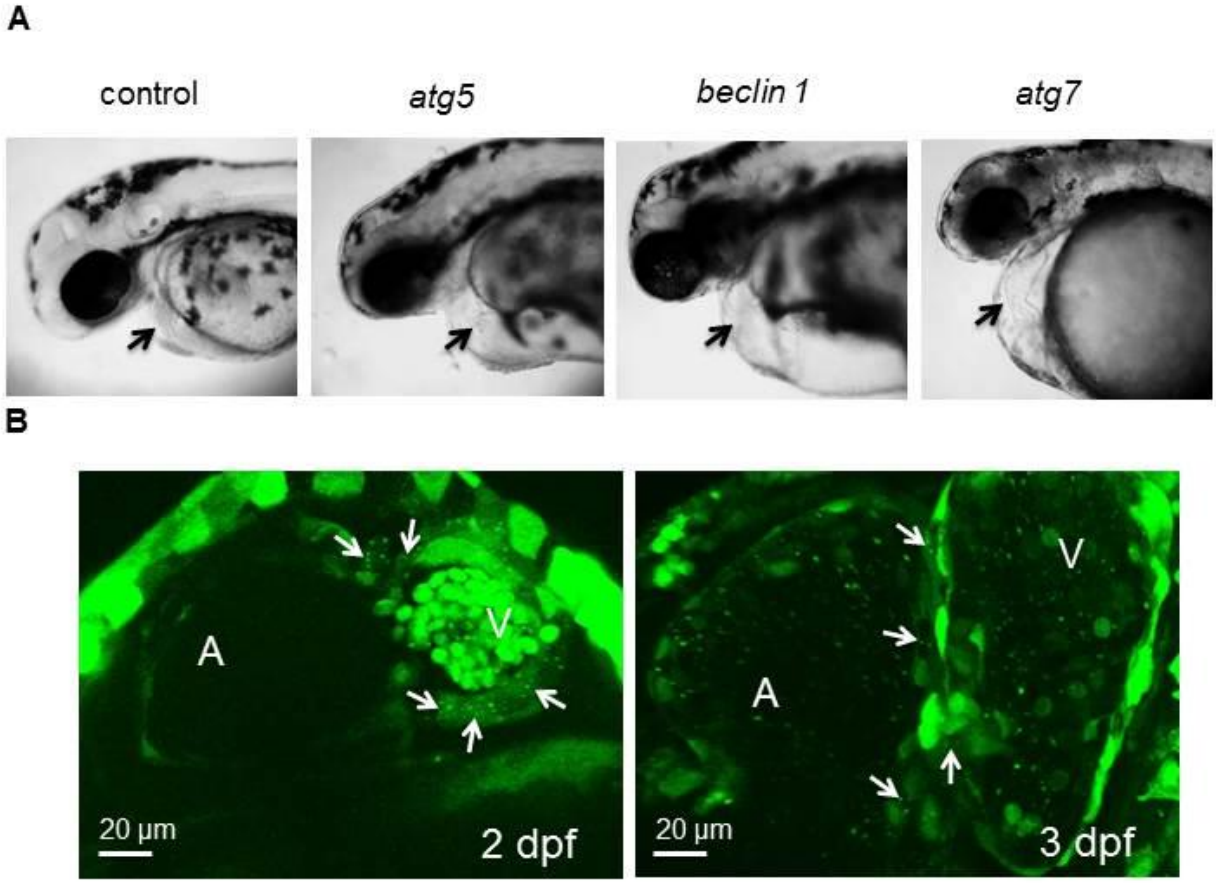

Figure 1.5. Autophagy is active during zebrafish cardiac development.

(A) Abnormal cardiac morphology in autophagy morphants which display mislooping, abnormal cardiac chambers, and linearized hearts monitored at 2 dpf. **(B)** *Tg(cmv:GFP-LC3)* embryos were examined for GFP-LC3 and imaged at 2 and 3 dpf using confocal microscopy. Representative images showing GFP-LC3 puncta (white arrows) in atrium (A), ventricle (V).

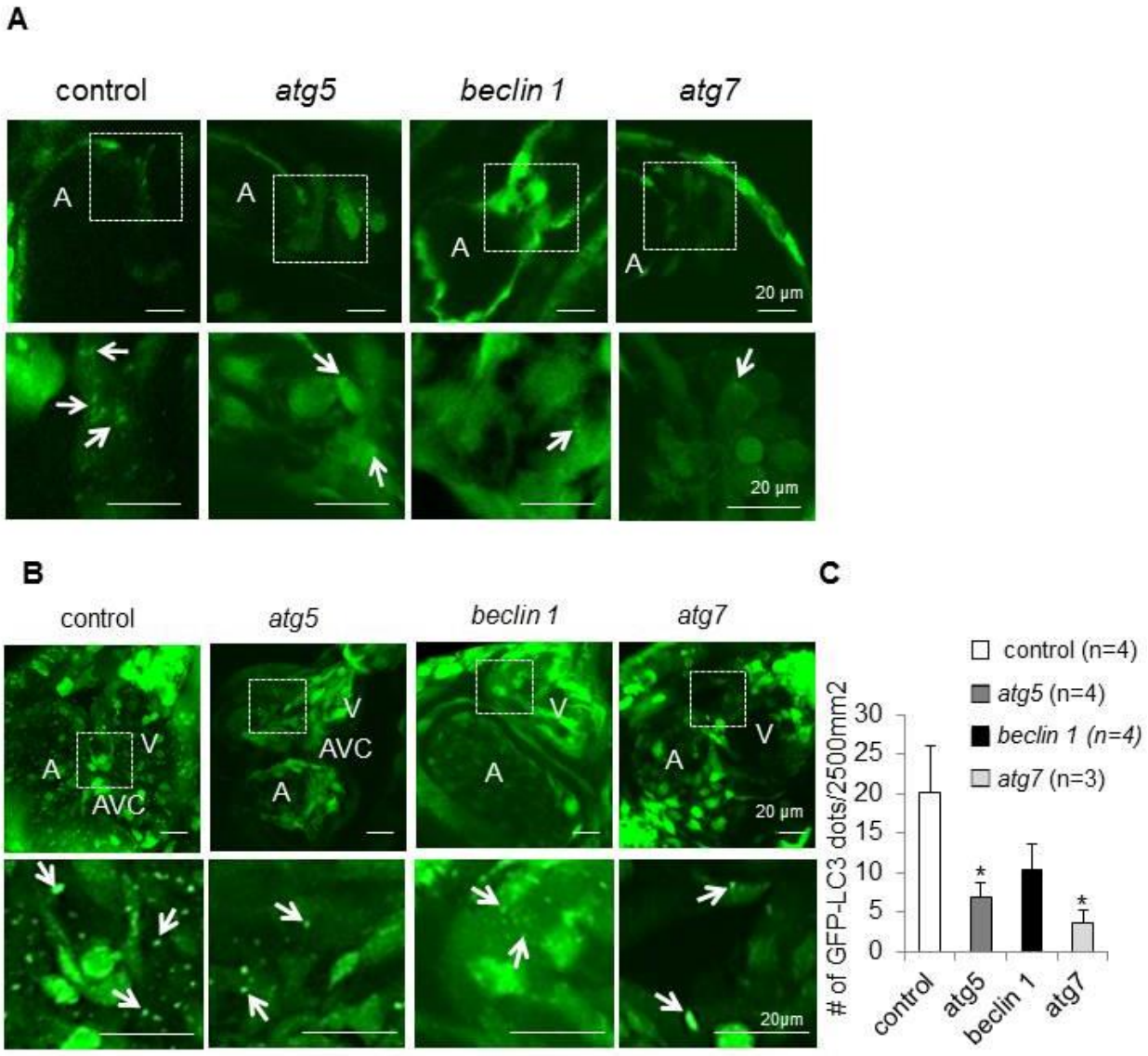

Figure 1.6. Autophagy is impaired in the heart by autophagy gene knockdown.

Autophagy is active during normal cardiac development and impaired by autophagy MOs. *Tg(cmv:GFP-LC3)* embryos were injected with either control or autophagy MOs and imaged at 2 and 3 dpf using confocal microscopy. Representative images showing GFP-LC3 puncta (white arrows) in atrium (A), ventricle (V) and AV canal (AVC). Scale bar=20 µm. **(A)** GFP-LC3 at 2 dpf. The areas delineated by the white dashed lines are shown as z-stack images at higher magnification in the bottom panel. (**B**) GFP-LC3 at 3 dpf. The areas delineated by the white dashed lines are shown at higher magnification in the bottom panel. (**C**) Quantification of data shown in **(B)**. Results represent the mean ± SEM from more than 3 embryos in each group. *P<0.05 vs. control morphants; one-tailed *t*-test.

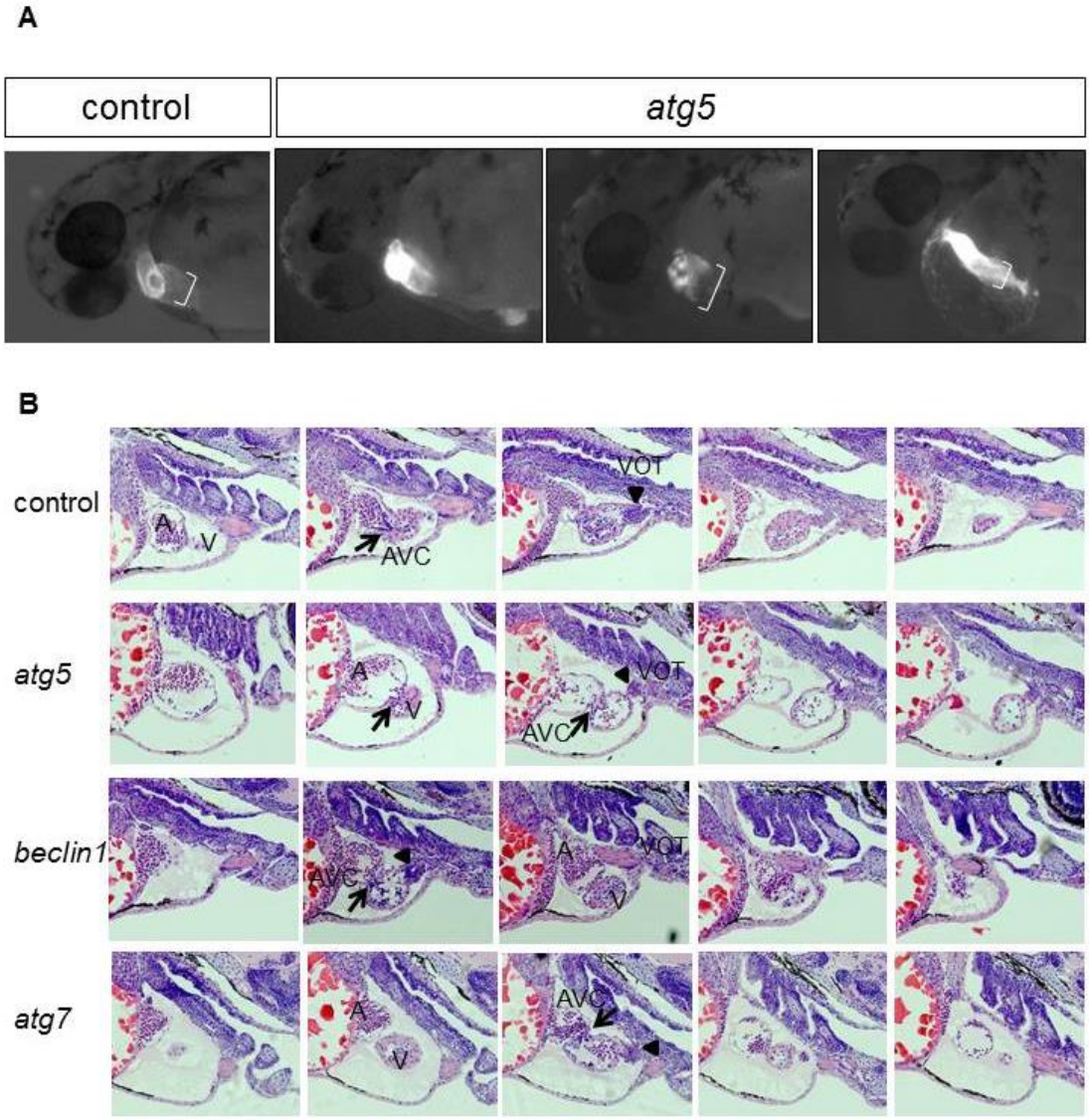

Figure 1.7. Autophagy gene knockdown results in abnormal cardiac development.

(A) *Atg5* morphants displayed abnormal cardiac morphology, such as incorrect looping (left), enlarged atria (middle), and linearized hearts (right). Control or autophagy MOs were injected into *Tg(cmlc2:GFP)* and hearts were visualized at 2 dpf. (**B**) Hematoxylin and eosin (H&E) staining of serial sagittal sections of hearts from representative control or autophagy morphants at 3 dpf. The head is positioned to the right. In the control morphant heart, the atrium, AV canal (arrow), ventricle, and ventricular outflow tract (arrow head) (from left to right) are visualized. All autophagy morphant hearts display pericardial edema. The *atg5* and *beclin 1* morphant hearts shown have enlarged atria compared to those from the control morphant. The *beclin 1* morphant heart displays an accumulation of blood cells in the atrium. All autophagy morphant hearts shown contain the atrium and ventricle in the same plane indicating incorrect cardiac looping. A, atrium; V, ventricle; AVC, atrioventricular canal; VOT, ventricular outflow tract.

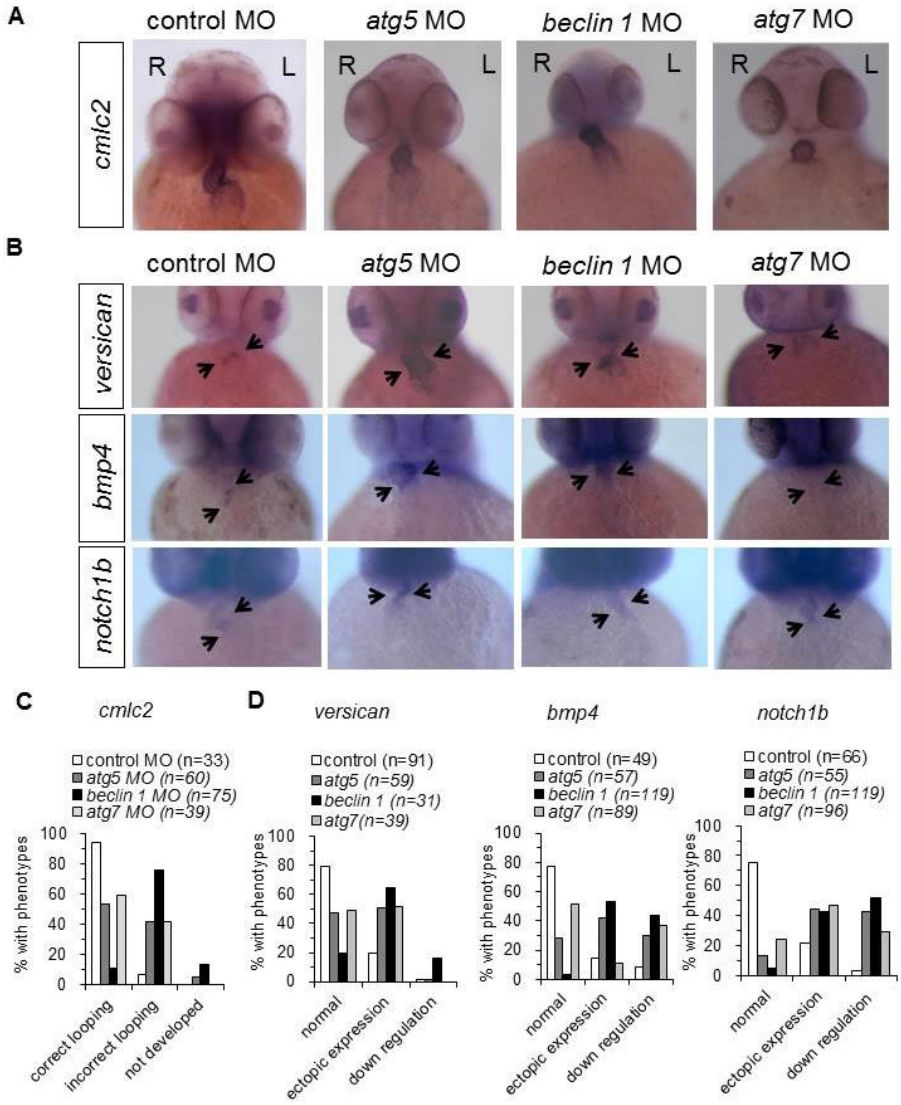

Figure 1.8. Autophagy gene knockdown results in abnormal cardiac looping and valve development.

(A and **C)** *In situ* hybridization with a *cmlc2* probe of morphant hearts at 48 hpf. **(A)** Representative images of a control morphant showing correct looping with the atrium placed left and caudal, and the ventricle right and rostral, and of autophagy morphants, showing linearized hearts without looping. **(C)** Quantification of data shown in **(A)**. More than 30 embryos were analyzed in each group. **(B** and **D)** *In situ* hybridization of morphants with probes that detect cardiac valve markers at 2 dpf. **(B)** Representative images of *versican*, *bmp4* and *notch1b* expression in the hearts of control and autophagy mutants. **(D)** Quantification of data shown in (**C**). More than 30 embryos in each group were analyzed. R, right; L, left.

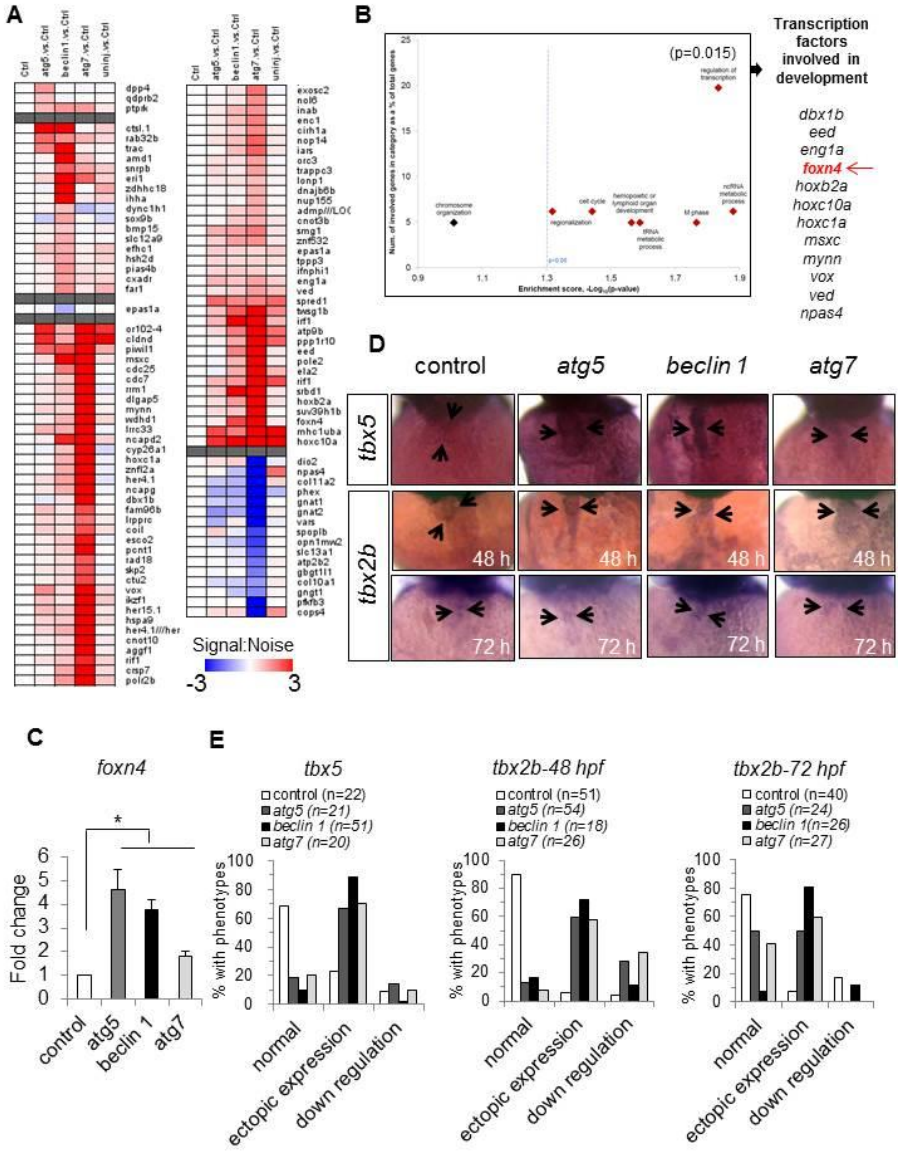

Figure 1.9. Autophagy gene knockdown results in up-regulation of transcription factors that are involved in development.

(A) Heat map of altered transcripts from the hearts of autophagy morphants at 3dpf. **(B)** Gene expression signature. Autophagy gene knockdown induced up-regulation of transcription factors that are involved in development, including *foxn4* (arrow). **(C)** Real-time PCR measurement of *foxn4* mRNA levels in purified hearts of autophagy morphants at 3 dpf. Results represent the mean ± SEM from triplicate samples. **P*<0.05 vs. control morphants; one-tailed *t*-test. **(D** and **E)** *In situ hybridization* to detect *tbx5* and *tbx2b* expression in morphant hearts. (**D**) Representative images of control and autophagy morphants, with the autophagy morphants showing stronger expression of *tbx5* and *tbx2b* throughout the heart (arrows). **(E)** Quantification of data shown in (**D**). More than 18 embryos in each group were analyzed.

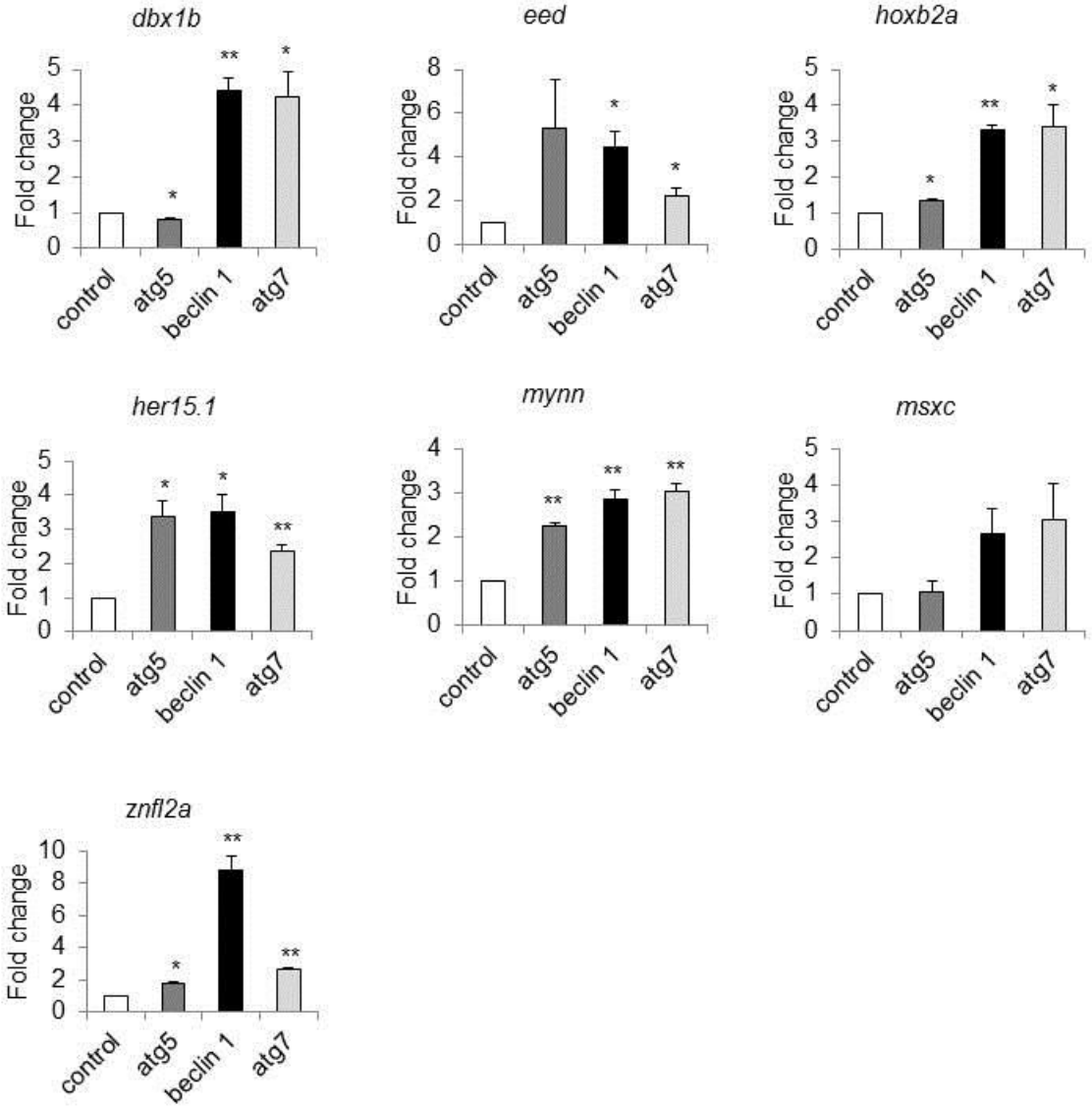

Figure 1.10. Autophagy gene knockdown results in up-regulation of transcription factors that are involved in development.

Real-time PCR measurement of transcripts for *dbx1b, eed, hoxb2a, her15.1, mynn, msxc,* and *znfl2a* in purified hearts of autophagy morphants at 3 dpf. Results represent the mean ± SEM from triplicate samples. ***P*<0.01, **P*<0.05 for autophagy morphants vs control morphants; t-test.

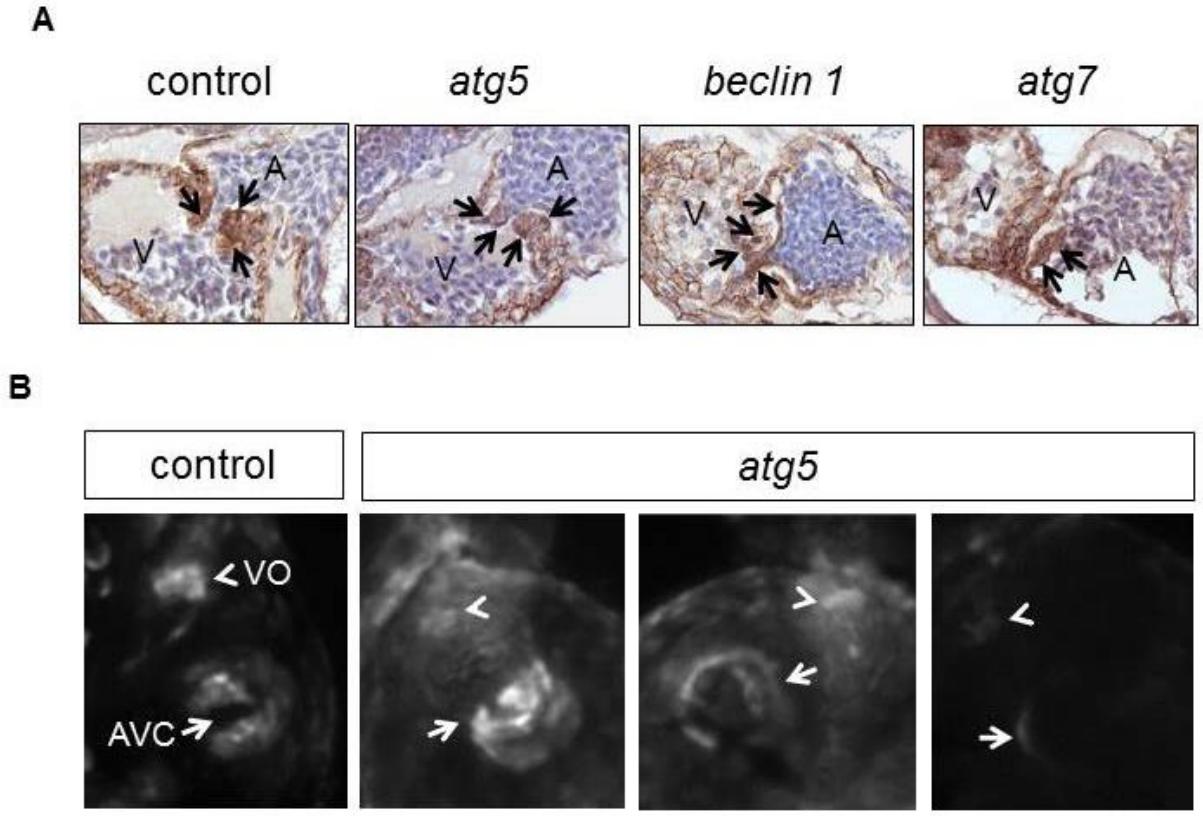

Figure 1.11. Autophagy gene knockdown alters Wnt signaling.

(A) Immunohistochemistry for β-catenin did not show wnt activation in *atg5* morphants but showed slight activation in *beclin 1* and *atg7* morphants. Sagittal sections of control or autophagy morphants hearts at 3 dpf stained for β-catenin. Arrows point to positive nuclei of endocardial cells. A, atrium; V, ventricle. **(B)** *Atg5* morphants showed deregulated Wnt/β-catenin signaling; up-regulation (left), normal (middle), and down-regulation (right). Control or *atg5* MO was injected into *Tg(tcfsiam:EGFP)* and hearts were imaged at 3 dpf. Arrows point to wnt positive endocardial cells. AVC, atrioventricular canal; VOT, ventricular outflow tract

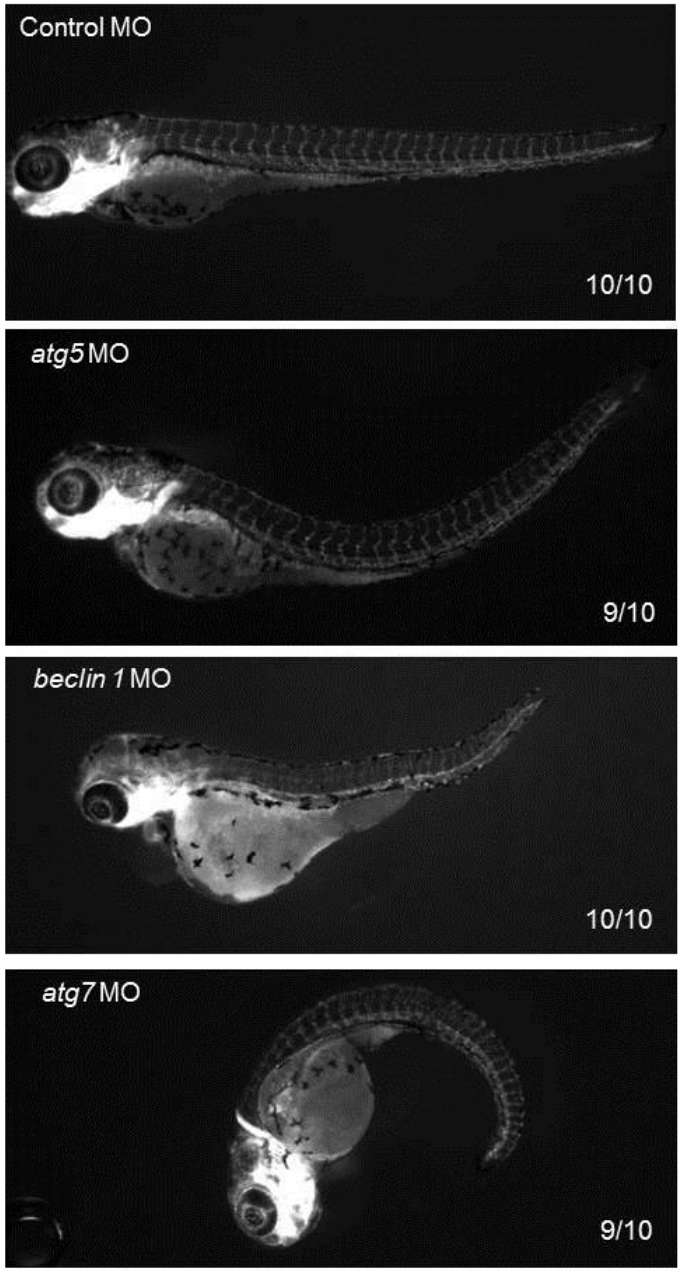

Figure 1.12. Autophagy morphants develop normal vasculature.

Representative images of the vasculature in control or indicated autophagy morphants using *Tg(fli1:EGFP)* fish at 3 dpf. None of the control or *beclin 1* morphants showed abnormal vasculature. Nine out of 10 *atg5* and 9 out of 10 *atg7* morphants showed normal vasculature.

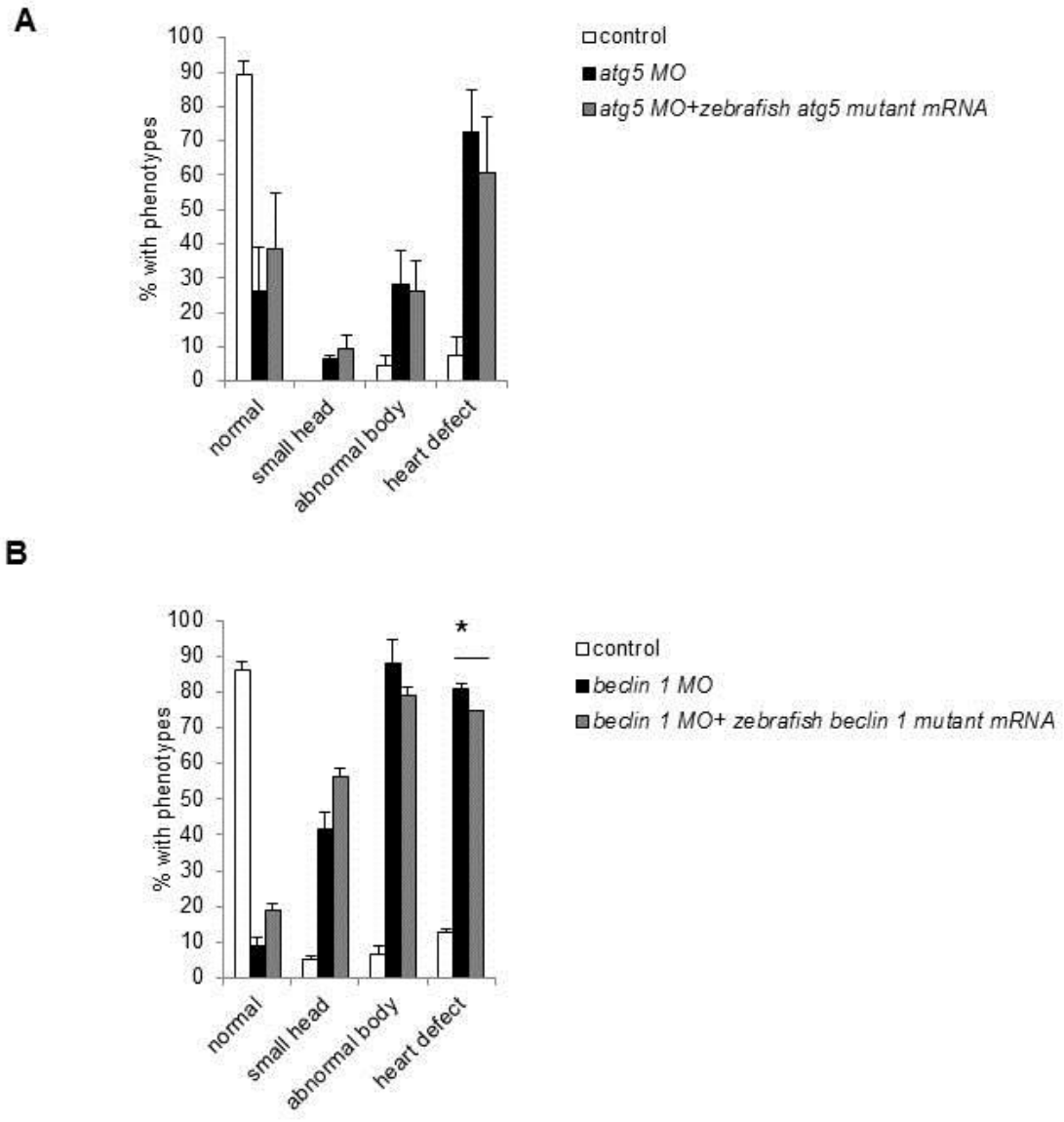

Figure 1.13. Cardiac defects are not fully rescued by mRNA injection.

(A) Quantification of phenotypes in *atg5* morphants injected with 16 pg of zebrafish mutated *atg5* mRNA. Results represent the mean ± SEM from 3 independent experiments. **(B)** Quantification of phenotypes in *beclin 1* morphants injected with 2 pg of zebrafish mutated *beclin 1* mRNA. Results represent the mean ± SEM from 2 independent experiments. **P*<0.05 for autophagy morphants vs. control morphants; one-tailed *t*-test.

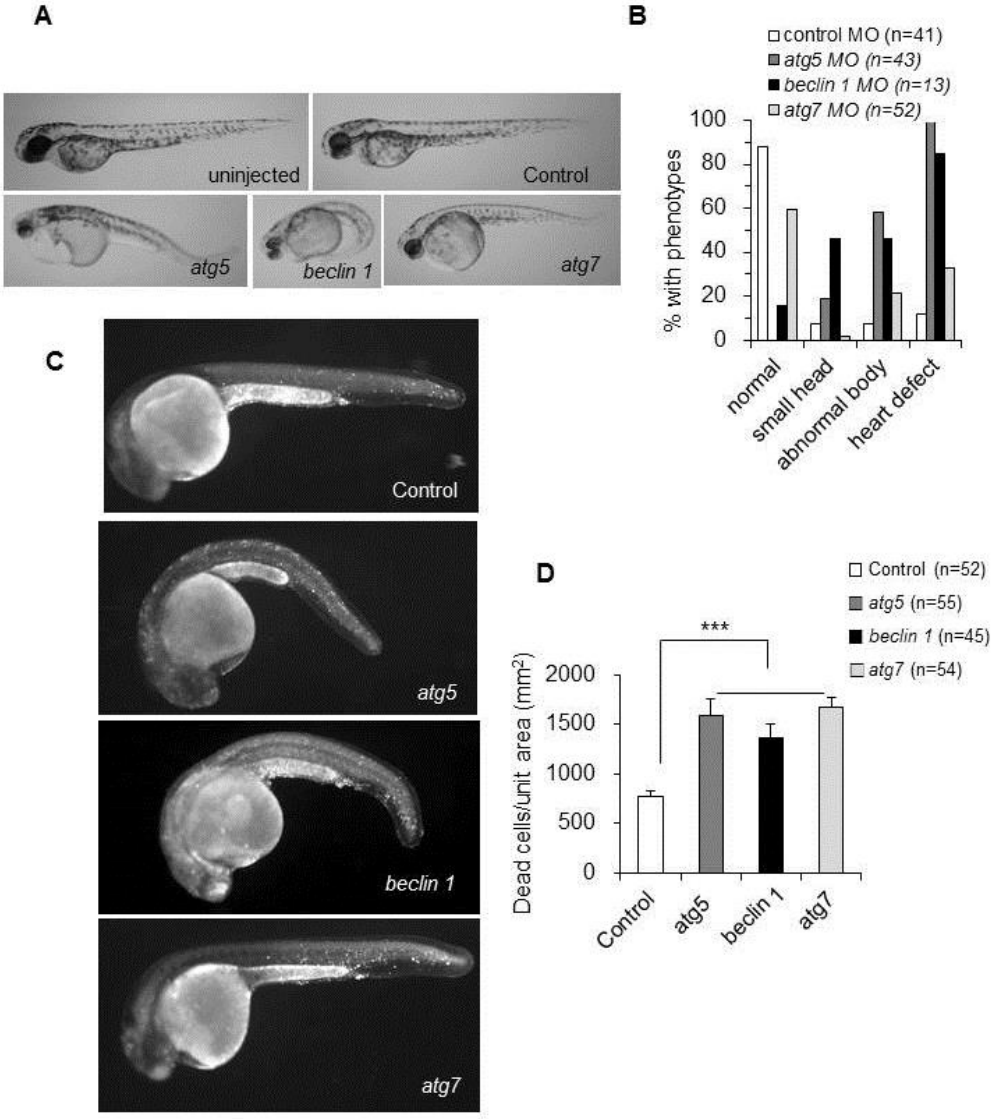

Figure 1.14. Autophagy gene knockdown results in developmental defects and increased numbers of dead cells in a p53 mutant background.

(A and **B)** Morphology of autophagy morphants in *tp53*^{M214K} mutant background at 2 dpf. Autophagy morphants showed small heads, twisted body shapes and cardiac defects at 2 dpf. **(B)** Quantification of data shown in (A). More than 10 embryos in each group were analyzed. **(C** and **D)** Acridine orange (AO) staining of control and autophagy morphants in *tp53*$^{M214K/M214K}$ mutant zebrafish at 1 dpf. AO-positive cells were counted in a region spanning from the end of the yolk tube extension to the end of the tail. (**D**) Quantification of data shown in (**C**). Results represent the mean ± SEM from more than 40 embryos in each group. ***P<0.001; one-tailed t-test.

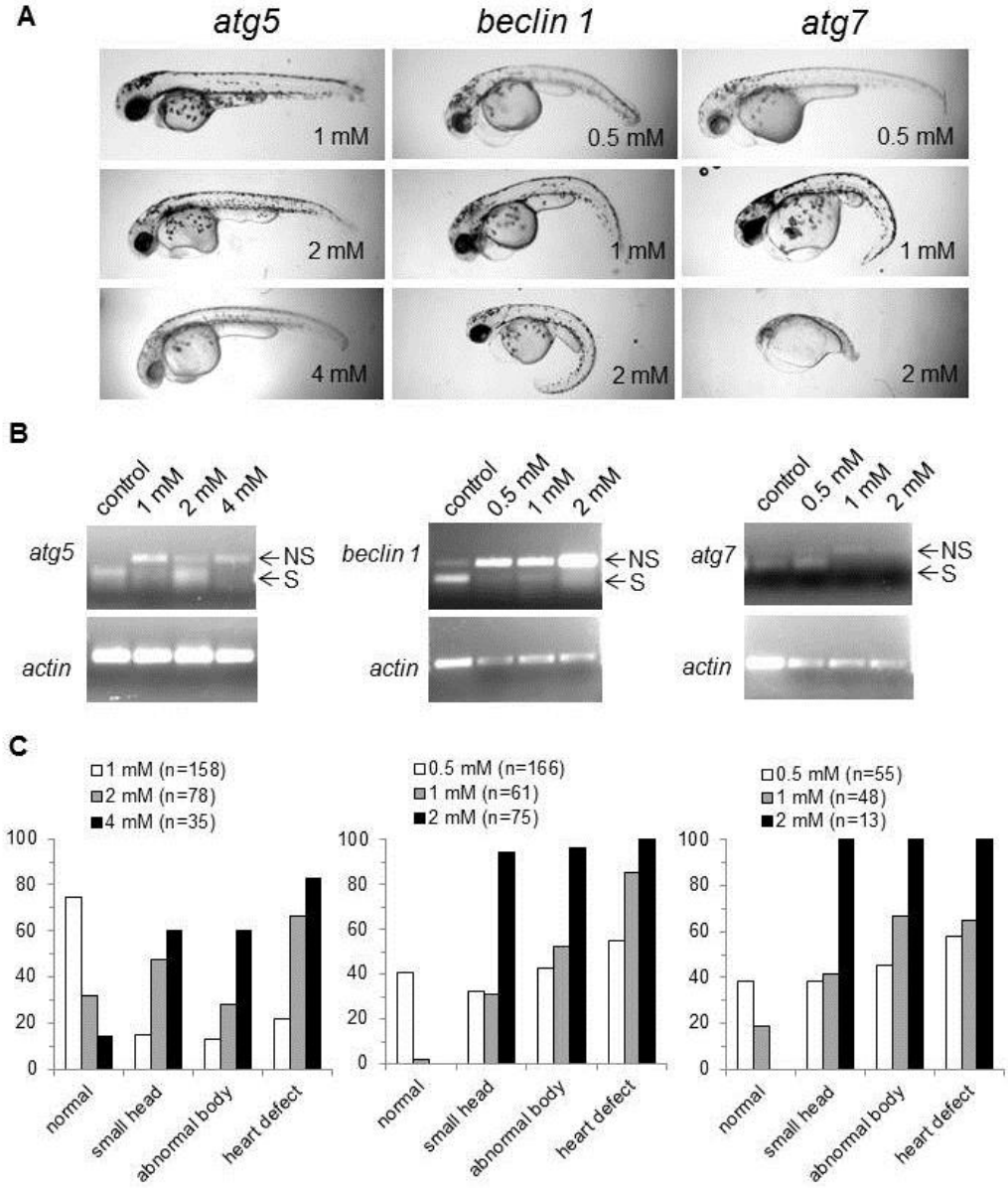

Figure 1.15. Autophagy is efficiently inhibited in a dose-dependent manner by splicing morpholinos (MOs).

(A) Morphology of autophagy morphants at 2 dpf. Embryos were injected with 3 different concentrations of each splicing MOs. Phenotypes, such as small heads, twisted body shapes and cardiac defects were dose-dependent. **(B)** Impaired splicing by splicing MO injections was confirmed by RT-PCR. RNAs were isolated from autophagy morphants at 2 dpf and PCR reactions were done using splicing site-specific primer sets. NS; not-spliced, S: spliced. **(C)** Quantification of data shown in **(A)**.

Chapter 3: *Novel role of autophagy in mouse cardiac morphogenesis*

3.3 Introduction

Autophagy is conserved from yeast to mammals [9]. An essential role for autophagy has been reported in various tissues or cells during development and differentiation, including heart, brain, neuron, liver, skeletal muscle, adipocyte, oocyte, and immune cells [13]. Mice lacking the autophagy gene *FIP200* are embryonic lethal, and have defective heart and liver development at embryonic day (E) 14.5 to E15.5 [21]. However, cardiac specific $Atg5^{-/-}$ mice develop cardiac dysfunction and left ventricular dilation only under pressure overloaded conditions during early cardiogenesis [86]. In adult cardiac tissue, temporally-controlled cardiac deletion of *Atg5* results in cardiac hypertrophy and dysfunction [86]. Thus, autophagy plays an important role in the heart but its role in cardiogenesis is still not clear.

The heart is the first organ which forms and functions during development. The heart consists of 2 layers: myocardial and endothelial layers. During mouse cardiogenesis, cardiac progenitor cells become aligned and migrate to the anterior-lateral region to form cardiac plates. The endothelial cells nearby this plate start to form linearized endocardiac tubes. At E8.0, these two tubes are combined and the developing heart starts beating. The heart starts to loop to the right by E8.5 and around E9.5 the heart forms primitive atrial and ventricular chambers [87]. The cardiac development of most organisms follows a similar pathway and autophagy is strikingly conserved in several different species. In the previous chapter, I showed that genetic knockdown of autophagy genes resulted in developmental cardiac defects in zebrafish. Next, we asked whether autophagy has also a role in mammalian cardiac development.

Here, we found that autophagy is active during cardiac development in mice. Cardiac tissue at E9.5 showed active autophagy as evidenced by GFP-LC3 puncta formation. Impaired autophagy by knockout of *Atg5*, led to altered expression of the cardiac patterning gene, *Tbx2*, improper AVC development shown by *Wnt4* expression and a ventricular septal defect (VSD) consistent with our finding in autophagy-deficient zebrafish.

3.2 Methodology

Mouse strain and maintainence

Autophagy reporter mice *GFP-LC3* and *Atg5* knockout mice have been previously described [22]. *Atg5*$^{-/-}$ mice were generated by obtaining offspring of *Atg5*$^{+/-}$ crosses. After harvesting the postnatal pups, tails were collected and lysed in DirectPCR Lysis Reagent(Tail) (Viagen Biotech, Cat#101-T) for genotyping. After heat inactivation at 85˚C for 45 mins, 1µl of lysate was used for PCR reactions. Primers for PCR reactions were as following:

Primers for mouse genotyping	
Exon	5’-GAATATGAAGGCACACCCCTGAAATG-3’
Check	5’-ACAACGTCGAGCACAGCTGCGCAAGG-3’
Short	5’-GTACTGCATAATGGTTTAACTCTTGC-3’

All animal protocols were approved by the UT Southwestern medical Center Institutional Animal Care and Use Committee.

Fluorescence microscopy

To measure autophagy in early embryonic mouse heart development, autophagy reporter GFP-LC3 mice were used. Embryos were prepared at E9.5 by perfusion with 4% PFA in PBS. Embryos were fixed in 4% PFA for 3 hours, 15% sucrose for 4 hours, and then 30% sucrose overnight. Frozen tissue sections were used for fluorescence microscopic analysis. Autophagosomes were visualized with Zeiss Axioplan2 microscope using Zeiss PLAN-APOCHROMAT 4x and 63x objective.

Histological analysis

Postnatal pups of *Atg5*$^{+/-}$ crosses were sacrificed and the heart was dissected, fixed in 4% PFA and dehydrated. Transverse sections were stained with H&E for tissue morphology.

Mouse in situ hybridization

Whole mount *in situ* hybridizations were performed using standard protocols on embryos at E9.5 and E10.5 to detect *Tbx2* and *Wnt4*. Riboprobes for *Tbx2* and *Wnt4* have been described previously [88].

3.3 Results

Autophagy is active during early embryonic cardiac development in mouse

Autophagy is induced by fertilization and detected as early as the 2 cell stage-embryo in mouse [14]. It has been known that autophagy is active in almost all organs during mammalian development [54]. In zebrafish, we detected active autophagy during cardiac development. To investigate whether autophagy is also active during embryonic cardiac development in mouse, autophagy reporter GFP-LC3 mice were used to monitor for GFP-LC3 puncta formation. At

E9.5, GFP-labeled autophagosomes were found in cardio myocytes and the atrioventricular canal, indicating that autophagy occurs during cardiac development in mice as well as in zebrafish (Figure 2.1).

Atg5 knockout mice exhibit cardiac defects

In zebrafish, autophagy knockdown induced developmental cardiac defects. We next asked if this role of autophagy is conserved in mammals, especially given the striking conservation of the autophagy pathway and its functions across diverse species [3]. To investigate whether autophagy plays a role in mammalian cardiac development, we examined postnatal day 0 (P0) *Atg5*-deficient mice. *Atg5*$^{-/-}$ mice have previously been shown to die within several hours of birth, due to defective nutrient and energy homeostasis [22]. *Atg5*$^{-/-}$ mice derived from crosses of *Atg5*$^{+/-}$ heterozygotes were significantly smaller than *Atg5*$^{+/+}$ or *Atg5*$^{+/-}$ mice at P0 (Figure 2.2A, B). *Atg5*$^{-/-}$ pups frequently had small heads and morphologically abnormal eyes, reminiscent of the defects seen in autophagy morphant zebrafish. Upon macroscopic analysis of P0 hearts, we noted enlarged right atria (relative to the size of total heart mass) in all *Atg5*$^{-/-}$ mice examined (Figure 2.2A, middle). Upon histologic analysis, 4 out of 9 *Atg5*$^{-/-}$ mice were found to have AV canal defects including abnormal valve morphology and a membranous ventricular septal defect (VSD) at P0 (Figure 2.2A, C). *Atg5*$^{+/+}$ mice or *Atg5*$^{+/-}$ mice did not show the same cardiac developmental abnormalities (n=11 in each group), although 1 out of 11 in each of the *Atg5*$^{+/+}$ and *Atg5*$^{+/-}$ groups exhibited a small muscular VSD.

Atg5 knockout mice exhibit an altered cardiac gene expression pattern in the developing heart

To determine whether impairment of autophagy in the murine heart leads to similar gene expression abnormalities as those we observed in the zebrafish autophagy morphants, we

isolated E9.5 embryos from crosses of *Atg5*$^{+/-}$ heterozygotes and performed *in situ* hybridization for *Tbx2* (Figure 2.3). At this stage, *Tbx2* expression is normally restricted to the myocardium of the AVC, the inner curvature and the outflow tract [89, 90]. Consistent with the results in zebrafish, 2 out of 4 *Atg5*$^{-/-}$ mice displayed increased *Tbx2* expression and the other 2 out of 4 showed ectopic *Tbx2* expression, These abnormal expression patterns were not observed in *Atg5*$^{+/+}$ littermates. These results indicate that the requirement of autophagy for developmental cardiac patterning is strongly conserved from fish to mammals.

Atg5 knockout mice show improper AVC development.

Autophagy occurs during mouse cardiac development, as evidenced by GFP-LC3 puncta at E9.5. As shown in postnatal pups, *Atg5*$^{-/-}$ embryos at E10.5 had smaller body and heart sizes compared to *Atg5*$^{+/-}$ embryos (Figure 2.4A). Analysis of *Tbx2* expression at E9.5 was performed to gain further insight into the cardiac defects shown at P0. To follow up on the aberrant expression of the cardiac patterning gene *Tbx2* and cardiac defects, VSD, we performed *in situ* hybridization for *Wnt4*,which labels endothelial cells in AVC at E10.5. *Atg5*$^{-/-}$ embryos showed decreased *Wnt4* expression compared to that of *Wnt4* in endothelial cells in the AVC of *Atg5*$^{+/-}$ embryo (Figure 2.4). This result indicated that *Atg5*$^{-/-}$ mice have defects in AV cushion formation, possibly due to either decreased numbers of endothelial cells in the AV cushion or reduced *Wnt4* expression (Figure 2.4).

3.4 **Discussion**

Here, I demonstrated that autophagy is essential in mouse cardiac morphogenesis, similar to our findings in zebrafish. Autophagy-deficient zebrafish embryos showed abnormal cardiac morphogenesis, including mislooping of chambers and mispatterning of gene expressions

involved in AVC development, indicating an essential role for autophagy in cardiac development. To understand whether these findings are specific to zebrafish or represent a more generally conserved role of autophagy in cardiac development, we carefully examined the phenotype of *Atg5*-deficient mice. We found that mice deficient in *Atg5* exhibit developmental defects of the AV canal and membranous VSDs. We also observed aberrant expression of the cardiac patterning gene *Tbx2* and *Wnt4* in autophagy-deficient *Atg5*$^{-/-}$ mice during AV cushion formation. These observations strongly resemble the cardiac phenotype of autophagy-deficient zebrafish, indicating that the essential role of autophagy genes in developmental morphogenic patterning is conserved throughout vertebrate evolution.

In the mouse, autophagy is detected as early as the fertilized oocyte-stage which undergoes massive morphological changes [14]. Genetically manipulated mouse models for key autophagy components suggested an important role for autophagy in mouse morphogenesis, including gene trap of *AMBRA1*, systemic knockout of *FIP200*, and hematopoietic-specific knockout of *Atg7* [20, 21, 30]. *Atg5* knockout mice have been described as histologically almost normal at birth, but die quickly cause of defective nutrient and energy homeostasis [22]. In our studies, postnatal *Atg5*$^{-/-}$ mice showed cardiac defects, in addition to smaller body and heart sizes than *Atg5*$^{+/+}$ or *Atg5*$^{+/-}$ mice. The different phenotypes of *Atg5*$^{-/-}$ mice could be explained by the dependency of phenotype penetrance on mouse genetic background [34]. Even though this mouse has systemic knockout of *Atg5*, the cardiac abnormal phenotype was not present in 100% of the mice, suggesting possible compensation mechanisms to overcome the loss of *Atg5*. Furthermore, at earlier stages of development which have active autophagy, *Atg5*$^{-/-}$embryos displayed abnormal expression of *Tbx2* and *Wnt4* in the AV cushion. It appears that impaired autophagy leads to

defects in the transcriptional patterning and morphogenesis of the AVC, and this is conserved across vertebrates.

The Wnt signaling pathway is one of the important pathways in AVC development [91]. Using mouse embryonic fibroblasts (MEFs) derived from *Atg5* knockout mice, Gao *et al*. showed negative regulation of Wnt signaling by autophagy [74]. In our zebrafish studies, inhibition of autophagy by MO injections induced altered regulation of Wnt signaling; however, it was not clear whether the alteration was directly caused by impaired autophagy. *In situ* hybridization to detect *Wnt4* showed reduced expression *in* $Atg5^{-/-}$embryos compared to $Atg5^{+/-}$ embryos. Wnt4 is one of the ligands for Wnt signaling but not a main one in cardiac development, so it is difficult to conclude that the regulation of Wnt signaling is by autophagy in this context or that differences in Wnt signaling explain the cardiac development defects in $Atg5^{-/-}$ mice. Future studies are needed to address this question.

Here, I demonstrated a conserved role for autophagy during cardiac development in vertebrates. Autophagy is active during cardiogenesis, and impaired autophagy deregulates cardiac patterning genes, which results in VSDs in neonatal mice. It will be interesting to determine whether there is a relationship between autophagy defects and the pathogenesis of congenital heart diseases.

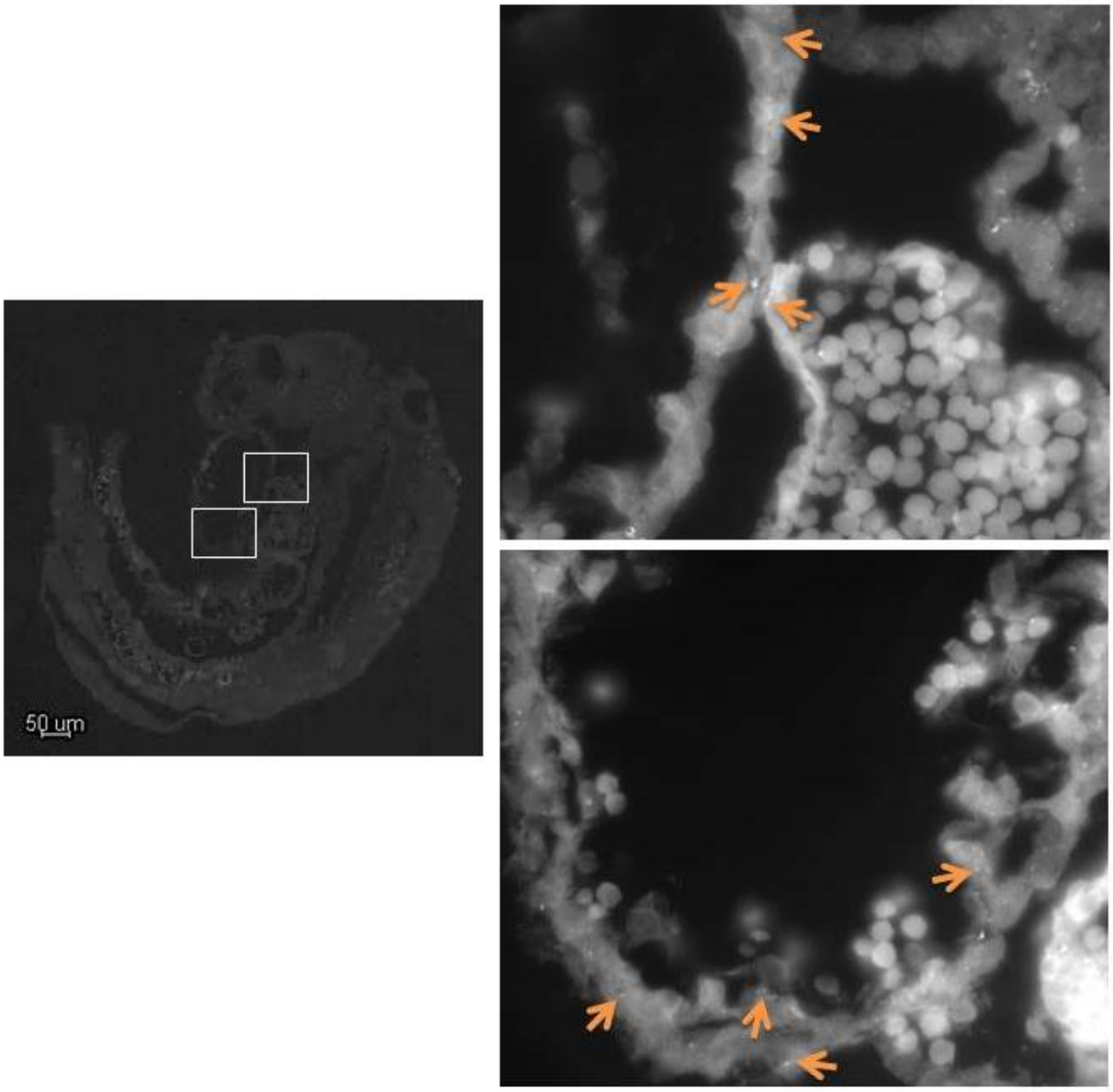

Figure 2.1. Autophagy is active during mouse cardiac development.

GFP-LC3 puncta were visualized with fluorescent microscopy. GFP-LC3 embryos at E9.5 were dissected and sectioned in a sagittal orientation. Whole animals were visualized at 4X (left) and GFP-LC3 puncta in AVC (right, top) and cardiomyocytes (right, bottom) were imaged at 63X. Arrows point to GFP-LC3 puncta.

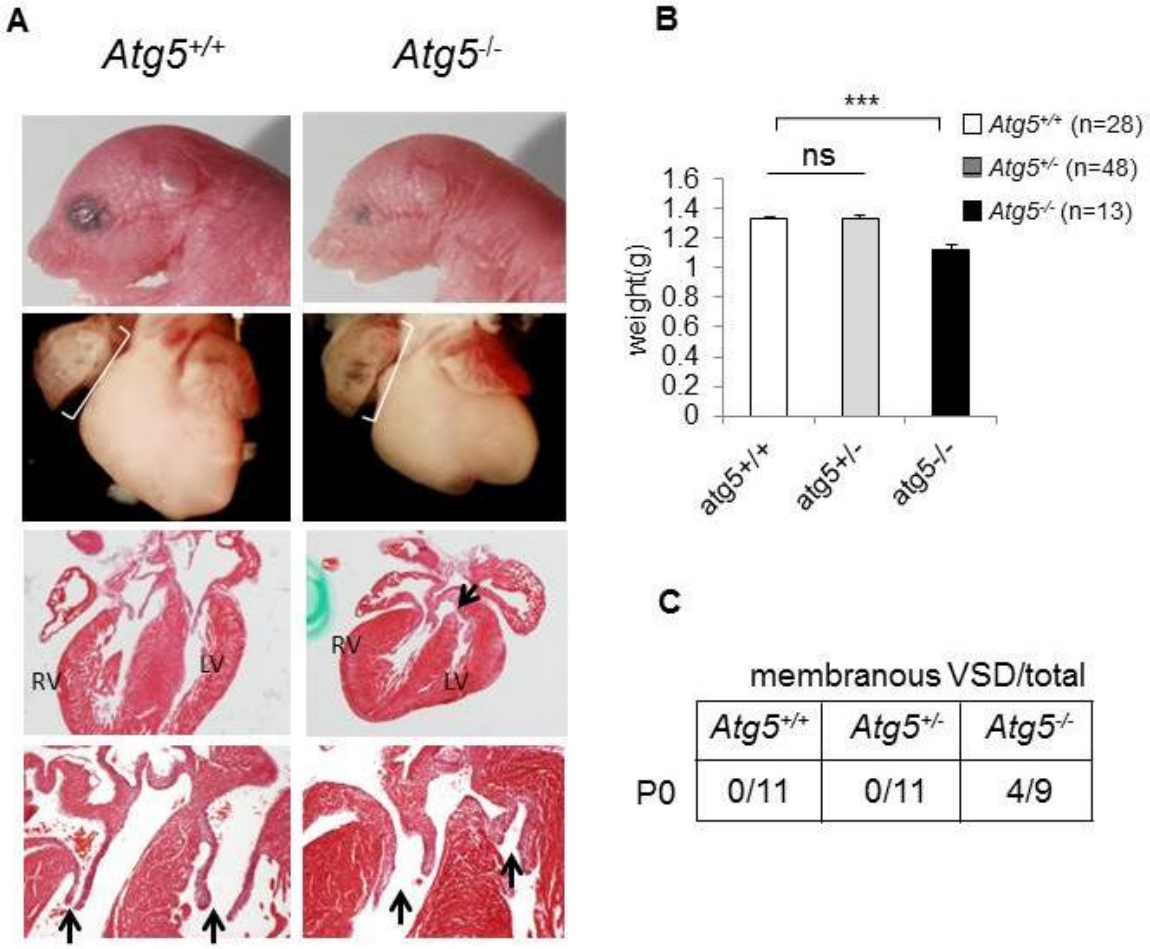

Figure 2.2. *Atg5*$^{-/-}$ mice exhibit defective cardiac development.

(A) Representative images of *Atg5*$^{-/-}$ and *Atg5*$^{+/+}$ mice (at day P0). Top row, photomicrographs of heads and eyes; second row from tops, photomicrographs of hearts; third and fourth rows, H & E sections of hearts. Arrow in third row denotes enlarged right atrium; arrow in third row denotes ventricular septal defect; arrows in the fourth row denotes AV valve thickening. **(B)** Body weights of *Atg5*$^{-/-}$, *Atg5*$^{+/-}$ and *Atg5* $^{+/+}$ mice. Results represent mean ± SEM. ****P*<0.005 for indicated comparison; one-tailed *t*-test. **(C)** Summary of prevalence of membranous ventricular septal defect (VSD) in mice of the indicated genotype at day P0.

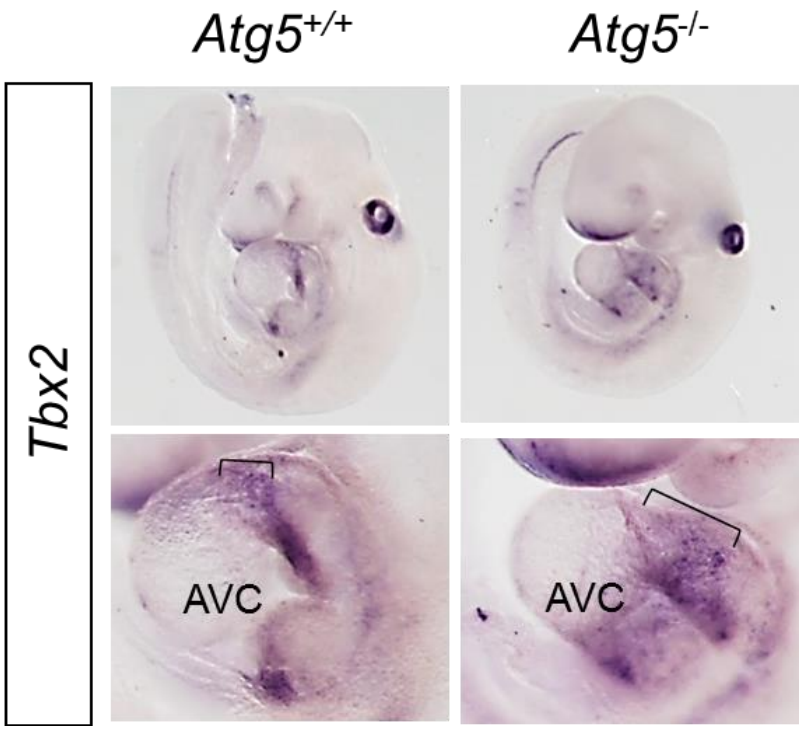

Figure 2.3. *Atg5*$^{-/-}$ mice display an altered cardiac gene expression pattern.

In situ hybridization to detect *Tbx2* expression in *Atg5*$^{-/-}$ and *Atg5*$^{+/+}$ mice (at day E9.5). Top panels, photomicrographs of *Tbx2* expression in the whole embryo; lower panels, photomicrographs of *Tbx2* expression in hearts. Arrow in lower panel denotes expanded *Tbx2* expression in the atrioventricular cushion (AVC). Results shown are representative of results from at least 4 embryos per genotype.

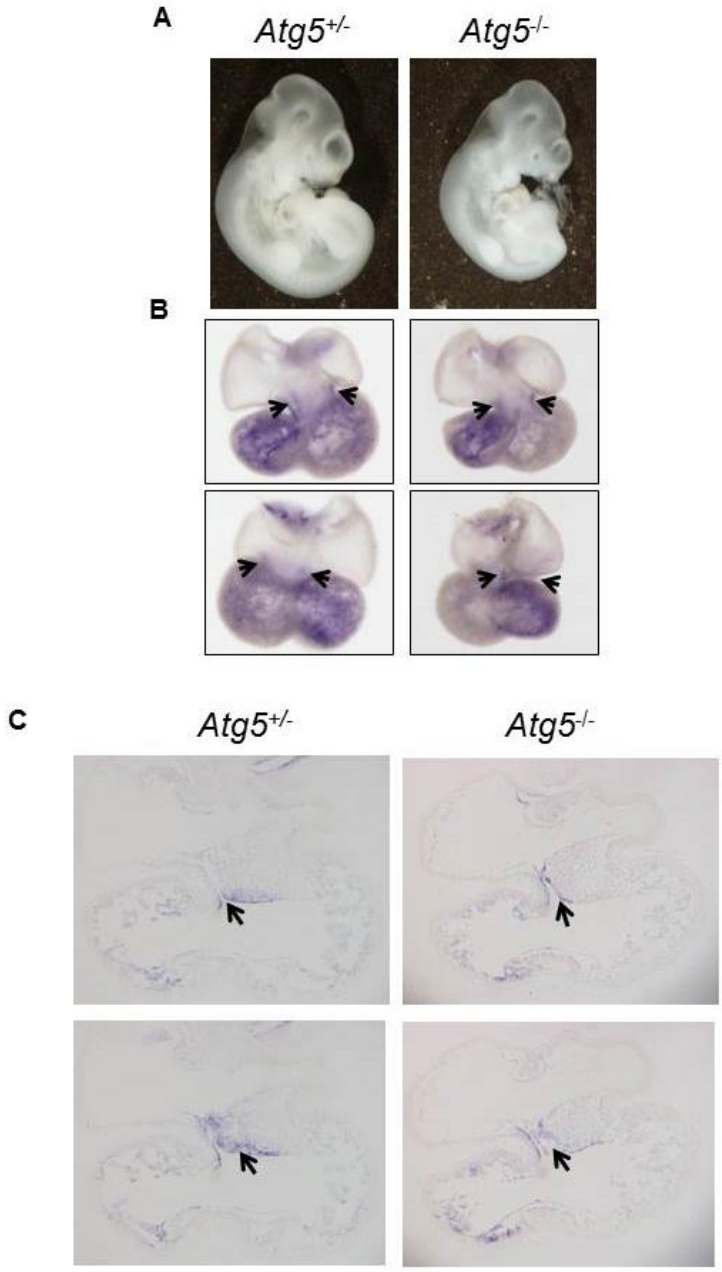

Figure 2.4. *Atg5*$^{-/-}$ mice show improper atrioventricular cushion (AVC) development.

In situ hybridization to examine AVC development in *Atg5*$^{-/-}$ and *Atg5*$^{+/+}$ mice using a *Wnt4* probe as a marker (at day E10.5). **(A)** Representative images of *Atg5*$^{-/-}$ and *Atg5*$^{+/+}$ mice (at E10.5). **(B)** *Wnt4* expression in the whole heart. Arrow denotes AVC. **(C)** *Wnt4* expression in sections of hearts. Arrow denotes diminished *Wnt4* expression in atrioventricular cushion (AVC).

Chapter 4: *The role of autophagy in tumor suppression*

4.1 Introduction

Autophagy has been suggested to be involved in tumor suppression based upon studies in several knockout models. *Atg4C* knockout mice have increased chemically-induced fibrosarcomas [36] and *Bif-1* deletion in mice results in an increased frequency of spontaneous lymphomas and solid tumors [38]. *Beclin 1* is frequently monoallelically deleted in human breast and ovarian cancers, and *beclin 1* heterozygous-deficient mice have an increased frequency of spontaneous malignancies [19]. Mice with mosaic deletion of *Atg5* and liver specific deletion of *atg7* develop benign liver adenomas [37]. Several hypotheses have been proposed to explain how autophagy functions as a tumor suppressor pathway including promoting genomic stabilities and reducing tumorigenic inflammation [34].

Zebrafish is well-established as an important model for development, and recently has also become a popular model for the study of cancer. Zebrafish develop many kinds of tumors that share similar morphology and comparable pathways with those in humans [49]. However, there are also several differences with respect to mammalian tumorigenesis including a low tumor incidence compared to the mouse models and a different tumor spectrum [51]. For example, zebrafish homozygous mutant $tp53^{M214K}$ fish develop malignant peripheral nerve sheath tumors at a prevalence at about 28% by 16-months of age [52]. However, 74% of homozygous *p53* knockout mice develop sarcomas and lymphomas before 6 months of age [53]. Although there are several differences between human and zebrafish tumorigenesis, there are also several advantages of using a zebrafish model system for the study of cancer including its suitability for genetic and chemical screening, and suitability for *in vivo* tumor progression imaging [51].

Taking advantage of zebrafish as a model system for studying tumorigenesis, I generated transgenic fish lines which express dominant-negative autophagy proteins. Recently, techniques have become available to target specific genes in zebrafish by the use of TALENs, but previously, gene targeting was not well-established in zebrafish. To inhibit autophagy in zebrafish, I used two different dominant-negative autophagy proteins, dnAtg5 and dnAtg4b. The K130R mutation in Atg5 protein inhibits the binding of Atg5 to Atg12 and inhibits autophagy [92]. The mutation of cysteine 74 to alanine in Atg4b blocks proteolytic cleavage of LC3 and blocks the formation of the Atg7-LC3 intermediate and leads to inhibition of autophagy [93].

To study the role of autophagy in tumor suppression, I utilized several techniques that are already established in the zebrafish field. The microphthalmia-associated transcription factor a (*mitfa)* promoter is expressed in the developing neural crest and in melanocytes [94], and a previous study showed that transgenic expression of mutant BRAF kinase under the control of *mitfa* promoter leads to melanoma in p53-mutant fish [95]. Therefore I reasoned that tissue-specific inhibition of autophagy under control of the *mitfa* promoter might cause the development of tumors. For *in vivo* imaging, I employed the viral 2A system to label cells that express the dominant-negative autophagy proteins, since fusion with other proteins could affect the dominant-negative activity [96]. In the 2A system, insertion of a peptide linker sequence derived from a picornavirus sequence between two proteins causes ribosome skipping, and the translation of two separate proteins [96].

To generate transgenic fish lines that stably express dominant-negative autophagy proteins, I used a transposon-based technique. Transposons are DNA-based repetitive sequences that move from one locus in the genome to another in a reaction catalyzed by a transposase [97]. In

zebrafish, the *Tol2* transposase system has been used for both somatic and germline transgenesis. To make dominant-negative autophagy transgenics, each expression construct was generated using the *Tol2* system and injected into cells of one cell-stage embryos.

By using these techniques, transgenic lines expressing dominant-negative autophagy proteins were generated. Stable transgenic fish expressing dnAtg5 as well as expression construct-injected fish displayed altered pigmentation and increased tumor incidence. The tumors that developed in transgenic fish expressing dnAtg5 in a p53 heterozygous mutant background were identified mostly as MPNSTs, which are also observed in p53 homozygous mutant fish. Furthermore, expression of dnAtg5 accelerates loss-of-heterozygosity (LOH) of p53 in a $p53^{M214K/+}$ background, which may result in accelerated tumor development and an increased incidence of tumors.

4.2 Methodology

Zebrafish strains and maintenance

Fish were raised and maintained under standard conditions [56]. Embryos from the wild type AB strain were used for injection to generate transgenic fish lines. Generated transgenic fish lines *Tg(mitfa:dnatg5)* and *Tg(mitfa:mcerry-dnatg4B)* were out-crossed with wild type AB, the autophagy reporter line *Tg(cmv:GFP-LC3)*, or the zebrafish *p53* mutant line $tp53^{M214K}$ and maintained. All animal protocols were approved by the UT Southwestern Medical Center Institutional Animal Care and Use Committee.

Cloning of expression constructs for transgenic line generation

Tol2 transposon-based transgenesis constructs were used to generate transgenic zebrafish lines (Invitrogen) [98].

Clones for transgenic line generation			
Transgenic line	*Tg(mitfa:dnatg5)*	*Tg(mitfa:GFP2A-dnatg5)*	*Tg(mitfa:mcherry-dnatg4b)*
5'-Entry	p5E-*mitfa*	p5E-*mitfa*	p5E-*mitfa*
Middle Entry	pDONR221	pME-GFP	pME-mcherry no stop
3'-Entry	p3E-polyA	pDONRP4-P1R	pDONRP4-P1R
Destination vector	pDESTtol2pA2		

To construct dominant-negative forms of zebrafish *atg4b* and *atg5,* zebrafish cDNA was prepared from 24 hpf embryos. Amplified *atg5* and *atg4b* cDNAs were cloned into the pGEM-T vector (Promega) and mutated using the Quick Change XL Site-Directed mutagenesis kit (Stratagene). After verifying the sequences of mutated *atg5*^{K130R} and *atg4b*^{C74A} clone, *att* sites for BP reactions were added to the ends of the *atg5*^{K130R} and *atg4b*^{C74A} DNA fragments by Phusion High-Fidelity DNA polymerase (NEB). The DNA fragments of the *atg5*^{K130R} and *atg4b*^{C74A} with *att* sites were purified by QIAquick Gel Extraction kit (Qiagen), and used for BP and LR reactions as specified in the Gateway manual to generate the final *Tol2* expression constructs. Final expression constructs were verified for their sequences before use. Primers used for mutagenesis and *Tol*2 cloning were as follows:

Primers for amplification of cDNAs	
Atg5 F	5'-ATGGCAGATGACAAGGATGTG -3'
Atg5 R	5'-TCAGTCACTCGGTGCAGGGAT -3'

Atg4b F	5’-ATGGATGCAGCTACTCTCACATACG -3’
Atg4b R	5’- TCACAAAGACAGGATTTCAAATTCTTCATCC-3’
Primers for site-directed mutagenesis	
Atg5^{K130R} F	5’- AGCACATTTCATGTCTTGCATTAGAGAGGCCGATGC-3’
Atg5^{K130R} R	5’-GCATCGGCCTCTCTAATGCAAGACATGAAATGTGCT-3’
Atg4b^{C74A} F	5’-ACTTCAGACACCGGCTGGGGCGCAATGCTTCGATGC-3’
Atg4b^{C74A} R	5’-GCATCGAAGCATTGCGCCCCAGCCGGTGTCTGAAGT-3’
Primers with *att* sites	
attB1-dnatg5 F	5’-GGGGACAAGTTTGTACAAAAAAGCAGGCTCCACCATGGCAGATGACAAGGATGTG -3’
dnatg5-attB2 R	5’-GGGGACCACTTTGTACAAGAAAGCTGGGTTTCAGTCACTCGGTGCAGG -3’
attB2-dnatg5 F	5’-GGGGACAGCTTTCTTGTACAAAGTGGAAATGGCAGATGACAAGGATGTG-3’
dnatg5-attB3 R	5’-GGGGACAACTTTGTATAATAAAGTTGATCAGTCACTCGGTGCAGG-3’
attB2-dnatg4b F	5’-GGGGACAGCTTTCTTGTACAAAGTGGAAATGGATGCAGCTACTCTCACATAC -3’
dnatg4b-attB3 R	5’-GGGGACAACTTTGTATAATAAAGTTGATCACAAAGACAGGATTTCAAATTC-3’

mRNA in vitro transcription assay and purification

The pCS2FA-transposase clone was used as a template for transposase mRNA synthesis. pCS2FA-transposase was linearized by NotI and purified with the Qiagen PCR Purification kit

(Qiagen). Using 2 µg of linearized DNA, transposase mRNA was synthesized using mMessage mMachine SP6 kit (Ambion). Synthesized transposase RNA was purified by lithium Chloride precipitation and quantified using spectrophotometrically (Nanodrop).

Transgenic fish generation, screening and genotyping

Expression constructs (50-100 ng/µL) with transposase mRNA(100 ng/µL) were injected into one cell stage-embryos. Injected embryos were raised to adulthood and in-crossed for transgenic screening. Pools of embryos were screened for transgene incorporation by PCR reactions. Once the embryos showed transgene incorporation, the parents of embryos were out-crossed for further germline founder screening.

The progeny of transgene founders were screened for transgenes by PCR. Fish were anesthetized with 0.2% Triacaine solution and clipped tails were lysed using Direct PCR Lysis Buffer (tail) (Viagen Biotech, Cat#101-T). After heat inactivation for 45 min at 85˚C, crude lysates containing genomic DNA were used for PCR analyses. Two different primer sets for each transgene were used to confirm their genotypes. Transgenic fish lines *Tg(mitfa: dnatg5)* and *Tg(mitfa:mcerry-dnatg4B)* out-crossed with the autophagy reporter line *Tg(cmv:GFP-LC3)* were further confirmed for GFP expression. Transgenic fish lines *Tg(mitfa:dnatg5)* and *Tg(mitfa:mcerry-dnatg4B)* out-crossed with zebrafish *p53* mutant line $tp53^{M214K}$ were also confirmed for their p53 status by sequence analysis. The primer sets used for genotyping are as follows:

Primers for genotyping	
mitfa F	5’- GGCCCATCAGACAACAAAGT -3’

atg5 F	5’- ATGGCAGATGACAAGGATGTG -3’
atg5 R	5’- TCAGTCACTCGGTGCAGGGAT -3’
atg5 377F	5’-GTCTTGCATTAGAGAGGcCG-3’
atg5 738R	5’-CTCTAGCAGGGGTTCAATGC-3’
atg4b F	5’- ATGGATGCAGCTACTCTCACATACG -3’
atg4b R	5’- TCACAAAGACAGGATTTCAAATTCTTCATCC -3’
Sc atg4b F	5’- AGCCTCGAGAGATGAATGGA -3’
Sc atg4b R	5’- GCAGCAATAGAAGGGTCGAG -3’
mcherry F	5’- CCTGTCCCCTCAGTTCATGT -3’
mcherry R	5’- TCTTGGCCTTGTAGGTGGTC -3’
GFP F	5’- CAACTACAACAGCCACAACGTC-3’
GFP R	5’- TCGTCCATGCCGAGAGTGATC -3’
P53 seq F	5’- GAGCAGCATCATGAAGCATC -3’
P53seq R	5’- GTGTCTGTCCATCTGTTTAACAG -3’
microsatellite F	5’- AGCAACCATATGCCCACTTC -3’
microsatellite R	5’- AAACACCCTTTTCCATTCCC -3’

Zebrafish RNA preparation and RT-PCR

RNA was extracted from *Tg(mitfa: dnatg5)* tumor tissue or cultured primary tumor cells using Trizol reagent (Invitrogen). After adding 0.5 ml of Trizol reagent, tissues or cells were lysed with blue pestle. cDNAs were synthesized using 5 μg of purified RNAs by RT^2 HT first-strand kit (Qiagen). To detect different autophagy transcripts, PCR was performed using the following primers:

Primers for RT-PCR	
atg5 F	5’- ATGGCAGATGACAAGGATGTG -3’
atg5 R	5’- TCAGTCACTCGGTGCAGGGAT -3’
atg5 377F	5’-GTCTTGCATTAGAGAGGcCG-3’
atg5 738R	5’-CTCTAGCAGGGGTTCAATGC-3’
Sc atg4b F	5’- AGCCTCGAGAGATGAATGGA -3’
Sc atg4b R	5’- GCAGCAATAGAAGGGTCGAG -3’
mcherry F	5’- CCTGTCCCCTCAGTTCATGT -3’
mcherry R	5’- TCTTGGCCTTGTAGGTGGTC -3’
GAPDH F	5’-TGGGTGTCAACCATGAGAAA-3’
GAPDH R	5’-TCAACGGTCTTCTGTGTTGC-3’

Histological analysis

Zebrafish were euthanized with 50% Tricaine solution, fixed in 4% PFA for 48 hours and decalcified for 5 days in 0.5M EDTA [99]. Tumor sections were stained with H&E for tissue pathological diagnosis.

Primary cell culture of zebrafish MPNST

Tumors were dissected from euthanized zebrafish in 50% Tricaine solution. Tissues were washed twice in PBS containing antibiotics (Gibco), and digested for 30 min at 37˚C using dispase (Becton Dickinson). Digested tissues were washed twice in PBS, plated on a multi-chamber slide (Nunc) in LDF (Leibovitz 50%, DMEM 35%, F-12 15%) medium containing antibiotics, and incubated at 25°C. Primary cells were carefully monitored until they attached to the plate. After 3 passages, cells were harvested and used for RT-PCR.

Tumor incidence assay

Tumor incidence was monitored weekly in *Tg(mitfa: dnatg5), Tg(mitfa:dnatg5)* in $p53^{WT/M214K}$ background, *Tg(mitfa:dnatg5)* in $p53^{M214K/M214K}$ background, heterozygous $tp53^{M214K}$, homozygous $tp53^{M214K}$ and wild-type zebrafish. Fish were genotyped and followed for tumor incidence. Fish with apparent cell masses were sacrificed and stained with H&E. Tumor incidence was analyzed statistically using the Log-rank test.

Immunohistochemistry

For immunostaining, slides were deparaffinized and baked for 15 min in Trilogy reagent (Cell Marque) in a pressure cooker for antigen retrieval. Endogenous peroxidase activity was quenched by 3% H_2O_2 in water for 30 min and nonspecific binding sites were blocked in 2.5% horse serum (Impress kit, Vector) for 30 min at room temperature. Slides were incubated for 1 hour with anti-p62 antibody (Progen) at 1:250, washed with PBST 4 times and incubated with biotinylated anti-guinea pig antibody for 30 min in a wet chamber. After several washes with PBST, slides were incubated with ABC mixture (1% A in PBS-10 µl/ml, 1% B) for 30 min, developed with DAB solution, and incubated in 0.5% $CuSO_4$ in 0.15M NaCl for 5 min. Slides were counterstained with hematoxylin (Invitrogen), dehydrated, and mounted with Permount mounting media (Fisher).

4.3 Results

Expression of dominant-negative autophagy genes alters the pigmentations pattern and enhances tumor development.

To investigate the role of autophagy in tumor suppression, an established zebrafish tumor model was modified and used. During zebrafish development, Mitf is expressed in neural crest and melanocytes and has been implicated as a key regulator in pigment cell development [94]. A previous report showed that transgenic zebrafish expressing activated BRAF mutant driven by *mitfa*-tissue-restricted promoter formed fish nevi and developed melanomas in a p53-mutant background [95].

To determine the role of autophagy in tumor suppression, I expressed dominant-negative Atg5 (dnAtg5) or dominant-negative Atg4b (dnAtg4b) from the *mitfa* promoter. To inhibit autophagy in a tissue-specific manner, three different Tol2 [98] constructs were used, including GFP-2A-dnAtg5 or mCherry-dnAtg4b and dnAtg5 without the GFP-2A tag (Figure 3.1A). The embryos were injected with expression constructs and transposase mRNA, and then monitored for their phenotypes.

Altered pigmentation and tumors arising from somatic transgenesis

Two of the fish injected with *mitfa:mCherry-dnatg4b* displayed altered pigmentation around 9 months of age. I noted that they had fewer pigmented cells on stripes than age-matched wild type fish. After 1 year, pigmented cells on the stripes were barely seen, but were detected on the tail and dorsal fin. Approximately 1 year of age, one of the injected fish developed a tumor on its dorsal fin, which was diagnosed patholigically as an angiosarcoma (Figure 3.1B, C). Similarly, one of the fish injected with *mitfa:GFP-2A-dnatg5* lost its pigment around 10 months of age and another fish formed a MPNST at 21 months of age, however *mitfa:dnatg5*-injected fish did not show any abnormal phenotypes (Figure 3.1B, C). The fish bearing tumors were monitored under

fluorescent microscopy to detect the expression of GFP or mcherry, but no fluorescent signal was detected in the tumor tissue.

Stable expression of mitfa:dnatg5 alters the pigmentation pattern and results in tumors in a $tp53^{M214K/+}$ *background.*

The appearance of tumors in fish bearing somatic transgene insertions suggested that the tissue-specific inhibition of autophagy might have oncogenic effects. However, the low incidence of tumors prevented a more detailed analysis of the effects of inhibiting autophagy. To generate transgenic fish lines stably expressing dominant-negative autophagy proteins in target tissues, each injected fish was screened to identify germline founders. Injected fish were in-crossed and their eggs were screened for transgene by PCR reaction. Screenings was done with 2 primer sets that target different regions of the transgene. The offspring showing transgenes positive in both screenings were labeled as transgenic fish and their parents were out-crossed for further founder screening. Two founders were screened from *mitfa:dnatg5*-injected fish (Figure 3.2A). Since the *mitfa* promoter becomes active beginning around 24 hpf [100], 2 dpf embryos were lysed and analyzed for their transgene expression. RT-PCR products were confirmed by sequence analysis and showed the expression of the dominant-negative form of *atg5* RNA as well as endogenous *atg5* RNA (Figure 3.2B).

The progeny from founders were raised to adulthood and monitored for their phenotypes. Interestingly, a small number of fish showed altered pigmentation at 1 year of age (2 out of 27) in similar manner as shown in the fish injected with *mitfa:mcherry-dnatg4b* or *mitfa:GFP-2A-.dnatg5* (Fig3.2C). However, transgenic fish did not develop tumors.

I reasoned that inhibition of autophagy alone might be insufficient to cause tumors. Therefore I tested the effect of the transgenes in the sensitized *tp53*-mutant background. Homozygous mutant *tp53*^{M214K} fish were previously shown to have defects in the apoptotic response to γ-irradiation, as well as tumor susceptibility. The most common tumors in these fish are MPNSTs [52]. In out cohort, 55% of *tp53*$^{M214K/M214K}$ homozygotes developed MPNSTs beginning at 7 months of age (median age of onset 16.5 months); *tp53*$^{M214K/+}$ heterozygotes exhibited lower incidence (17%) and longer latency, suggesting that loss-of-heterozygosity (LOH) of the wildtype *tp53* allele is required for tumorigenesis (Fig 3.3A).

Transgenic expression of dominant-negative autophagy constructs increased tumor incidence and decreased latency in p53-deficient fish. The effect was slight in transgenic *tp53*$^{M214K/M214K}$ homozygotes (60% incidence: median age of onset 16 months). The effect of the transgene was more significant in the p53-heterozygous background; nearly 40% of transgenic *tp53*$^{M214K/+}$ heterozygotes developed tumors, with a median age of onset of 27 months. Tumors predominantly occurred in the abdominal region and were characterized by the presence of more prominent blood vessels. There are also a small number of tumors in the eyes, jaw, and gills (Figure 3.2D).

Log-rank tests were performed to analyze differences in time-to-tumor incidence among groups with or without the transgene in *tp53*$^{M214K/+}$ or *tp53*$^{M214K/M214K}$ backgrounds. The difference between *Tg(mitfa:dnatg5)* in heterozygous *tp53*^{M214K} background and heterozygous *tp53*^{M214K} fish was significant ($p<0.0001$). Expression of dnAtg5 in *tp53*$^{M214K/M214K}$ background showed a trend towards earlier and slightly higher tumor incidence than homozygous

tp53^{M214K}mutant fish, but the difference did not reach statistical significance (p=0.3277) (Fig 3.3A).

I obtained similar results from *Tg(mitfa:mcherry-dnatg4b)* fish. Transgenic fish did not show any phenotypes in a wild-type background, but developed tumors, including central PNET-like retinoblastomas, in heterozygous p53 mutant background around 15 months of age (4 tumors out of 47) (Figure 3.2 F). Expression of the transgene was confirmed by RT-PCR using tumor tissue, but the expression of mCherry was not detected (Figure 3.2E).

Tumor histology

Macroscopically, some of the tumors showed intensely pigmented regions, indicating the possibility of melanoma (figure 3.3B). Histological examination identified the tumors mostly as MPNSTs as well as smaller numbers of neuroendocrine tumors, vascular tumors, and small cell malignant tumors (Figure 3.3C; Table 1).

Autophagy is inhibited in Tg(mitfa:dnatg5)tumor tissues

Tg(mitfa:dnatg5) fish in a *tp53*$^{M214K/+}$ background showed a significantly higher tumor incidence than *tp53*$^{M214K/+}$ heterozygous mutant fish. However, both fish lines developed MPNSTs, which was somewhat surprising in *Tg(mitfa:dnatg5)*, because the *mitfa* promoter is thought to be active mainly in melanocytes [94]. To confirm the tumor incidence in *Tg(mitfa:dnatg5)* in a *tp53*$^{M214K/+}$ background is due to inhibition of autophagy, RT-PCR analysis was performed of tumor tissues. Tumor samples were digested and followed in primary cell culture for up to 3 passages to get homogeneous cells. After 3 passages, cultured cells were harvested and analyzed for the expression of *dnatg5*. PCR products were confirmed by sequence

analysis and showed the expression of *dnatg5* RNA in tumor tissue (Figure 3.4A). Furthermore, tumor tissues from *Tg(mitfa:dnatg5)* in a *tp53*$^{M214K/+}$ background and heterozygous *tp53*$^{M214K/+}$ mutant fish were stained for p62 to determine autophagy activity. Compared to tumors from heterozygous *tp53*$^{M214K/+}$ fish, tumors from *Tg(mitfa::dnatg5)* in a *tp53*$^{M214K/+}$ showed significantly increased p62 staining, indicating impaired autophagy (Figure 3.4B). Tumors with more epithelioid cells feature showed stronger p62 staining than spindle-like cells. In summary, expression of dominant-negative Atg5 driven by the *mitfa* promoter resulted in enhanced tumor formation, mostly MPNSTs, and was associated with autophagy inhibition.

Inhibition of autophagy accelerates loss-of-heterozygosity (LOH) in p53+/- background

We did not observe tumors in fish that stably express dnAtg5 in a p53 wild-type background. Most tumors observed in the other genotypes were MPNSTs. Since increased tumor incidence due to dnAtg5 expression was only detected in a p53 heterozygous mutant background, we hypothesized that expression of dnAtg5 might affect the function of p53. p53 functions as a homotetramer in cells, and the defective apoptosis phenotype of heterozygous *tp53*$^{M214K/+}$ mutant fish was found to be intermediate compared to that of the homozygous *tp53*$^{M214K/M214K}$ mutant fish [52], implying that the total cellular level of p53 protein is functionally important. We also noted that the tumor incidence in *Tg(mitfa:dnatg5)*in a *tp53*$^{M214K/+}$ background resembles that of p53 homozygous *tp53*$^{M214K/M214K}$ mutant (non-transgenic) fish, with a slightly later onset. It has been demonstrated that loss of the wild-type p53 allele occurs frequently tumors arising in p53-heterozygous mutant backgrounds [101]. To explore the mechanism by which dnAtg5 expression accelerates tumor incidence in *Tg(mitfa:dnatg5) fish*, we analyzed tumors for LOH of p53 in their tumor tissues. Pair-matched

tumor and non-tumorigenic tissue genomic DNA was prepared from the individual tumor-bearing fish, and the relevant part of the *tp53* gene was PCR-amplified and sequenced. The sequencing results showed clear LOH in both fish lines, *Tg(mitfa:dnatg5)* in a $tp53^{M214K/+}$ background and heterozygous mutant $tp53^{M214K/+}$ fish. Both of the lines showed LOH in over 70% of tumors [22/30 tumors from *Tg(mitfa:dnatg5)* in a $tp53^{M214K/+}$ background (73.3%) and 7/10 tumors in heterozygous *Tg(mitfa:dnatg5)* in a $tp53^{M214K/+}$ fish (70%)] (Figure 3.5). Given the significantly shortened latency of tumorigenesis in the *Tg(mitfa:dnatg5)*fish, these data suggested inhibition of autophagy by the expression of dnAtg5 accelerates LOH of p53. These results further suggest a possible role for autophagy in tumor suppression by regulating LOH of tumor suppressor genes.

4.4 Discussion

There is some controversy regarding the role of autophagy in tumorigenesis. Autophagy may play a role in tumor suppression, as suggested by studies involving genetic deletion of autophagy proteins. However, autophagy may also act as a survival signal in established tumors. Here, I presented two possible roles for autophagy, one regulating cell fate decision and the other regulating genomic stability during tumorigenesis.

After injection of expression constructs, small numbers of fish displayed slightly reduced pigmentation as compared to wild type fish. Even though only small numbers of fish showed this phenotype, it was reproducible through several generations of a stable transgenic fish line that expresses dnAtg5. Since mitfa has been known to be involved in cell fate decision during migration of melanocyte precursors derived from neural crest cells [102], we expected that dominant-negative autophagy genes driven by the *mitfa* promoter may be expressed in these

cells. Interestingly, this phenotype was only observed around 1 year of age, even though the activation of *mitfa* promoter starts around 24 hpf. In view of a possible role for autophagy in cell death, one possibility is that older melanocytes may be more sensitive to the loss of autophagy leading to increased cell death at older ages and diminished replacement of melanocytes. Alternately, dominant-negative autophagy gene expression may inhibit the production of melanin and result in stripes consisting of reduced numbers of pigmented cells. To address these possibilities, transgenic fish *Tg(mitfa:dnatg5)* were out-crossed with another transgenic reporter line, *Tg(sox10::GFP),* which expresses GFP in neural crest cells. These fish will be further monitored for effects on neural crest cells and their derivatives.

The other phenotype observed in transgenic fish lines that express a dominant-negative autophagy gene was the development of tumors. Fluorescent proteins were not detected in the tumor tissue of the fish injected with *mitfa:GFP-2A-dnatg5* or *mitfa:mcherry-dnatg4b* expression constructs or in stable transgenic line *Tg(mitfa:mcherry-dnatg4b).* However, *dnatg5* RNAs or mCherry RNAs were detected in tumor tissues from *Tg(mitfa:dnatg5)*and *Tg(mitfa:mcherry-dnatg4b),* as well as in embryonic lysates from *Tg(mitfa:dnatg5),* indicating that the transgenes are expressed in tumors but not at a level detectable by fluorescent microscopy. The finding that two independent transgenic lines incorporating two different dominant-negative autophagy constructs all accelerated tumorigenesis strongly argues that the effect was due to the inhibition of autophagy, and not an artifact of transposon insertion.

It is somewhat surprising that most of tumors found in *Tg(mitfa:dnatg5)* in a $tp53^{M214K/+}$ background were MPNSTs and not melanomas, given that the expression constructs are driven by the *mitfa* promoter. In vertebrates, the origin of pigment cells is neural crest cells. In

zebrafish, neural crest cells are differentiated into peripheral neurons, glia, Schwann cells and pigment cells during migration from dorsal neural tube into target tissues [103]. There is the possibility that dominant-negative autophagy proteins driven by *mitfa* promoter affect the fate decision of melanocyte precursors and as a result, that they are expressed in different types of tissue, peripheral nerve sheath tumors. Supporting this hypothesis, some of tumors displayed intensively pigmented regions. Another possibility is that the *mitfa* promoter fragment used in these studies (~5 kb of genomic DNA) does not perfectly recapitulate the activity of the endogenous *mitfa* locus, leading to ectopic transgene expression in peripheral nerve tissues. Alternatively, inhibiting autophagy in another neural-crest derived tissue, such as mast cells, may accelerate MPNST formation in a non cell-autonomous fashion. A relationship between mast cell haploinsufficiency for *Nf1* and the incidence of MPNSTs has previously been shown in a mouse model of *Nf1* deficiency [104]. Further studies will be required to distinguish these possibilities.

MPNST is the most common type of tumor that develops in zebrafish cancer models, including those harboring mutations in p53, ribosomal proteins or mismatch repair proteins, and mutations causing genomic instability [79, 105-107]. These mutant lines share the common characteristic of genomic instability. In this regard, it is particularly interesting that inhibition of autophagy has also been reported to cause genomic instabilities [6]. Thus the mechanism of accelerated MPNST development in fish with impaired autophagy may well be increased genomic instability.

The transgenic fish line *Tg(mitfa:dnatg5)* was prone to develop tumors in either homozygous or heterozygous *tp53* ^{M214K} mutant backgrounds. Expression of dnAtg5 significantly

increased tumor incidence in a *tp53*$^{M214K/+}$ background, compared to the control heterozygous *tp53*$^{M214K/+}$ mutant line. Berghmans *et al.* reported tumor incidence only in homozygous mutant *tp53* ^{M214K} fish [52], whereas in our studies, *p53* heterozygous mutant fish also developed MPNSTs after 16 months of age. The inconsistency in tumor phenotypes may due to the late onset of tumors in the heterozygous mutant fish line, arising after 16 months of age, beyond the age range reported by Berghmans *et al.* The study of Li-Fraumeni syndrome (LFS) and Knudson's 'two-hit hypothesis' suggested that biallelic mutation of p53 is necessary for tumor suppression and tumor development [108]. To address this hypothesis in fish, each tumor bearing-fish was analyzed for its p53 status. Strikingly, more than 70% of tumors showed LOH both in the *Tg(mitfa:dnatg5)* heterozygous *tp53* ^{M214K} mutant background or heterozygous *tp53* $^{M214K/+}$ mutant line, suggesting LOH may be an important cause of tumors in a *tp53*$^{M214K/+}$ background. In zebrafish cancer models, LOH has not been reported except in one *p53*^{I166T} mutant fish line [109]. Here, I showed that expression of dnAtg5 did not increase the frequency of LOH but clearly accelerated LOH of p53 in a *tp53*$^{M214K/+}$ background and led to enhanced tumor development. The precise mechanisms are not yet clear, but may relate to genomic instability caused by impaired autophagy.

In this study, I generated a transgenic fish line which expressed a dominant-negative autophagy protein to determine the role of autophagy in oncogenesis. I found that expression of dnAtg5 altered pigment pattern in stripes and significantly increased tumor incidence in a *tp53*$^{M214K/+}$ background likely by increasing LOH at the p53 locus. Further mechanisms should be investigated regarding how LOH is regulated and how dnAtg5 may trigger genomic instability. Transgenic models that can accelerate p53 LOH would provide unique opportunities for the study of tumorigenesis and for genetic and chemical modifier screens.

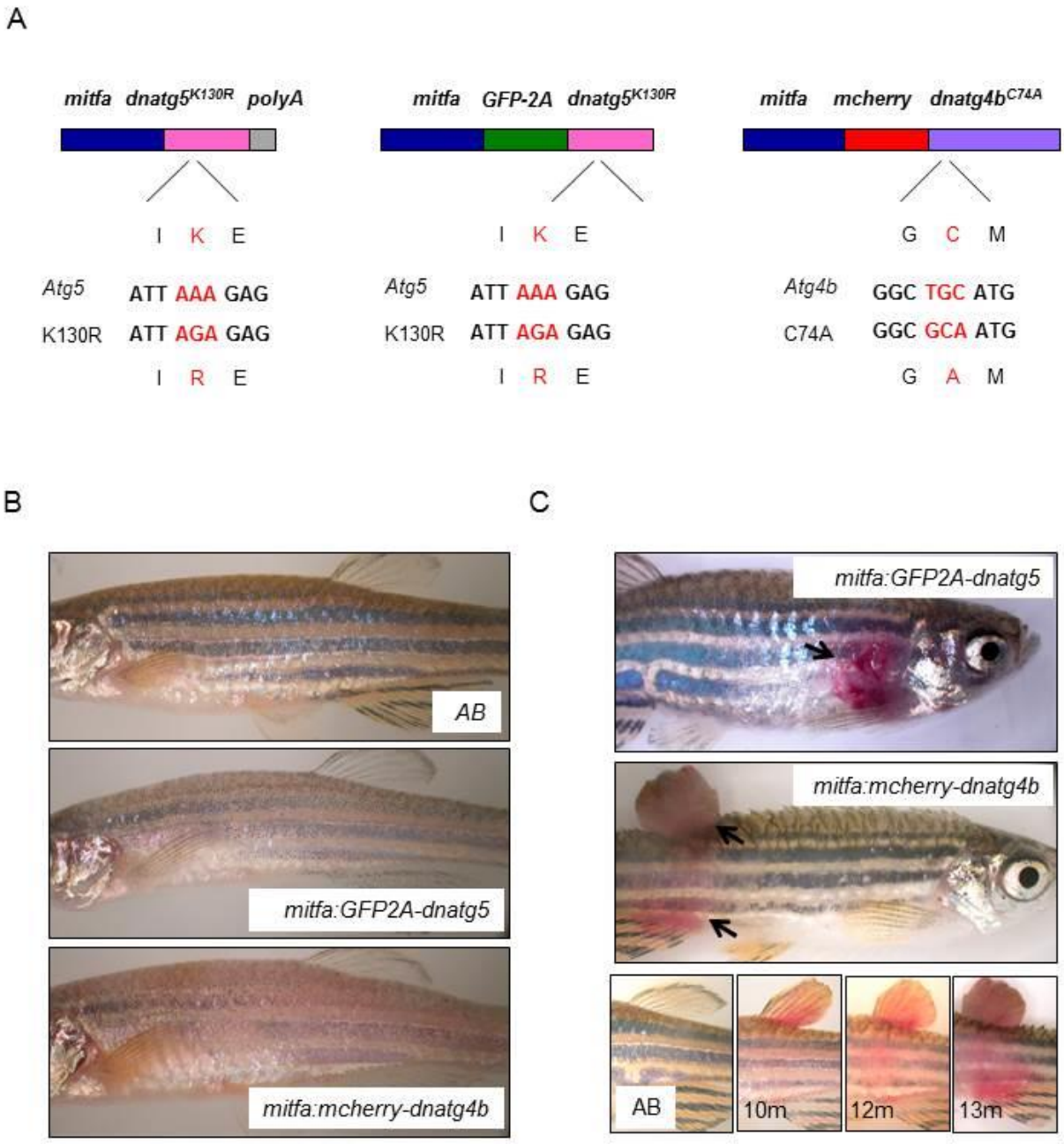

Figure 3.1. Expression of dominant-negative autophagy proteins induces altered pigmentation and tumor development.

(A) Expression construct used for generation of transgenic fish. **(B)** Altered pigmentation in the fish injected with *mitfa:GFA2A-dnatg5* or *mitfa:mcherry-dnatg4b* at 10-month old. **(C)** Fish injected with *mitfa:GFA2A-dnatg5* or *mitfa:mcherry-dnatg4b* developed tumor, *mitfa:GFA2A-dnatg5* at 21-months of age; *mitfa:mcherry*-dnatg4b at 10-months of age. Arrow points to tumor area.

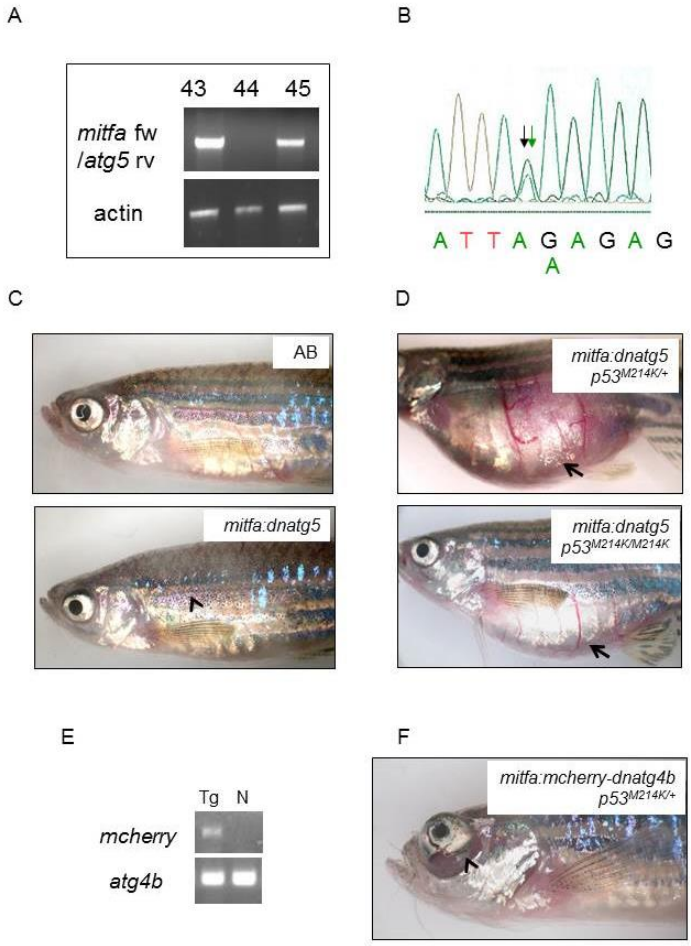

Figure 3.2. *Tg(mitfa:dnatg5)* fish display altered pigmentation and develop tumors in a p53-mutant background.

(A) Germ-line transmission of transgene *mitfa:dnatg5*. Genomic DNA from progeny of injected fish was used for founder screening. PCR reactions were performed for two different regions of the target gene. Two founder fish were identified (43 and 45). **(B)** Expression of the transgene was confirmed by RT-PCR. PCR reactions were performed using RNA from 48-hpf old embryos and PCR products were validated by sequence analysis. **(C)** *Tg(mitfa:dnatg5)* exhibited an example of altered pigmentation at 12-month of age. Arrow points to altered pigmentation. **(D)** *Tg(mitfa:dnatg5)* in p53-mutant background with a tumor. Most of the tumors arose on the abdomen. *Tg(mitfa::dnatg5)* were out-crossed with p53 mutant fish $tp53^{M214K/M214K}$ to introduce a tumor-prone mutant background. **(E)** Expression of transgene was confirmed by RT-PCR. PCR reactions were performed using tumor tissue from *Tg(mitfa:mcherry-dnatg4b)* or *p53 mutant fish* $tp53^{M214K/+}$. Tg, *Tg(mitfa:mcherry-dnatg4b)*; N, *p53 mutant fish* $tp53^{M214K/+}$. **(F)** *Tg(mitfa:mcherry-dnatg4b)* in p53 mutant background develop tumor, retinoblastoma. Arrow points to tumor.

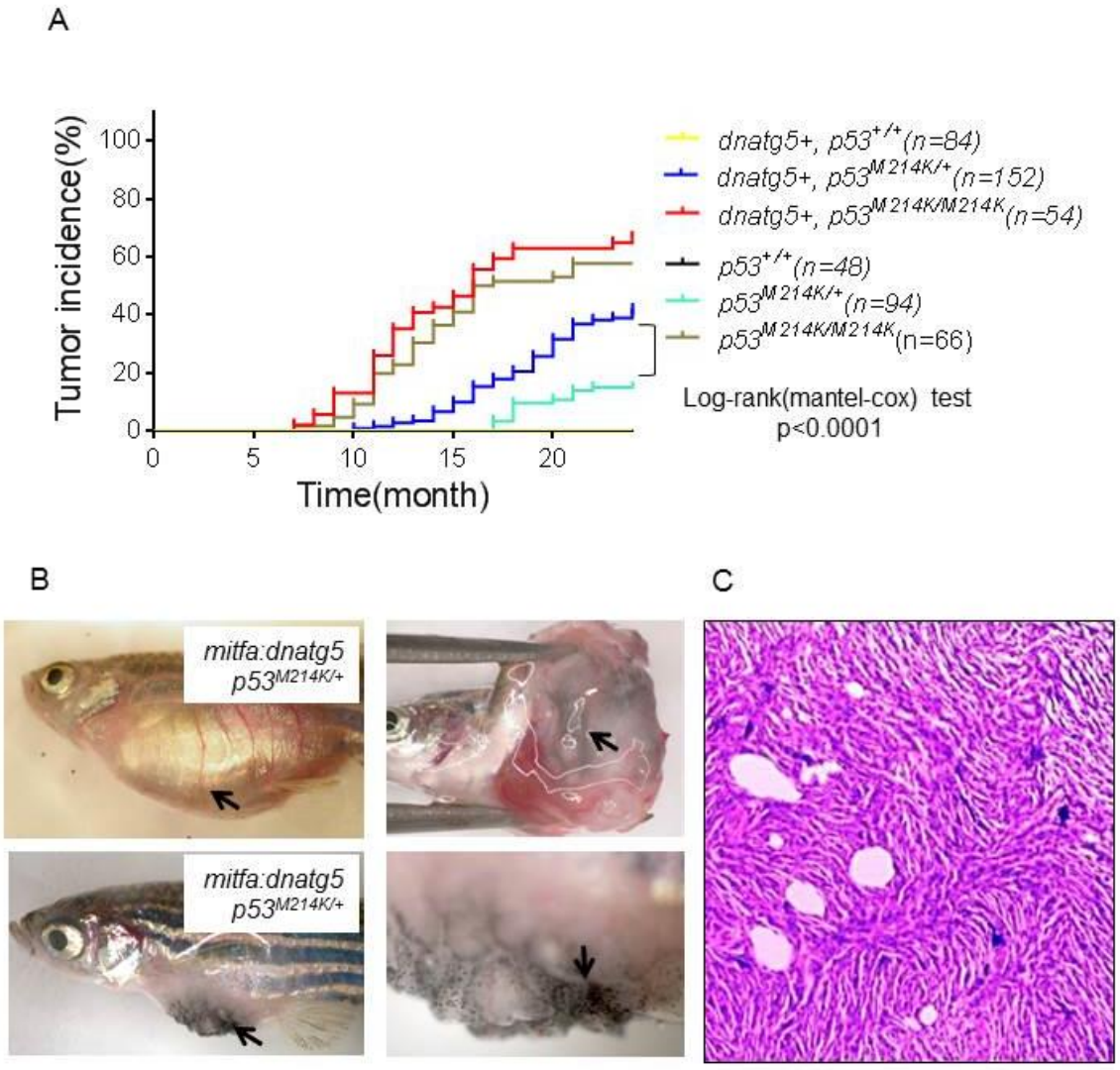

Figure 3.3. *Tg(mitfa:dnatg5)* fish line develops malignant peripheral nerve sheath tumors in a p53-mutant background.

(A) Time-to-tumor incidence. More than 40 fish in each genotype were followed for their tumor burden. The difference of tumor incidence between *Tg(mitfa:dnatg5)* in a $tp53^{M214K/+}$ background and control a $tp53^{M214K/+}$ was significant by log-rank test ($p<0.0001$). However, the difference between *Tg(mitfa:dnatg5)* in a $tp53^{M214/M214K}$ background and control mutant line $tp53^{M214/M214K}$ was not significant. **(B)** Photograph of a pigmented tumor. Some of the tumors from *Tg(mitfa:dnatg5)* in $tp53^{M214/+}$ displayed intense pigmentation. Top. 16 month-old fish; bottom, 24 month-old fish. Arrow points to pigmented region in tumor. **(C)** Tg(*mitfa:dnatg5)* in p53-mutant background develop malignant peripheral nerve sheath tumors (MPNSTs)

Table 1. Tumor histology in different genomic background

Genotype	$p53^{+/+}$	$p53^{M214K/+}$	$p53^{M214K/M214K}$	*dnatg5+* $p53^{+/+}$	*dnatg5+* $p53^{M214K/+}$	*dnatg5+* $p53^{M214K/M214K}$	*dnatg4b+* $p53^{M214K/+}$
Total # per genotype	48	94	66	84	152	54	66
Total # with tumor	0	14 (15%)	39 (58%)	0	61 (40%)	36 (67%)	4
MPNST	0	11	26	0	43	26	1
Neuroendocrine tumor	0	3	3	0	5	2	0
Vascular tumor	0	0	2	0	0	1	0
Small cell tumor	0	0	0	0	7	0	0
Abnormal feature (Hemangioma, Cystoadenoma)	0	0	0	0	2	0	0
Retinoblastoma	0	0	0	0	0	0	3
Not determined	0	0	8	0	4	7	0

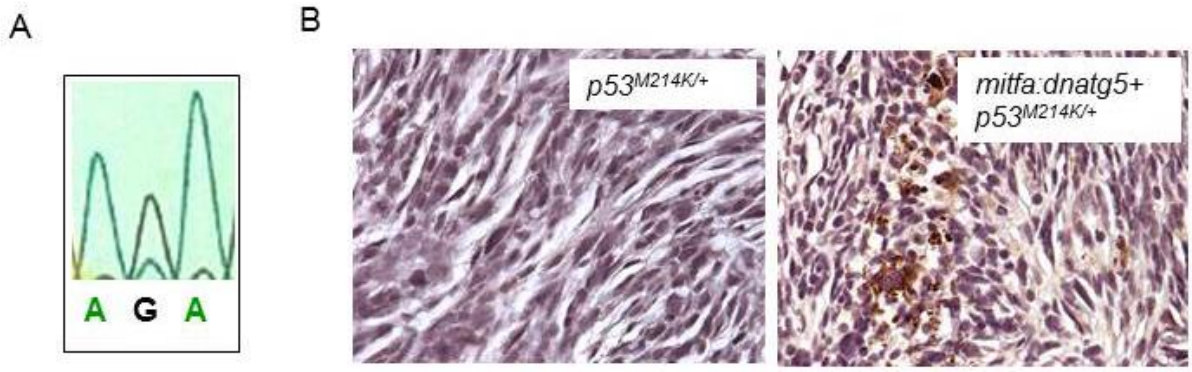

Figure 3.4. Autophagy is impaired in tumor tissues from a *Tg(mitfa:dnatg5)* fish line.

(A) RT-PCR showed transgenic mRNA in tumor tissues. RNA was isolated from tumor primary cells. After 3 passages, cells were harvested and PCR products were confirmed by sequencing. **(B)** Immunohistochemistry staining of p62 showed impaired autophagy. Tumor from *Tg(mitfa:dnatg5)* in a $tp53^{M214K/+}$ background was compared to control a $tp53^{M214K/+}$ tumor. *Tg(mitfa:dnatg5)* in a $tp53^{M214K/+}$ background displayed more brown dots than control mutant $tp53^{M214K/+}$ fish.

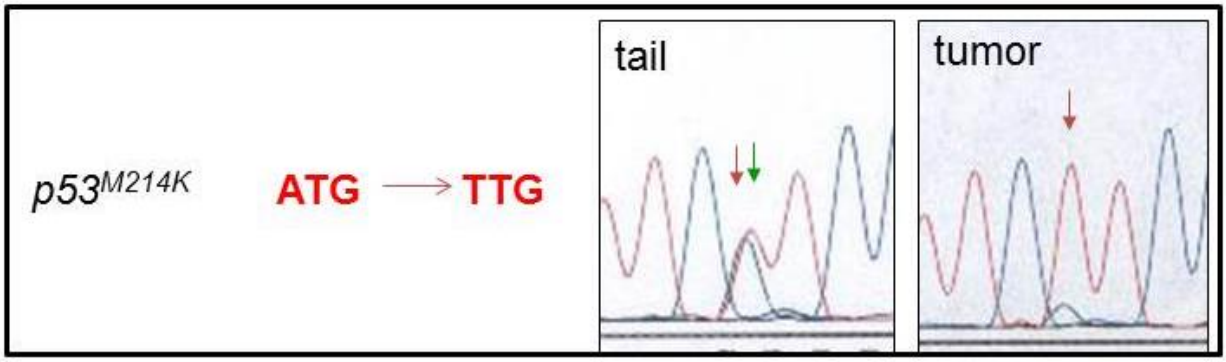

Loss of heterozygosity

Genotype	$p53^{M214K/+}$(n=10)	atg5+, $p53^{M214K/+}$(n=30)
%	70%	73.4%

Figure 3.5. ***Tg(mitfa:dnatg5)*** **fish line accelerates loss-of-heterozygosity in** a ***tp53*** $^{M214K/+}$ **background.**

Sequence analysis of the PCR products from *Tg(mitfa:dnatg5)* in a *tp53* $^{M214K/+}$ comparing normal (tail) and tumor genomic DNA. The compound red and green trace at codon position (arrow) indicates heterozygosity, whereas a trace with red only indicates LOH in tumor sample.

BIBLIOGRAPHY

1. Maiuri, M.C., Zalckvar, E., Kimchi, A., and Kroemer, G., *Self-eating and self killing: crosstalk between autophagy and apoptosis.* Nat. Rev. Mol. Cell. Biol., 2007. **8**: p. 741-752.
2. Levine, B., Kroemer, G., *Autophagy in the pathogenesis of disease.* Cell, 2008. **132**(1): p. 27-42.
3. Levine, B. and D.J. Klionsky, *Development by self-digestion: molecular mechanisms and biological functions of autophagy.* Dev Cell, 2004. **6**(4): p. 463-77.
4. Nakatogawa, H., et al., *Dynamics and diversity in autophagy mechanisms: lessons from yeast.* Nat Rev Mol Cell Biol, 2009. **10**(7): p. 458-67.
5. Qu, X., Zou, Z., Sun, Q., Luby-Phelps, K., Cheng, P., Hogan, RN., Gilpin, C., Levine, B., *Autophagy gene-dependent clearance of apoptotic cells during embryonic development.* Cell, 2007. **128**(5): p. 931-946.
6. Mathew, R., et al., *Autophagy suppresses tumor progression by limiting chromosomal instability.* Genes Dev, 2007. **21**(11): p. 1367-81.
7. Melendez, A., et al., *Autophagy genes are essential for dauer development and life-span extension in C. elegans.* Science, 2003. **301**(5638): p. 1387-91.
8. Mizushima, N., *Autophagy: process and function.* Genes Dev., 2007. **21**(22): p. 2861-73.
9. Kroemer, G., G. Marino, and B. Levine, *Autophagy and the integrated stress response.* Mol Cell, 2010. **40**(2): p. 280-93.
10. Klionsky, D.J., et al., *Guidelines for the use and interpretation of assays for monitoring autophagy.* Autophagy, 2012. **8**(4): p. 445-544.
11. Levine, B., Mizushima, N., Yoshimori, T. , *Methods in mammalial autophagy reserch.* Cell, 2010. **140**(3): p. 313-26.
12. Komatsu, M. and Y. Ichimura, *Physiological significance of selective degradation of p62 by autophagy.* FEBS Lett, 2010. **584**(7): p. 1374-8.
13. Mizushima, N., Levine, B., *Autophagy in mammalian development and differentiation.* Nat. Cell Biol., 2010. **12**(9): p. 823-830.
14. Tsukamoto, S., Kuma, A., Murakami, M., Kishi, C., Yamamoto, A., Mizushima, N., *Autophagy is essential for preimplantation development of mouse embryos.* Science, 2008. **321**(5885): p. 117-120.
15. Tsukamoto, S., et al., *Autophagy is essential for preimplantation development of mouse embryos.* Science, 2008. **321**(5885): p. 117-20.
16. Huang, S., et al., *Autophagy genes function in apoptotic cell corpse clearance during C. elegans embryonic development.* Autophagy, 2013. **9**(2): p. 138-49.
17. Sato, M. and K. Sato, *Degradation of paternal mitochondria by fertilization-triggered autophagy in C. elegans embryos.* Science, 2011. **334**(6059): p. 1141-4.
18. Al Rawi, S., et al., *Postfertilization autophagy of sperm organelles prevents paternal mitochondrial DNA transmission.* Science, 2011. **334**(6059): p. 1144-7.
19. Yue, Z., et al., *Beclin 1, an autophagy gene essential for early embryonic development, is a haploinsufficient tumor suppressor.* Proc Natl Acad Sci U S A, 2003. **100**(25): p. 15077-82.
20. Fimia, G.M., et al., *Ambra1 regulates autophagy and development of the nervous system.* nature, 2007. **447**(7148): p. 1121-5.

21. Gan, B., Peng, X., Nagy, T., Alcaras, A., Gu, H., Guan, J., *Role of FIP200 in cadiac and liver development and its regulation of TNFalpha and TSC-mTOR signaling pathways.* J. Cell Biol, 2006. **175**: p. 121-133.
22. Kuma, A., et al., *The role of autophagy during the early neonatal starvation period.* nature, 2004. **432**(7020): p. 1032-6.
23. Sou, Y.S., et al., *The Atg8 conjugation system is indispensable for proper development of autophagic isolation membranes in mice.* Mol Biol Cell, 2008. **19**(11): p. 4762-75.
24. Komatsu, M., et al., *Impairment of starvation-induced and constitutive autophagy in Atg7-deficient mice.* J Cell Biol, 2005. **169**(3): p. 425-34.
25. Saitoh, T., et al., *Atg9a controls dsDNA-driven dynamic translocation of STING and the innate immune response.* Proc Natl Acad Sci U S A, 2009. **106**(49): p. 20842-6.
26. Saitoh, T., et al., *Loss of the autophagy protein Atg16L1 enhances endotoxin-induced IL-1beta production.* nature, 2008. **456**(7219): p. 264-8.
27. Tsukada, M. and Y. Ohsumi, *Isolation and characterization of autophagy-defective mutants of Saccharomyces cerevisiae.* FEBS Lett, 1993. **333**(1-2): p. 169-74.
28. Otto, G.P., et al., *Dictyostelium macroautophagy mutants vary in the severity of their developmental defects.* J Biol Chem, 2004. **279**(15): p. 15621-9.
29. Kundu, M., et al., *Ulk1 plays a critical role in the autophagic clearance of mitochondria and ribosomes during reticulocyte maturation.* Blood, 2008. **112**(4): p. 1493-502.
30. Mortensen, M., Ferquson, DJ., Edelmann, M., Kessler, B., Morten, KJ., Komatsu, M., Simon, AK., *Loss of autophagy in erythroid cells leads to detective removal of mitrochondria and sever anemia in vivo.* Proc. Natl. Acad. Sci., 2010. **107**(2): p. 832-7.
31. Miller, B.C., et al., *The autophagy gene ATG5 plays an essential role in B lymphocyte development.* Autophagy, 2008. **4**(3): p. 309-14.
32. Stephenson, L.M., et al., *Identification of Atg5-dependent transcriptional changes and increases in mitochondrial mass in Atg5-deficient T lymphocytes.* Autophagy, 2009. **5**(5): p. 625-35.
33. Pua, H.H., et al., *Autophagy is essential for mitochondrial clearance in mature T lymphocytes.* J Immunol, 2009. **182**(7): p. 4046-55.
34. Rubinsztein, D.C., P. Codogno, and B. Levine, *Autophagy modulation as a potential therapeutic target for diverse diseases.* Nat Rev Drug Discov, 2012. **11**(9): p. 709-30.
35. Qu, X., Yu, J., Bhagat, G., Furuya, N., Hibshoosh, H., Troxel, A., Rosen, J., Eskelinen, EL., Mizushima, N., Ohsumi, Y., Cattoretti, G., Levine, B., *Promotion of tumorigenesis by heterozygous disruption of the beclin 1 autophagy gene.* J. Clin. Invest., 2003. **112**(12): p. 1809-1820.
36. Marino, G., et al., *Tissue-specific autophagy alterations and increased tumorigenesis in mice deficient in Atg4C/autophagin-3.* J Biol Chem, 2007. **282**(25): p. 18573-83.
37. Takamura, A., et al., *Autophagy-deficient mice develop multiple liver tumors.* Genes Dev, 2011. **25**(8): p. 795-800.
38. Takahashi, Y., et al., *Bif-1 interacts with Beclin 1 through UVRAG and regulates autophagy and tumorigenesis.* Nat Cell Biol, 2007. **9**(10): p. 1142-51.
39. Choi, A.M., S.W. Ryter, and B. Levine, *Autophagy in human health and disease.* N Engl J Med, 2013. **368**(7): p. 651-62.
40. Yang, S., et al., *Pancreatic cancers require autophagy for tumor growth.* Genes Dev, 2011. **25**(7): p. 717-29.

41. Stainier, D., *Zebrafish genetics and vertbrate heart formation.* Nat. Rev. Genet., 2001. **2**(1): p. 39-48.
42. Beis, D., Stainier, DY., *In vivo cell biology: following the zebrafish trend.* Trends Cell Biol., 2006. **16**(2): p. 105-12.
43. Clark, K.J., et al., *Transgenic zebrafish using transposable elements.* Methods Cell Biol, 2011. **104**: p. 137-49.
44. Handel, E.M. and T. Cathomen, *Zinc-finger nuclease based genome surgery: it's all about specificity.* Curr Gene Ther, 2011. **11**(1): p. 28-37.
45. Zu, Y., et al., *TALEN-mediated precise genome modification by homologous recombination in zebrafish.* Nat Methods, 2013.
46. Mione, M.C. and N.S. Trede, *The zebrafish as a model for cancer.* Dis Model Mech, 2010. **3**(9-10): p. 517-23.
47. Liu, j., Stainier, DY., *Zebrafish in the study of early cardiac development.* Circ. Res., 2012. **110**(6): p. 870-4.
48. Yelon, D., *Cardiac patterning and morphogenesis in zebrafish.* Dev Dyn, 2001. **222**(4): p. 552-63.
49. Amatruda, J., Shepard, JL., Stern, HM., Zon, LI., *Zebrafish as a cancer model system.* Cancer cell, 2002. **1**(3): p. 229-31.
50. Langenau, D.M., et al., *Cre/lox-regulated transgenic zebrafish model with conditional myc-induced T cell acute lymphoblastic leukemia.* Proc Natl Acad Sci U S A, 2005. **102**(17): p. 6068-73.
51. Feitsma, H. and E. Cuppen, *Zebrafish as a cancer model.* Mol Cancer Res, 2008. **6**(5): p. 685-94.
52. Berghmans, S., Murphey, RD., Wienholds, E., Neuberg, D., Kutok, JL., Fletcher, CD., Morris, JP., Liu, TX., Schulte-Merker, S., Kanki, JP., Plasterk, R., Zon, LI., Look, AT., *tp53 mutant zebrafish develop malignant peripheral nerve sheath tumors.* Proc. Natl. Acad. Sci., 2005. **102**(2): p. 407-12.
53. Donehower, L.A., et al., *Mice deficient for p53 are developmentally normal but susceptible to spontaneous tumours.* nature, 1992. **356**(6366): p. 215-21.
54. Di Bartolomeo, S., F. Nazio, and F. Cecconi, *The role of autophagy during development in higher eukaryotes.* Traffic, 2010. **11**(10): p. 1280-9.
55. Fimia, G., Stoykova, A., Romagnoli, A., Giunta, L., Di Bartolomeo, S., Nardacci, R., Corazzari, M., Fuoco, C., Ucar, A., Schwarts, P., Gruss, P., Piacentini, M., Chowdhury, K. Cecconi, F., *Ambra1 regulates autophagy and development of the nervous syste.* Nature, 2007. **447**(1121-1125).
56. Westerfield, M., *The zebrafish book. A guide for the laboratory use of zebrafish (Danio rerio).* . 4th ed2000, Eugene, Oregon: University of Oregon Press.
57. He, C., Bartholomew, CR., Zhou, W., Klionsky, DJ., *Assaying augophagic activity in transgenic GFP-Lc3 and GFP-Gabarap zebrafish embryos.* Autophagy, 2009. **5**(54): p. 520-6.
58. Burns, C.G., et al., *High-throughput assay for small molecules that modulate zebrafish embryonic heart rate.* Nat Chem Biol, 2005. **1**(5): p. 263-4.
59. Moro, E., et al., *In vivo Wnt signaling tracing through a transgenic biosensor fish reveals novel activity domains.* Dev Biol, 2012. **366**(2): p. 327-40.
60. Lawson, N., Weinstein, BM. , *In vivo imaging of embryonic vascular development using transgenic zebrafish.* Dev. Biol., 2002. **248**(2): p. 307-18.

61. Dodge, M.E., et al., *Diverse chemical scaffolds support direct inhibition of the membrane-bound O-acyltransferase porcupine.* J Biol Chem, 2012. **287**(27): p. 23246-54.
62. Burns, C., MacRae, CA., *Purification of hearts from zebrafish embryos.* Biotechniques, 2006. **40**(3): p. 278-281.
63. Verduzco, D. and J.F. Amatruda, *Analysis of cell proliferation, senescence, and cell death in zebrafish embryos.* Methods in cell biology, 2011. **101**: p. 19-38.
64. Neumann, J.C., et al., *Mutation in the type IB bone morphogenetic protein receptor Alk6b impairs germ-cell differentiation and causes germ-cell tumors in zebrafish.* Proceedings of the National Academy of Sciences of the United States of America, 2011. **108**(32): p. 13153-8.
65. Mellen, M.A., E.J. de la Rosa, and P. Boya, *Autophagy is not universally required for phosphatidyl-serine exposure and apoptotic cell engulfment during neural development.* Autophagy, 2009. **5**(7): p. 964-72.
66. Melendez, A. and B. Levine, *Autophagy in C. elegans.* WormBook : the online review of C. elegans biology, 2009: p. 1-26.
67. Mizushima, N. and B. Levine, *Autophagy in mammalian development and differentiation.* Nat Cell Biol, 2010. **12**(9): p. 823-30.
68. Bill, B.R., et al., *A primer for morpholino use in zebrafish.* Zebrafish, 2009. **6**(1): p. 69-77.
69. Hurlstone, A., Haramis, AP., Wienholds, E., Begthel, H.,Korving, J., Van Eden, F., Cuppen, E., Zivkovic, D., Plasterk, RH., Clevers, H., *The wnt/beta-catenin pathway regulates cardiacl valve formation.* Nature, 2003. **425**: p. 633-637.
70. Beis, D., Bartman, T., Jin, SW., Scott, IC., D'Amico, LA., Ober, EA., Verkade, H., Frantsve, J., Field, HA., Wehman, A., Baier, H., Tallafuss, A., Bally-Cuif, L., Chen, JN., Stainier DY, Junhblut, B., *Genetic and cellular analysis of zebrafish atrioventricular cushion and valve development.* Development, 2005. **132**(18): p. 4193-4205.
71. Chang, C., Neilson, JR., Bayle, JH., Gestwicki, JE., Kuo, A., Stankunas, K., Graef, IA., Crabtree, GR., *A field of myocardial-endocardial NFAT signaling underlies heart valve morphogenesis.* Cell, 2004. **118**(5): p. 649-63.
72. Chi, N., Show, RM, De val, S., Kang, G., Jan, LY., Black, BI, Stainier, DY., *Foxn4 directly regulates tbx2b expression and atrioventricular canal formation.* Genes Dev., 2008. **22**: p. 734-739.
73. Zimmerman, Z.F., R.T. Moon, and A.J. Chien, *Targeting Wnt pathways in disease.* Cold Spring Harb Perspect Biol, 2012. **4**(11).
74. Gao, C., Cao, W., Bao, L., Zuo, W., Xie, G., Cai, T., Fu, W., Zhang, J., Wu, W., Zhang, X., Chen, YG., *Autophagy negatively regulates Wnt signalling by promoting Dishevelled degradation.*

. Nat. Cell Biol., 2010. **12**(8): p. 781-90.
75. Lin, Y.F., I. Swinburne, and D. Yelon, *Multiple influences of blood flow on cardiomyocyte hypertrophy in the embryonic zebrafish heart.* Dev Biol, 2012. **362**(2): p. 242-53.
76. Forouhar, A., Liebling, M., Hickerson, A., Nasiraei-Moghaddam, A., Tsai, H., Hove, JR., Fraser, SE., Dickinson, ME., Gharib, M., *The embryonic vertebrate heart tube is a dynamic suction pump.* Science, 2006. **312**(5774): p. 751-3.

77. Vermont, J., Forouhar, AS., Liebling, M., Wu, D., Plummer, D., Gharib, M., Fraser, SE., *Reversing blood flows act through klf2a to ensure normal valvulogenesis in the developing heart.* PLoS Biol., 2009. **7**(11): p.):e1000246.
78. Robu, M.E., et al., *p53 activation by knockdown technologies.* PLoS genetics, 2007. **3**(5): p. e78.
79. Berghmans, S., et al., *tp53 mutant zebrafish develop malignant peripheral nerve sheath tumors.* Proceedings of the National Academy of Sciences of the United States of America, 2005. **102**(2): p. 407-12.
80. Benato, F., et al., *Ambra1 knockdown in zebrafish leads to incomplete development due to severe defects in organogenesis.* Autophagy, 2013. **9**(4): p. 476-95.
81. Hu, Z., Zhang, J., Zhang, Q., *Expression pattern and functions of autophagy-related gene atg5 in zebrafish organogenesis.* Autophagy, 2011. **7**(12): p. 1514-1527.
82. Robu, M., Larson, JD., Nasevicius, A., Beiraqhi, S., Brenner, C., Farber, SA., Ekker, SC., *p53 activation by knockdown technologies.* PLoS Genet., 2007. **25**(3(5)): p. e78.
83. Nasevicius, A. and S.C. Ekker, *Effective targeted gene 'knockdown' in zebrafish.* Nat Genet, 2000. **26**(2): p. 216-20.
84. Potts, J., Runyan, RB., *Epithelial-mesenchymal cell transformation in the embryonic heart can be mediated, in part, by transforming growth factor beta.* Dev. Biol., 1989. **134**(2): p. 392-401.
85. Timmerman, L., Grego-Bessa, J., Raya, A., Bertrán, E., Pérez-Pomares, JM., Díez,J., Aranda, S., Palomo, S., McCormick, F., Izpisúa-Belmonte, JC., de la Pompa, JL., *Notch promotes epithelial-mesenchymal transition during cardiac development and oncogenic transformation.* Genes Dev., 2004. **18**(1): p. 99-115.
86. Nakai, A., Yamaguchi, O., Takeda, T., Higuchi, Y., Hikoso, S., Tanike, M., Omiya, S., Mizote, I., Matsumura, Y., Asahi, M., Nishida, K., Hori, M., Mizushima, N., Otsu, K., *The role of autophagy in cardiomyocytes in the basal state and in response to hemodynamic stress.* Nat. Med., 2007. **13**(5): p. 619-624.
87. Savolainen, S.M., J.F. Foley, and S.A. Elmore, *Histology atlas of the developing mouse heart with emphasis on E11.5 to E18.5.* Toxicol Pathol, 2009. **37**(4): p. 395-414.
88. Cecconi, F. and B. Levine, *The role of autophagy in mammalian development: cell makeover rather than cell death.* Dev Cell, 2008. **15**(3): p. 344-57.
89. Christoffels, V.M., et al., *T-Box Transcription Factor Tbx2 Represses Differentiation and Formation of the Cardiac Chambers.* Developmental Dynamics, 2004. **229**(4): p. 763-770.
90. Harrelson, Z., et al., *Tbx2 is essential for patterning the atrioventricular canal and for morphogenensis of the outflow tract during heart development.* Development, 2004. **131**(20): p. 5041-5052.
91. Armstrong, E.J. and J. Bischoff, *Heart valve development: endothelial cell signaling and differentiation.* Circ Res, 2004. **95**(5): p. 459-70.
92. Pyo, J., Jang, MH., Kwon, YK., Lee, HJ., Jun, JI., Woo, HN., Cho, DH., Choi, B., Lee, H., Kim, JH., Mizushima, N., Oshumi, Y., Jung, YK., *Essential role of Atg5 and FADD in autophagic cell death: dissection of autophagic cell death into vacuole formation and cell death.* J Biol. Chem., 2005. **280**(21): p. 20722-9.
93. Fujita, N., Hayashi-Nishino, M., Fukumoto, H., Omori, H., Yamamoto, A., Noda, T., Yoshimori, T., *An Atg4B mutant hampers the lipidation of LC3 paralogues and causes defects in autophagosome closure.* Mol Biol Cell, 2008. **19**: p. 4651-4659.

94. Widlund, H.R. and D.E. Fisher, *Microphthalamia-associated transcription factor: a critical regulator of pigment cell development and survival.* Oncogene, 2003. **22**(20): p. 3035-41.
95. Patton, E.E., et al., *BRAF mutations are sufficient to promote nevi formation and cooperate with p53 in the genesis of melanoma.* Curr Biol, 2005. **15**(3): p. 249-54.
96. Provost, E., J. Rhee, and S.D. Leach, *Viral 2A peptides allow expression of multiple proteins from a single ORF in transgenic zebrafish embryos.* Genesis, 2007. **45**(10): p. 625-9.
97. Suster, M.L., et al., *Transgenesis in zebrafish with the tol2 transposon system.* Methods Mol Biol, 2009. **561**: p. 41-63.
98. Kwan, K.M., et al., *The Tol2kit: a multisite gateway-based construction kit for Tol2 transposon transgenesis constructs.* Dev Dyn, 2007. **236**(11): p. 3088-99.
99. Moore, J.L., et al., *Fixation and decalcification of adult zebrafish for histological, immunocytochemical, and genotypic analysis.* Biotechniques, 2002. **32**(2): p. 296-8.
100. Curran, K., D.W. Raible, and J.A. Lister, *Foxd3 controls melanophore specification in the zebrafish neural crest by regulation of Mitf.* Dev Biol, 2009. **332**(2): p. 408-17.
101. Levine, A.J., *The p53 tumor-suppressor gene.* N Engl J Med, 1992. **326**(20): p. 1350-2.
102. Rawls, J.F., E.M. Mellgren, and S.L. Johnson, *How the zebrafish gets its stripes.* Dev Biol, 2001. **240**(2): p. 301-14.
103. Mellgren, E.M. and S.L. Johnson, *The evolution of morphological complexity in zebrafish stripes.* Trends Genet, 2002. **18**(3): p. 128-34.
104. Yang, F.C., et al., *Nf1-Dependent Tumors Require a Microenvironment Containing Nf1(+/-) and c-kit-Dependent Bone Marrow.* Cell, 2008. **135**(3): p. 437-448.
105. Amsterdam, A., et al., *Many ribosomal protein genes are cancer genes in zebrafish.* PLoS Biol, 2004. **2**(5): p. E139.
106. Moore, J.L., et al., *Zebrafish genomic instability mutants and cancer susceptibility.* Genetics, 2006. **174**(2): p. 585-600.
107. Feitsma, H., et al., *Zebrafish with mutations in mismatch repair genes develop neurofibromas and other tumors.* Cancer Res, 2008. **68**(13): p. 5059-66.
108. Berger, A.H. and P.P. Pandolfi, *Haplo-insufficiency: a driving force in cancer.* J Pathol, 2011. **223**(2): p. 137-46.
109. Parant, J.M., et al., *Genetic modeling of Li-Fraumeni syndrome in zebrafish.* Dis Model Mech, 2010. **3**(1-2): p. 45-56.